THE SYNERGIC EFFECTS OF FLOW AND SPHINGOSINE 1-PHOSPHATE ON SPROUTING ANGIOGENESIS INTO THREE-DIMENSIONAL COLLAGEN MATRICES

A Dissertation

by

HO JIN KANG

Submitted to the Office of Graduate Studies of
Texas A&M University
in partial fulfillment of the requirements for the degree of

DOCTOR OF PHILOSOPHY

May 2011

Major Subject: Biomedical Engineering

THE SYNERGIC EFFECTS OF FLOW AND SPHINGOSINE 1-PHOSPHATE ON SPROUTING ANGIOGENESIS INTO THREE-DIMENSIONAL COLLAGEN MATRICES

A Dissertation

by

HO JIN KANG

Submitted to the Office of Graduate Studies of
Texas A&M University
in partial fulfillment of the requirements for the degree of

DOCTOR OF PHILOSOPHY

Approved by:

Chair of Committee,	Roland R. Kaunas
Committee Members,	Kayla J. Bayless
	Alvin T. Yeh
	Christopher M. Quick
Head of Department,	Gerard L. Cote

May 2011

Major Subject: Biomedical Engineering

ABSTRACT

The Synergic Effects of Flow and Sphingosine 1-Phosphate on

Sprouting Angiogenesis Into

Three-Dimensional Collagen Matrices. (May 2011)

Ho Jin Kang, B.A., Korea University;

M.S., Korea University

Chair of Advisory Committee: Dr. Roland R. Kaunas

The vascular endothelium continually senses and responds to both biochemical and mechanical stimuli to regulate vascular function in health and disease. The purpose of this dissertation was to understand the molecular mechanisms by which endothelial cells (ECs) respond to sphingosine 1-phosphate (S1P) and fluid wall shear stress (WSS) to initiate angiogenesis. To accomplish this, a novel cell culture system was developed to study the combined effects of S1P and WSS on inducing EC invasion into three-dimensional (3-D) collagen matrices. EC invasion required the presence of S1P, with the effects of S1P being enhanced by WSS to an extent comparable with S1P combined with pro-angiogenic growth factor stimulation. The extent of EC invasion depended on the magnitude of WSS in a biphasic manner, with the greatest induction occurring at 5.3 dyn/cm^2 WSS. Several proteins have been implicated in EC invasion, including calpain, Akt, vimentin, p21-activated kinase (PAK), and membrane type 1-matrix metalloproteinase (MT1-MMP). Interestingly, activations of calpain and MT1-MMP and phosphorylations of Akt, PAK, and vimentin coincided with, and were required for,

S1P- and WSS- induced EC invasion. Further, inhibitors of calpain, MT1-MMP, Akt and PAK all attenuated invasion induced by WSS and S1P. Calpain inhibition reduced Akt phosphorylation, vimentin cleavage, and MT1-MMP membrane translocation, suggesting that calpain regulates MT1-MMP via Akt phosphorylation and vimentin remodeling. Akt inhibition also completely blocked MT1-MMP membrane translocation and decreased phosphorylation of PAK and vimentin. In summary, these results suggest a new molecular pathway by which the combination of S1P and WSS stimulates EC invasion through calpain, Akt, PAK and vimentin to regulate activation and membrane translocation of MT1-MMP in 3-D collagen matrices.

DEDICATION

This dissertation is dedicated to God, my parents, and loving wife, Jeong Eun

ACKNOWLEDGEMENTS

I am extremely grateful to my co-advisors, Drs. Roland Kaunas and Kayla Bayless, for their support and guidance during my graduate studies. They have always been patient with me, helped me through some difficult times, ended up becoming my friends, and provided great advice that allowed me to complete this dissertation. I would not be here without their assistance. They have provided dual perspectives on science. I did not have a background in chemistry or cell biology, but Drs. Bayless and Kaunas have taught me biochemistry, cell biology and biomedical engineering. I also would like to thank to my committee members, Dr. Alvin T. Yeh and Dr. Christopher M. Quick for their thoughtful advice, encouragement, and their time and effort in reviewing this dissertation. I also would like to thank to Dr. James Moore for providing important equipment and Dr. Wayne Orr for providing PAK peptide. I especially like to express my thanks to my lab colleagues Dr. Henry Kwak and Shichi, for the good times and their constant support throughout my graduate studies and Adriana Mendoza for maintenance of endothelial cell cultures. I would like to express my thanks and gratitude to my wife Jeongeun Joo and my parents Gilsun Kang, Kyungja Kim, Younghoon Joo and Youngsun Shim for their trust and encouragement throughout my studies.

TABLE OF CONTENTS

LIST OF FIGURES

FIGURE Page

FIGURE Page

CHAPTER I

INTRODUCTION

The vascular endothelium continually senses and responds to biochemical and mechanical stimuli in the flowing blood to regulate vascular function in health and disease. Angiogenesis is the formation of new blood vessels from pre-existing vessels during numerous processes including development, wound healing and tumor vascularization. Sprouting angiogenesis is influenced by both biochemical and mechanical stimuli and occurs in several stages. Normally, endothelial cells (ECs) form a quiescent monolayer lining the inside of blood vessels. Under angiogenic stimulation, they are activated to detach from the monolayer and migrate into the underlying tissue through matrix proteolysis. The EC sprouts form individual sprouts containing a lumen [1-3]. Thus, the ECs are primarily responsible for initiating and directing angiogenesis. Biochemical growth factors (GF) such as vascular endothelial growth factor (VEGF) and basic fibroblast growth factor (bFGF) are well known stimulators of angiogenesis [2-5]. Sphingosine-1-phosphate (S1P), a signaling sphingolipid deposited by activated platelets during wound healing, has been recently recognized to be a major regulator of angiogenesis in vivo and in vitro [4, 6-9].

This dissertation follows the format of *American Journal of Physiology - Heart and Circulatory Physiology.*

Sphingosine 1-phosphate (S1P)

S1P is a signaling sphingolipid and bioactive lipid mediator. S1P directs a number of fundamental biological processes including EC migration [10-12] and junction formation [13-16] and is important in cancer, atherosclerosis, immunity, asthma, wound healing and angiogenesis [17] [18]. Sphingosine can be released from ceramides by the enzyme ceramidase in platelets and S1P is the product of phosphorylation of sphingosine catalyzed by sphingosine kinase. Intracellular S1P is increased by growth factors, cytokines and hormones [18]. The biological effects of S1P are mediated by its binding to five specific G protein-coupled receptors located on the cell surface [19]. Thus, understanding the mechanism of S1P is important.

Effects of wall shear stress on endothelial cells

ECs are constantly exposed to, and respond to, both fluid shear stress and cyclic mechanical stretch caused by hemodynamic forces. Specifically, WSS affects cellular functions such as proliferation, migration, apoptosis, permeability and gene expression through intracellular signals [20]. ECs also become aligned and elongated with cytoskeletal changes by the direction and magnitude of fluid shear stress [21, 22]. WSS is crucial for normal vascular remodeling during development [23] and stimulate the growth of microvessels in tumors [24]. Parallel-plate flow chambers are often used for applying controlled WSS to culture ECs via pressure-driven flow. The fluid flow can be

modeled using Poiseiuelle's Equation, which describes fully-developed laminar flow of a Newtonian fluid in a rectangular channel,

$$\tau = 6\mu Q / wh^2 \quad (1)$$

where τ = wall shear stress, μ = fluid viscosity (0.7 cP), Q = flow rate (from 14 to 32 ml/min), w = the width of the flow chamber (29.21 mm), and h = distance between plates (from 0.254 to 2.54 mm). Here, $h<<w$ which justifies the assumption of 2-D flow.

Proteins related to EC signaling pathways

Calpain

Calpains, Ca^{2+}-dependent cysteine endopeptidases, are composed of a unique 80 kDa catalytic subunit (calpains 1, 2 and 3) associated with a common 28 kDa regulatory subunit (calpain 4) that is subdivided into four functional domains [25]. Calpastatin is a calpain specific endogenous inhibitor protein that tightly calpain activity [26] [27]. A key function of calpain is to degrade cellular proteins involved in pathways that influence cell apoptosis, migration and proliferation [28]. Dourdin et al. [29] demonstrated that calpain 4 knock-out mouse embryos die at around 10 days post-conception and exhibit a defect in vascular development. Carragher and colleagues reported that inhibitors of calpain suppressed focal adhesion disruption, reduced substrate adhesion and slowed cell migration [30, 31]. Thus, calpain activity is expected to play a key role in the transition of ECs into an invasive phenotype.

Akt

The serine/threonine kinase Akt (also known as protein kinase B) constitutes an important molecular link in signaling cascades involving cell survival, growth, migration, proliferation, polarity, and metabolism [32]. There are three known isoforms of Akt and each possess a Pleckstrin Homology (PH) domain that binds to phosphoinositides with high affinity; Akt binds either PIP_3 (phosphatidylinositol (3,4,5)-trisphosphate) or PIP_2 (phosphatidylinositol (3,4)-bisphosphate) phosphorylated by only PI3-kinases. The PI3-kinases activated by either a G protein coupled receptor or receptor tyrosine kinase phosphorylate PIP_2 to form PIP_3 at the membrane. As a result, Akt can be phosphorylated by its activating kinases, phosphoinositide dependent kinase 1 (PDK1 at threonine 308) and mTORC2 (at serine 473). Akt may also be activated by cAMP-elevating agents through protein kinase A.

There is significant evidence that Akt is involved in angiogenesis. In an *ex vivo* aortic ring invasion assay, the average length of sprouts was significantly reduced in Akt1 knockout mice [33].Since Akt is an important protein in EC sprouting *in vitro* and angiogenesis *in vivo* [34], we will investigate the role of Akt in S1P- and WSS-induced EC invasion.

PAK

The p21 activated kinases (PAKs) are 65-kDa serine-threonine kinases that are activated by Akt, PDK1, and the small GTPases Rac and Cdc42 to regulate cellular proliferation, differentiation, survival, and migration [35-37]. PAKs regulate protein kinase

cascades such as ERK [38, 39] and c-Jun N-terminal kinase (JNK) [40, 41]. In addition, PAKs activation is mediated by direct interaction with Nck, non-catalytic tyrosine kinase adaptor protein located at the cell membrane [39, 42, 43]. Nck is comprised of three SH3 domains and interacts with a proline-rich region in the N-terminus of PAK through the second SH3 domain [44, 45]. PAK2 is the predominant isoform in ECs [46, 47].Motivated by these results, we hypothesized that PAK2 may be involved downstream of Akt in S1P- and WSS-induced EC invasion. To study this, we used a PAK inhibitory synthetic peptide that selectively binds Nck and disrupts PAK membrane localization [36].

MT1-MMP

Matrix metalloproteinases (MMPs) are zinc-dependent endopeptidases that cleave extracellular matrix proteins. Most MMP's are secreted as inactive propeptides which are activated when they themselves are cleaved by extracellular proteinases. Membrane type 1-matrix metalloproteinase (MT1-MMP), however, is maintained on the cell membrane and its activity has been shown to play an essential role in sprouting events. One mechanism of MT1-MMP functions is through activated MMP-2 [48-51]. MT1-MMP consists of an N-terminal zinc-dependent metalloproteinase domain, a transmembrane domain and a cytoplasmic tail that can be phosphorylated. Langlois and Beliveau [52] demonstrated that phosphorylation of tyrosine 573 on the cytoplasmic tail of MT1-MMP in response to S1P stimulation directly correlates with proteolytic activity and membrane localization. However, the effects of WSS on MT1-MMP activity have not been reported. Thus, we investigated here whether WSS synergized with S1P to activate and translocate MT1-MMP to the membrane during sprouting

angiogenesis in 3-D matrices. Further, we identified the molecules that control MT1-MMP membrane translocation and activation during S1P- and WSS-induced EC invasion in 3-D collagen matrices.

Vimentin

Vimentin is the most abundant intermediate filament (IF) protein isoform in ECs. Vimentin spreads from the nucleus to the plasma membrane and attaches to the nucleus, endoplasmic reticulum, and mitochondria [53]. Vimentin is required for epithelial cell [54] and fibroblast migration [55]. Vimentin proteins consist of a central rod domain flanked by N-terminal head and C-terminal tail domains. The N-terminal head and C-terminal tail domains of adjacent vimentin proteins bind each other to result in filament assembly. This interaction is disrupted when a phosphate group is added to the head region, resulting in filament disassembly [56, 57]. PAK and Akt may be the kinase responsible for phosphorylating vimentin [58-60]. All domains of vimentin also have the cleavage site for calpains and are degraded by calpains [61] [62]. As a result, vimentin filaments can be partially disassembled and rearranged in cells [63]. Perlson [64] and Goldman [65, 66] reported that vimentin fragments cleaved by calpains binds and transports phosphorylated ERK along the axon of neural cells via dynein motor proteins. Based on these results, we hypothesized that vimentin fragments produced by either cleavage by calpains or phosphorylation by Akt-regulated PAK can bind with MT1-MMP and then translocate to the membrane to facilitate matrix proteolysis.

CHAPTER II

FLUID SHEAR STRESS MODULATES ENDOTHELIAL CELL INVASION INTO THREE-DIMENSIONAL COLLAGEN MATRICES [+]

Overview

Endothelial cells are chronically subjected to biochemical and mechanical stimuli, which regulates their angiogenic potential. We developed a novel system to study the synergistic effects of S1P and WSS on the initiation of angiogenic sprouting into 3-D collagen matrices. Polymerized collagen gels were incorporated into a parallel-plate flow chamber to apply controlled WSS to the surface of endothelial monolayers over a period of 18h. We show that EC invasion required the presence of S1P, with the effects of S1P being enhanced by shear stress to an extent comparable with S1P combined with angiogenic growth factor stimulation. The number of invading cells depended on the magnitude of WSS in a biphasic manner, with highest induction at 5.3 dyn/cm^2 WSS. The invasion distance was proportional to the magnitude of shear stress, however. These responses were observed in several EC cell types. Thus, these results provide strong evidence that shear stress is a positive modulator of S1P-induced EC invasion into 3-D collagen matrices.

[+]Reprinted with permission from Fluid Shear Stress Modulates Endothelial Cell Invasion Into Three-dimensional Collagen Matrices by Hojin Kang, Kayla J. Bayless, and Roland R. Kaunas, 2008 *American Journal of Physiology Heart and Circulatory Physiology*, 295: H2087-2097, Copyright 2008 by the American Physiological Society.

Introduction

Angiogenesis, the development of new blood vessels from pre-existing vessels, is a critical step in physiological and pathological events such as wound healing and tumor vascularization [1]. Sprouting angiogenesis *in vivo* involves EC degradation of the basement membrane, cell proliferation and migration toward angiogenic stimuli. These events are coordinated with eventual formation of a lumen within the endothelial sprout and the joining of sprouts to form a capillary bed [67, 68]. Importantly, both biochemical and mechanical forces influence these newly-developing structures.

Several biochemical factors are recognized to enhance angiogenesis with VEGF and bFGF being among the best characterized. *In vitro,* they induce proliferation, and invasion into 3-D collagen matrices, as well as the formation of tubular structures [69, 70]. More recently, S1P has been identified as a potent pro-angiogenic factor [8]. S1P can act as an intracellular signaling molecule and is also deposited by activated platelets during wound healing [5, 71]. Exogenous S1P administration or endogenous S1P production by sphingosine kinase over-expression promotes post-ischemic angiogenesis and blood flow recovery in mouse ischemic hind limb models [72]. Bayless and Davis previously reported that S1P-induced EC invasion and lumen formation required integrin cell surface receptors and membrane-associated metalloproteinase activity [4].

While the roles of biochemical factors have studied extensively, the role of hemodynamic forces in angiogenesis are not well understood. ECs are constantly subjected to a tangential WSS caused by blood flow. Nearly a century ago it was

observed that capillary growth from sprouting vessels was enhanced by increasing blood flow rate in the tails of frog larvae, while it regressed when flow ceased [73]. Ichioka et al. [74] also observed that elevated WSS caused by the vasodilator prazosin increased microvascular growth. Nasu et al. [75] demonstrated that tumor angiogenesis depended more on flow than on vascular growth factors. Dickinson and colleagues [23] demonstrated that shear forces are crucial for vascular remodeling during development.

Although simple two-dimensional (2-D) models have been used extensively to recognize cellular behaviors involved in sprouting angiogenesis, including migration and EC network formation [76-78], additional steps to sprouting including matrix proteolysis and lumen formation can only be observed when ECs invade into 3-D matrices. Consequently, a number of groups have begun to employ 3-D models [48, 50, 79-81]. The 3-D model of cell invasion used in the present studies provides an environment that is much more representative of the environment sprouting ECs find *in vivo*. Importantly, we also incorporate the effects of fluid flow on EC invasion, which turns out to have profound effects on EC invasion. Using this system, we evaluated the ability of S1P, growth factors, and WSS to promote invasion using human umbilical vein endothelial cells (HUVEC) into 3-D collagen matrices. We also compared invasion responses between HUVEC and human dermal and retinal microvascular ECs. Lastly, we determined whether S1P-induced EC invasion was dependent on the magnitude of shear stress or shear rate.

Materials and methods

Cell Culture

Unless otherwise indicated, all reagents were obtained from Sigma (St. Louis, MO). Human umbilical vein endothelial cells (HUVECs) were purchased from Lonza BioProducts (San Diego, CA) and were used in all experiments at passage 4-6. ECs were cultured in growth media supplemented with 500 ml Medium 199 (Invitrogen, Carlsbad, CA), 20% fetal bovine serum (FBS, Lonza BioProducts), 0.1 mg/ml heparin, 50 mg/ml gentamicin (Invitrogen), antibiotic-antimycotic (Invitrogen) and 0.4 mg/ml lyophilized bovine hypothalamic extract (Pel-freeze Biologicals, Rogers, AR) purified as previously described [82] at 37°C in a humidified 5% CO_2 incubator. Cells were passaged to allow formation of a confluent monolayer once weekly on flasks coated with 1 mg/ml sterile porcine gelatin in HEPES and fed 24 h prior to beginning experiments.

Collagen Matrix Invasion Assay

Rat tail collagen type I was purified as described [83] and used to prepare collagen matrices at 3.75 mg/ml as previously described [4]. D-Erythro-sphingosine-1-phosphate (S1P; Avanti Polar Lipids, Alabaster, AL) was added to the collagen matrices (unless otherwise noted) to a final concentration of 1 μM and thoroughly mixed. 7 mm circular wells (45 μl/ 0.38 cm^2) were formed by attaching a silicone rubber gasket (Specialty Manufacturing, Inc., Saginaw, MI), of 1 mm thickness and perforated with eight holes, on 50 x 75 mm glass microscope slide (Fig. 1). The collagen matrices

were added to the wells and allowed to polymerize for 1 h at 37°C in a humidified 5% CO_2 incubator (Thermoscientific). ECs were fed 24h before seeding cells onto collagen matrices. The cells were rinsed with 14 ml HEPES and removed with 2 ml of 0.25% trypsin-EDTA (Invitrogen) at 37°C for 1 min. The trypsin was neutralized with 2 ml FBS. Cells were counted with a hemocytometer, washed once in 10 ml serum-free M199, and plated as a confluent monolayer at a density of 60000 cells/ 0.38cm^2 in M199 containing 5% FBS and 50 µg/ml ascorbic acid. The cells were allowed to attach for 1h and then washed twice with serum-free M199 before applying the defined media and WSS as previous described in detail [84].

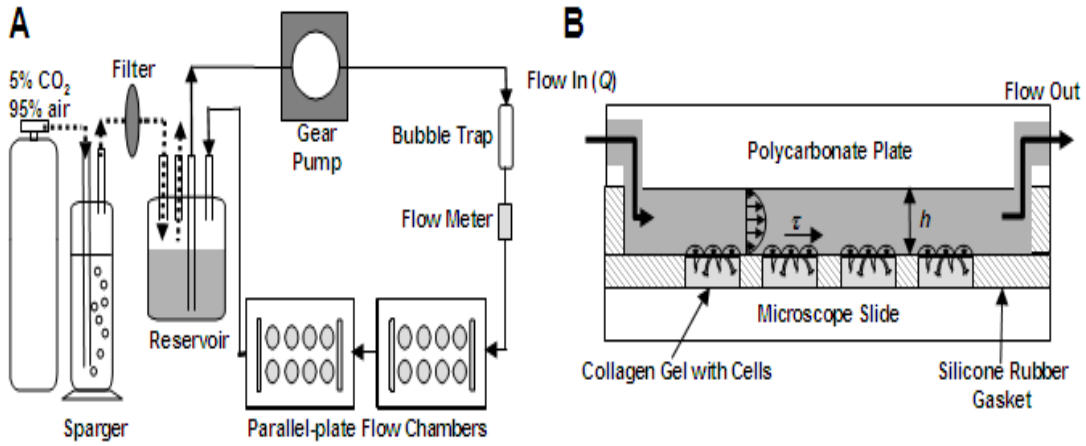

Figure 1. Apparatus to apply controlled varying levels of wall shear stress (WSS) to human umbilical vein endothelial cells (ECs) seeded on 3-D collagen matrices. A: multiple flow chambers (2 shown) were connected in series into a pressure-driven flow circuit in which media pH was controlled with humidified 5% CO_2-95% air (dashed lines). **B:** ECs were cultured on 8 (4 shown) circular collagen gels that were polymerized in the bottom plate of a parallel-plate flow chamber. Medium 199 media (dark grey shaded area) was perfused through the chamber to subject the cell monolayers to steady, uniform WSS.

Shear Stress Experiments

The plates containing ECs seeded on collagen matrices were assembled into parallel-plate flow chambers designed to apply uniform steady WSS to the cell monolayer (cf. Fig. 1). The WSS magnitude was calculated as $\tau = 6\mu Q / wh^2$, where τ is wall shear stress, μ is fluid viscosity (0.7 cP), *Q* is flow rate, *w* is the width of the flow channel (29.21 mm), and *h* is the height of flow channel (0.254mm ~ 2.54mm). The flow of the culture medium was provided by a sterile continuous-flow loop, with the flow rate controlled with a pulse-free gear pump (Ismatec) and monitored with an ultrasonic tubing flow sensor (Transonic Systems). The perfusion medium consisted of M199 containing reduced serum II (RSII) and 50 μg/ml ascorbic acid. RSII consisted of 2 mg/ml bovine serum albumin (BSA), 20 ng/ml human holo-transferrin, 20 ng/ml insulin, 17.1 ng/ml sodium oleate, and 0.02 ng/ml sodium selenite. Media pH was maintained at 7.4 by perfusing 5% CO_2-95% air first through a sparger containing sterilized water and then through the head gas of the media reservoir. Bubbles were removed from the media using a bubble trap. The entire system was enclosed by an acrylic box in which temperature was maintained at 37°C using a heat gun with feedback temperature control (Omega Engineering, Stamford, CT).

Imaging and Analysis

Following each experiment, collagen matrices containing invading cells were washed briefly in HEPES buffer, fixed in 3% glutaraldehyde in PBS for 2 h, stained with 0.1% toluidine blue in 30% methanol for 12 min, and washed with water to clearly

identify invading cells. Cross-sections were prepared using a razor blade and imaged using an Olympus CKX41 inverted microscope equipped with an Olympus Q-Color 3 camera. From the digital images of the cross-sections, the *invasion distance* was measured for individual sprouts as the distance from the bottom of the cell monolayer and the point of deepest penetration into the matrix. The *nucleus traveling distance* was also measured for individual sprouts as the distance from the bottom of the cell monolayer and the center of the nucleus into the matrix (important for situations where nuclear penetration into the matrix was attenuated with inhibitors). In addition, the *invasion diameter* was measured for individual sprouts as the width between the left and the right side of the nucleus. To quantify *invasion density*, *en face* images were observed using bright-field illumination with a 10X objective on an Olympus BH-2 upright microscope. The microscope was focused on the invading cells, which were located immediately below the EC monolayer. Each data point represents a field in the center of a well, where the number of invading cells was counted manually using an eyepiece equipped with an ocular grid covering an area of 1 mm^2. A single measurement was recorded for each well.

Proliferation Assay

To subject ECs to WSS magnitudes of 5.3 and 12 dyn/cm^2, in a single experiment, a flow system was run with six parallel-plate flow chambers arranged in series; WSS magnitude within an individual chamber depended on the channel gap height and individual chambers were removed after different time points (1, 12 and 24h). Ki-67 is a protein expressed in cell nuclei of dividing, but not resting, cells (69). Collagen matrices containing invading cells were fixed in 4% paraformaldehyde and immunostained with polyclonal rabbit anti-Ki-67 primary antibody and FITC-conjugated (goat anti-rabbit) secondary antibody. The collagen matrices were then mounted with DAPI mounting medium. To quantify proliferation density, *en face* images were observed at 20X focusing on the FITC signal in cell nuclei of cell in the monolayer. Each data point represents a field in the center of a well, where the number of proliferation cells was counted manually. The number of nuclei that stained positively and negatively for Ki-67 was quantified.

Modifying Media Viscosity

High molecular weight, neutral dextran was added to the perfusion media (3g/100ml) to investigate the role of viscosity in S1P- and WSS-induced EC invasion. WSS (dyn/cm^2) is defined as:

$$\tau = \frac{du}{dy}\mu \tag{2}$$

where τ = wall shear stress, μ = fluid viscosity (centipoises [cp]) and $\frac{du}{dy}$ = shear rate (s^{-1}). We can control shear stress and shear rate by varying μ and $\frac{du}{dy}$. The viscosity of the culture media with and without dextran was measured using a glass capillary viscometer (Cannon Instruments).

Statistical Analysis

Data are presented as the mean and standard deviation for each group of samples. Statistical analysis was performed using SAS software (Cary, NC). Comparisons between two groups were performed using Studentized T-tests. Comparisons between three or more groups were performed by one-way ANOVA followed by Student-Newman-Keuls post-hoc pairwise comparison testing. A two-way ANOVA was used to compare the time courses under different test conditions for the MMP-2 zymogram data.

Results

WSS Enhanced S1P-induced EC Invasion Into 3-D Collagen Matrices

Dr. Bayless has previously shown that S1P synergizes with growth factors (10 ng/ml each of VEGF and bFGF) to potently induce EC invasion and lumen formation into 3-D collagen matrices [4]. VEGF and WSS have been reported to increase the expression of the S1P receptor, $S1P_1$, and augment S1P-stimulated EC migration in 2-D culture [85, 86]; thus we hypothesized that WSS would enhance S1P-induced EC invasion. To test this hypothesis, ECs cultured on collagen matrices containing or lacking S1P (1 μM) were treated with either growth factors (GFs), WSS (5.3 dyn/cm^2), or no treatment for 18 h (Fig. 2). In this model, a confluent monolayer of primary human umbilical vein ECs was seeded on the surface of a polymerized 3-D collagen matrix. Over time, a subset of ECs moved from the surface and invaded into the matrix below. Photographs of fixed cultures illustrate the invasion process and these results were summarized in Fig. 2I. In these assays, 1μM S1P was mixed into the collagen matrices. No invasion was observed in control collagen matrices (Fig. 2A), and this was not changed by the application of either GFs (Fig. 2B), S1P (Fig. 2C), or WSS (Fig. 2D) alone. The simultaneous application of GFs and WSS induced a slight but insignificant amount of EC invasion (Fig. 2E). Simultaneous application of S1P and GFs (Fig. 2F) or S1P and WSS (Fig. 2G) induced significant EC invasion. Finally, application of GFs, S1P, and WSS all together resulted in the highest level of EC invasion (Fig. 2H), although this was not significantly greater than the combined application of S1P and WSS. These results indicate that S1P synergized with GFs and WSS to promote EC

invasion and that no individual stimulus (i.e., S1P, GFs, or WSS) alone was capable of promoting a response. Of potential concern with the WSS studies are the release of S1P into the perfusate and the generation of other proangiogenic soluble factors by the ECs subjected to WSS. With the assumption that all the S1P is released from the collagen matrices into the perfusate, the maximal concentration of S1P in the perfusate would be 0.16 μM, which is higher than the dissociation constant (K_d) for S1P to its receptors (10 to 30 nM) hence may activate the S1P receptors [87]. WSS has also been shown to induce the expression of bFGF and VEGF [77, 88]. Applying freshly collected conditioned media from cultures under the combined S1P and WSS condition did not upregulate EC invasion after 24h in separate static cultures of ECs on S1P-incorporated gels, however (data not shown). These results indicate that the effects of WSS on EC invasion into 3-D collagen matrices were not due to the generation of proangiogenic soluble factors and that S1P incorporation within the matrix is required to promote directed invasion of ECs into collagen matrices. For all subsequent flow experiments, S1P was incorporated into collagen matrices and GFs were not added to the perfusion media.

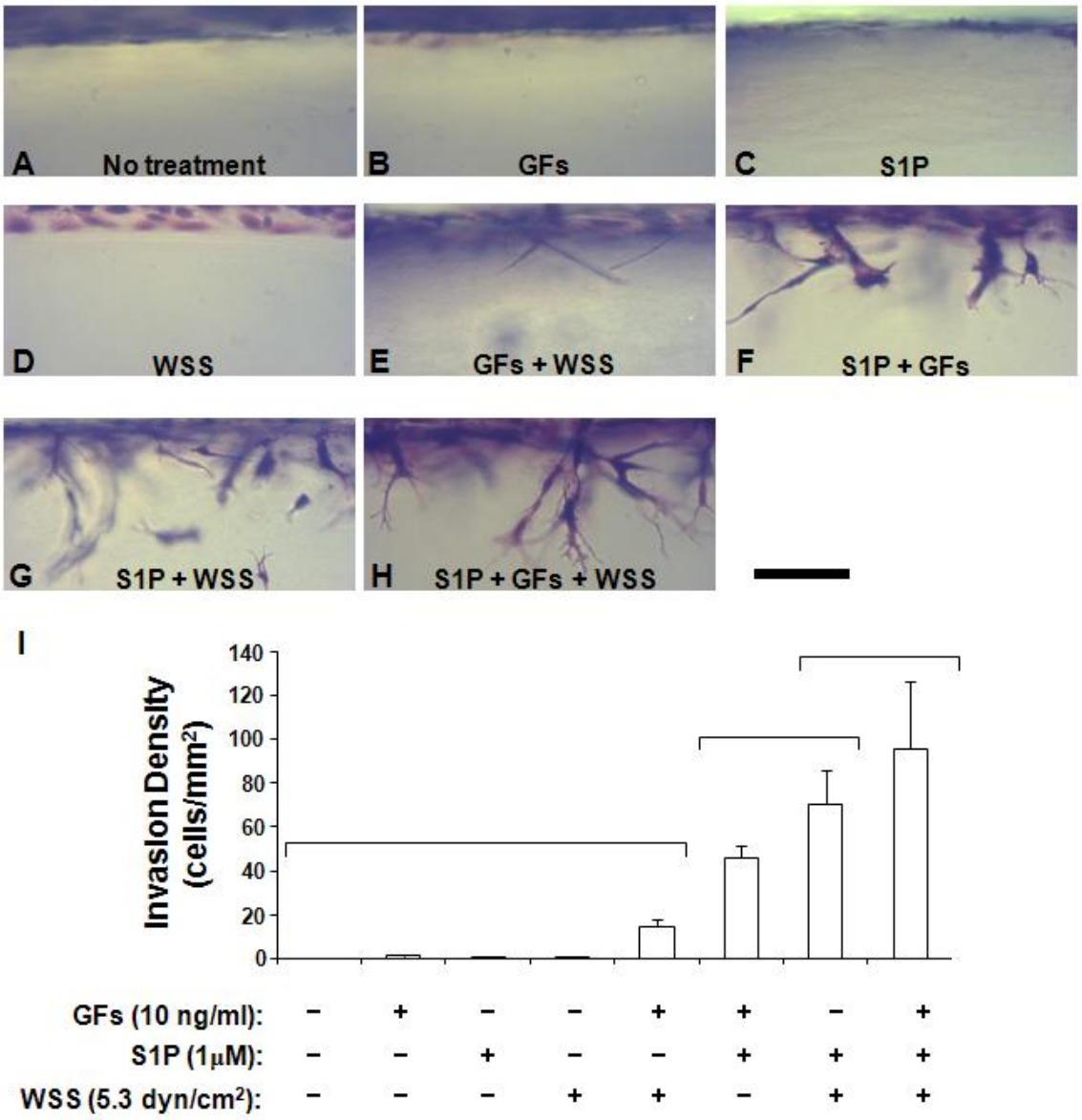

Figure 2. S1P synergizes with WSS and GFs to induce EC invasion. Representative cross-sectional micrographs are shown for ECs left untreated **(*A*)** and treated with 10 ng/ml each VEGF + bFGF (GFs; ***B***), S1P (1 μM; ***C***), 5.3 dyn/cm2 WSS **(*D*)**, GFs + WSS **(*E*)**, S1P + GFs **(*F*)**, S1P + WSS **(*G*)**, and GFs + S1P + WSS **(*H*)**. The cell monolayer is located at the *top* of each figure. Invasion density (*I*) for each condition was quantified (means ± SD; $n = 4$ fields) as described in MATERIALS AND METHODS from samples observed en face. Conditions that were not significantly different ($P<0.05$) as tested by ANOVA and multiple comparison testing are grouped in brackets. Scale bar, 100 μm.

WSS Enhanced EC Invasion in a Time- and Magnitude Dependent Manner

The effects of WSS magnitude on EC invasion were next characterized by quantifying both depth and density of EC invasion. Both invasion depth and density increased with time in ECs subjected to 5.3 dyn/cm^2 WSS into 3-D collagen matrices containing S1P (Fig. 3). To compare the effects of WSS magnitude in the same experiment, multiple chambers were connected in series and subjected to WSS for 24h. Since flow rate was the same in each chamber, the WSS within individual chambers was modified by varying chamber gap height to subject the ECs to WSS ranging from 0.12 to 12 dyn/cm^2. The invasion depth increased monotonically with increasing WSS (Fig. 4, *A*"–*C*" and *D*), with cells invading approximately twice the distance at 12 dyn/cm^2 than at 0.12 dyn/cm^2. The density of EC invasion showed a biphasic response, however, with EC invasion density initially increasing with WSS up to a maximum value of 64 ±23 cells/mm^2 at 5.3 dyn/cm^2 but then decreasing to 15 ±5 cells/mm^2 at 12 dyn/cm^2 (Fig. 4, *A*'–*C*' and *E*). To test whether WSS influenced invasion through direct effects on collagen matrices, we applied 0, 0.12, 5.3, and 12 dyn/cm^2 WSS to collagen matrices containing S1P for 48 h and then seeded ECs on the presheared matrices in media containing VEGF and bFGF to quantify invasion. The invasion density was unchanged by preconditioning the matrices with WSS regardless of the WSS magnitude (Fig. 4*F*), indicating that the matrices were not altered by perfusion in a manner that affected cell invasiveness. Low invasion responses observed with 12 dyn/cm^2 WSS could potentially be explained by alterations in cell proliferation or cell viability. Low WSS has been associated with increasing EC turnover through elevated rates of proliferation and

apoptosis [89], and high WSS can reduce EC proliferation in a dose-dependent manner [90]. We examined the expression of Ki-67 [a protein expressed in cell nuclei of dividing, but not resting, cells [91]] in ECs subjected to different magnitudes of WSS for 24 h. An average of 23.1 ± 6.0% of ECs subjected to 0.12 dyn/cm^2 WSS stained positively for Ki-67 compared with 13.0 ± 6.8% (at 5.3 dyn/cm^2) and 14.9 ± 1.2% (at 12 dyn/cm^2). These data are consistent with reports that relatively high WSS (>1.5 dyn/cm^2) suppresses DNA synthesis [92, 93]; however, there was no significant difference in the levels of Ki-67 staining between samples subjected to 5.3 and 12 dyn/cm^2 WSS. Based on these data, proliferation rates cannot explain reduced invasion observed with 12 dyn/cm^2 WSS compared with 5.3 dyn/cm^2 WSS. An alternate possibility is that apoptosis rates are altered between treatment groups. However, we did not detect any significant levels of cleaved caspase-3 (a marker of apoptosis) in response to any of the WSS treatments (data not shown). These results indicate that the effects of WSS magnitude on EC invasion do not occur through changes in the rates of cell proliferation or apoptosis but rather occur through biochemical changes as a result of different WSS magnitudes, which we investigate below.

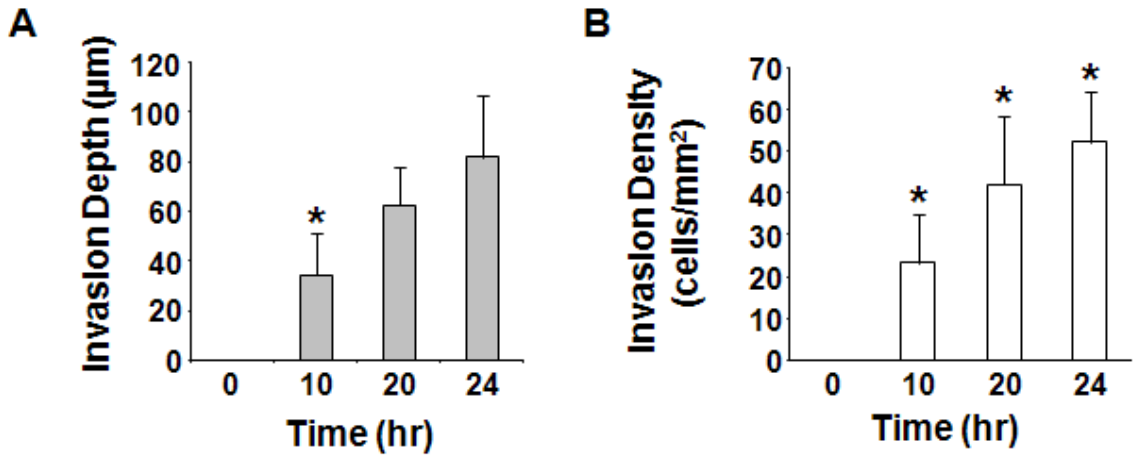

Figure 3. WSS-induced EC invasion progresses steadily over time. ECs were subjected to 5.3 dyn/cm^2 WSS for the times indicated in the presence of S1P. Cultures were fixed and stained with toloudine blue for morphometric analysis. The invasion distance (**A**; n=50 sprouts) and density (**B**; n=100 cells from 15 fields) are plotted as a function of time (means ±s.d). * Significantly difference from 0 h (P<0.05).

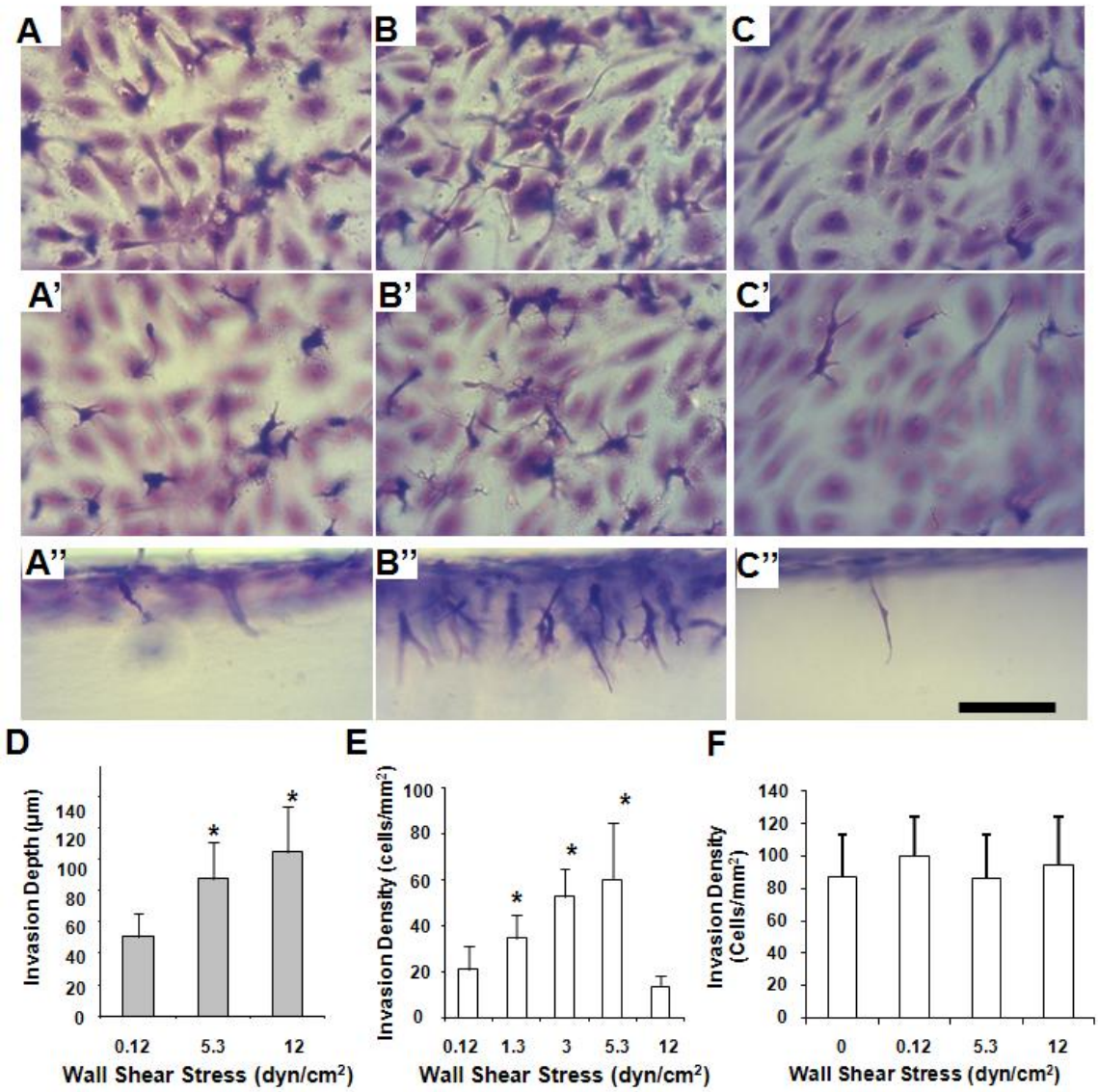

Figure 4. Invasion density and distance are dependent on the magnitude of WSS. *A-E*: ECs were subjected to steady WSS ranging from 0.12 to 12 dyn/cm^2 for 24 h in the presence of S1P, fixed, and stained with toloudine blue for morphometric analysis. Representative cross-sectional micrographs are shown of en face preparations focusing on the EC monolayer **(*A*–*C*)** and immediately below the monolayer **(*A'*–*C'*)** and of cross sections **(*A''*–*C''*)** for ECs subjected to WSS magnitudes of 0.12 **(*A*-*A''*)**, 5.3 **(*B*-*B''*)**, and 12 **(*C*-*C''*)** dyn/cm^2. The invasion distance (***D***; *n* =150 sprouts) and density (***E***; *n* =20 fields) of invading ECs are plotted as a function of WSS magnitude (means ±SD). ***F*:** collagen matrices containing S1P were subjected to different WSS magnitudes for 48 h before seeding and measuring the extent of cell invasion after 17 h under static conditions with 10 ng/ml VEGF and bFGF in the media. *Significant difference from value at 0.12 dyn/cm^2 WSS (P<0.05). Scale bar, 100 μm.

WSS Enhanced EC Invasion in Other EC Types

We next measured the effects of WSS magnitude in S1P-induced EC invasion of other EC types in 3-D collagen matrices. Human dermal microvascular endothelial cells (HDMVEC) and human retinal microvascular endothelial cells (HRMVEC) were each cultured on collagen matrices and subjected to WSS ranging among 0.12, 5.3, and 12 dyn/cm^2. After 24h, they were fixed in 3% glutaraldehyde, and stained with toluidine blue to observe EC invasion. Similar responses were also observed in HDMVEC and HRMVEC (Fig. 5). These results indicate that the biphasic dependence of invasion on WSS magnitude is not only limited to only HUVECs (cf. Fig. 4E).

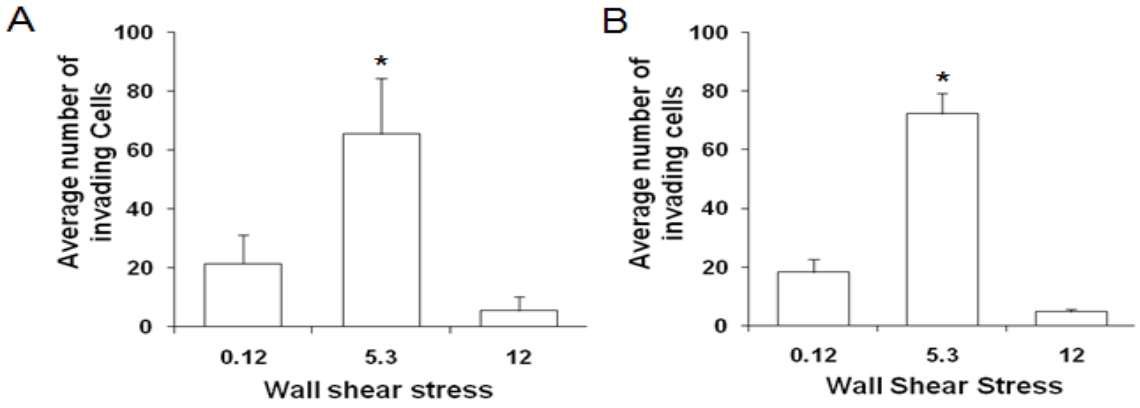

Figure 5. Quantification of invasion responses observes as a result of treatment with different magnitude of WSS in two different ECs. Steady WSS of at 0.12, 5.3 and 12 dyn/cm^2 WSS was applied to either Human Dermal Microvascular Endothelial Cells (HDMVEC:**A**) or Human Retinal Microvascular Endothelial Cells (HRMVEC:**B**) monolayers seeded on 3-D collagen matrices containing 1 μM S1P for 22h. Cultures were fixed, stained with toluidine blue for morphometric analysis and analyzed for invasion density. Density (**A and B**:n=8 fields) of invading ECs are plotted as a function of WSS magnitude (means ±SD). * indicates the condition is significantly different from value at 12 dyn/cm^2 WSS (ANOVA followed by Student-Newman-Keuls post-hoc test; $P<0.01$).

WSS Enhanced EC Invasion Is Dependent on Shear Rate

The magnitude of WSS is proportional to the viscosity and shear rate of the flowing fluid. To determine whether S1P-induced EC invasion depends on the magnitude of shear stress or shear rate, we used perfusion media including 3% dextran to increase viscosity (Figs. 6, 7, and 8). ECs on collagen matrices containing S1P were exposed to perfusion media in the presence and absence of 3% dextran with the same shear rate. Holding viscosity constant (i.e., in the absence of dextran), an increase in shear rate (from 760 to 1710 s^{-1}) resulted in a decrease in S1P- and WSS-induced EC invasion. Holding shear rate constant, increasing shear stress by increasing the viscosity resulted in 1) absence of cell alignments in the flow direction (Fig. 6C vs 6B); and 2) increased invasion density (Fig. 7). Invasion depth did not vary significantly with a change in a condition, however lumen diameter decreased with increasing shear stress, but not increasing shear rate (Fig. 8). Thus, the response to changes in flow demonstrates a complicated dependence on both shear rate and shear stress.

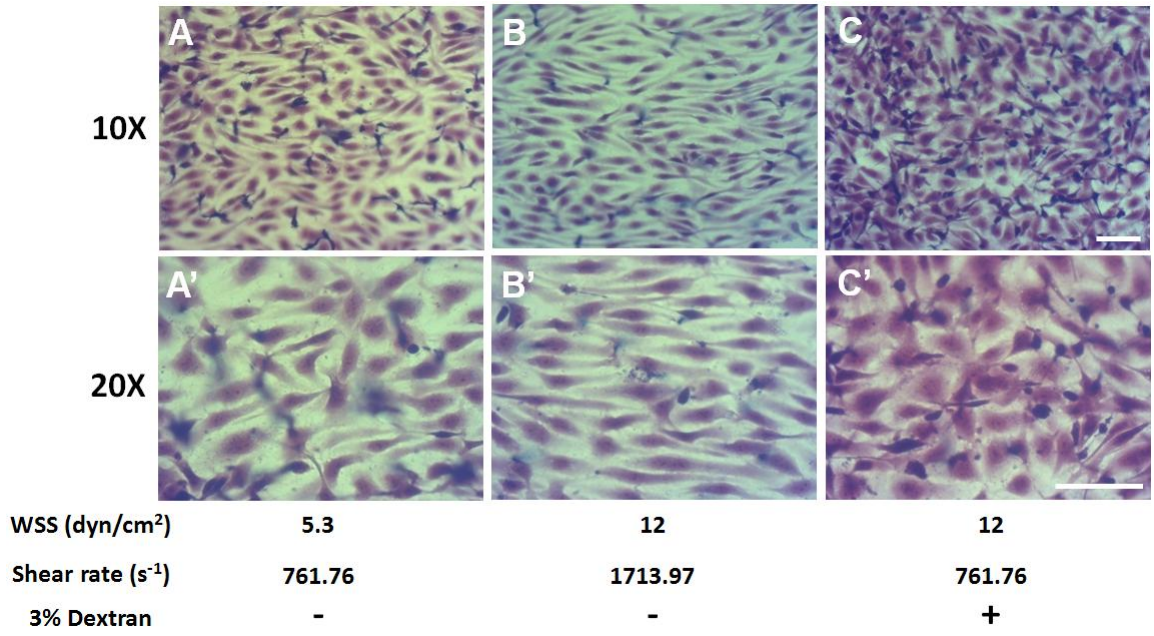

Figure 6. EC monolayer was not aligned in the direction of flow in the presence of perfusion media containing 3% dextran. *A-C'*: ECs were subjected to steady 5.3 and 12 dyn/cm^2 WSS for 24 h in the presence of perfusion media containing and lacking 3% dextran, fixed, and stained with toloudine blue for morphometric analysis. Representative cross-sectional micrographs are shown of en face preparations focusing on the EC monolayer with 10X **(*A–C*)** and 20X **(*A'–C'*)** for ECs subjected to WSS magnitudes of 5.3 **(A, A')**, and 12 dyn/cm^2 **(B,B',*C, C'*)**. Scale bar, 100 μm.

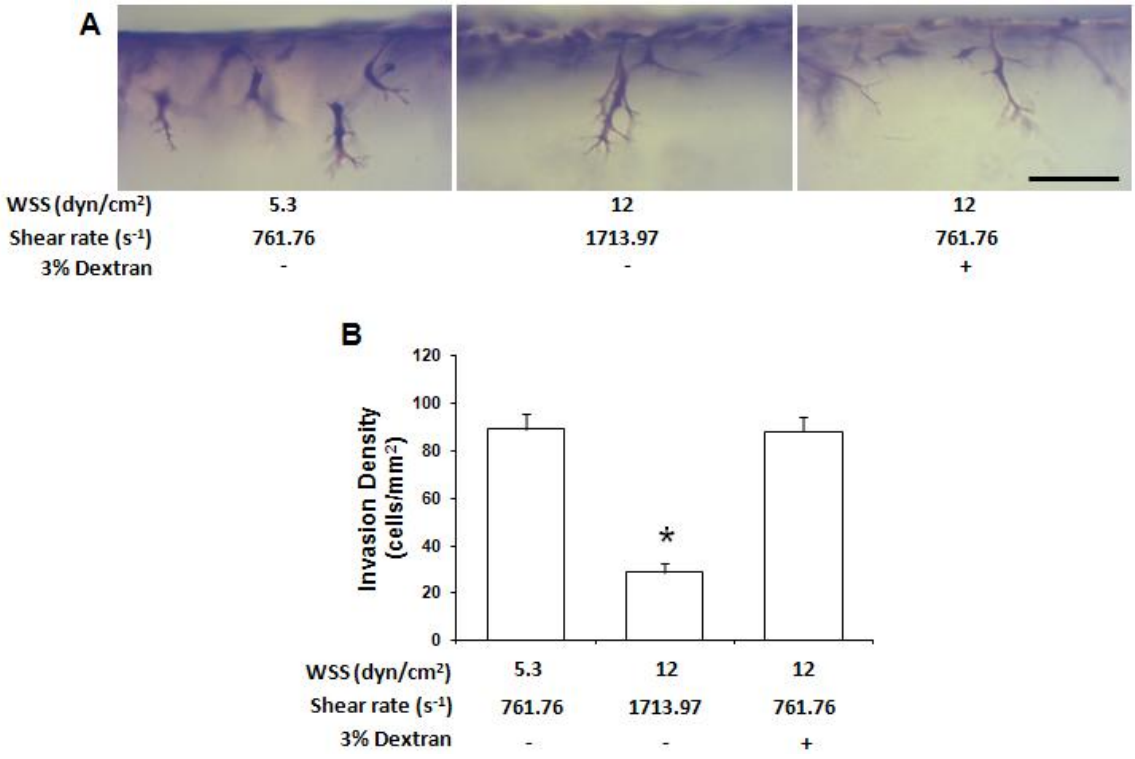

Figure 7. Invasion density is dependent on the shear rate. *A*: ECs were subjected to steady 5.3 and 12 dyn/cm^2 WSS in the presence of S1P, fixed, and stained with toloudine blue for morphometric analysis. Representative cross-sectional micrographs are shown of en face preparations focusing on the cross sections **(*A*)**. Invasion density (***B;*** *n* =12 fields) of invading ECs are plotted as a function of WSS magnitude (means ±SD). *Significant difference from value at 0.12 dyn/cm^2 WSS (P<0.05). Scale bar, 100 μm.

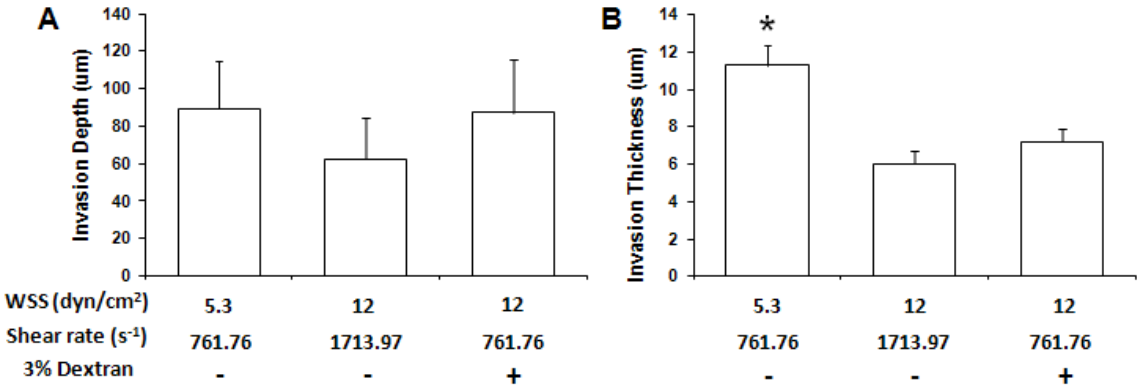

Figure 8. Invasion thickness is dependent on the magnitude of WSS. The invasion distance (***D***; *n* =116 sprouts) and width (***E***; *n* =80 fields) of invading ECs are plotted as a function of WSS magnitude (means ±SD). *Significant difference from value at 0.12 dyn/cm^2 WSS (P<0.05).

Discussion

Normally, ECs are maintained in a quiescent monolayer. However, under certain circumstances, ECs can be stimulated to escape from the monolayer and invade the underlying extracellular matrix to produce new vessels. In wound healing, for example, platelets from damaged blood vessels accumulate into the wound [94] where they can create a provisional matrix and release their abundant stores of proangiogenic factors including S1P, VEGF, and bFGF [95-97]. The high concentration of these factors in the wound stimulates EC invasion from nearby preexisting vessels and provides a directional cue for their migration toward the provisional matrix. We speculate that the WSS experienced by ECs in these neighboring vessels will modulate the extent of invasion and subsequent formation of new vessels. Specifically, our results support the notion that increasing WSS will enhance the rate of sprout growth; however, the invasion density will be diminished if the magnitude of WSS is too high. Thus, WSS may provide a negative feedback on the recruitment of new sprouts under conditions of high tissue perfusion (i.e., high WSS). In contrast, when tissue perfusion is inadequate (i.e., low to intermediate WSS), the enhanced recruitment of new vessels provides a mechanism to improve blood perfusion to wounded tissue.

In our experimental model, invasion requires the presence of S1P in the collagen matrix. We confirmed our previous result that bFGF and VEGF synergize with S1P to stimulate EC invasion into collagen matrices [4]. Importantly, we demonstrated that WSS is also a proangiogenic stimulus that can enhance the effects of S1P on EC

invasion. This is supported by the observation that WSS alone did not induce invasion, but WSS did enhance invasion in the presence of S1P to an extent comparable with angiogenic growth factor stimulation. Synergism between S1P, VEGF, and WSS has been observed in EC migration and proliferation in 2-D cultures. Specifically, Hughes et al. [85] showed that WSS and VEGF independently enhanced S1P-induced EC migration into a wound, and these effects were not further increased by combining WSS and VEGF. In their study, Hughes et al. [85] found that WSS or VEGF alone induced a greater degree of wound healing than S1P alone. In the present study, EC invasion was not observed when either VEGF/bFGF or WSS alone was applied. In our model, ECs require a directional cue for invasion into the matrix, which is provided by S1P incorporation in the collagen matrix. The VEGF and bFGF were added to the media and hence did not provide a concentration gradient directing cell migration into the matrix. Immobilization of VEGF and bFGF to collagen matrices via covalent binding has been shown to promote cell invasion [98]. It remains to be determined whether WSS enhances invasion of ECs into matrices containing immobilized growth factors in the absence of S1P. Our results show similarities to, as well as important differences from, previous studies that explored the role of WSS on angiogenesis responses in vitro. Cullen and colleagues [78] reported that subjecting bovine aortic ECs to WSS caused Transwell migration and tubule formation to increase monotonically with increasing WSS ranging from 0 to 20 dyn/cm^2. In these studies, Cullen et al. [78] applied WSS to bovine aortic ECs before placing them onto Transwell chambers to assay migration or onto 2-D Matrigels to measure tubule formation. In our experiment, where WSS was applied

during the 3-D invasion assay, invasion distance increased monotonically with increasing WSS; however, EC invasion density shows a bimodal dependence on WSS magnitude. It is possible that the inhibitory effect of high WSS observed in our study only occurs during the application of WSS and hence would not occur when ECs are presheared and then angiogenic assays are later performed under static conditions. Furthermore, the assays used to characterize angiogenic responses in their study are significantly different from those used in the present study. For example, migration through a Transwell filter would not require MMP activity, whereas migration through a collagen matrix does. Gloe and colleagues [77] presheared porcine aortic ECs with 16 dyn/cm^2 WSS for 6 h and demonstrated the formation of capillary-like structures after 24 h of static culture, which they attributed to shear-induced bFGF expression and secretion into the culture media. We were unable to stimulate invasion of ECs in a static system using conditioned media from WSS-treated invasion cultures, indicating the enhancement of invasion caused by WSS was not due to the generation of soluble proangiogenic factors. It is worth noting that these two studies [77, 78, 81]were performed using media containing 10–20% FBS or FCS. Given that FBS and FCS contain 141–180 nM S1P, and that the *K*d for S1P to its receptors is ~20 nM [87], the possibility exists that S1P receptor activation may have contributed to the angiogenic events observed in these studies. The 3-D model utilized in these studies provides a realistic environment to study angiogenic sprouting events and observe the complex interactions between invading cells and their surrounding matrix protein network. Importantly, these studies are carried out in collagen type I, the most abundant

extracellular matrix protein encountered by ECs during sprout formation. Ueda et al. [81] developed the first perfusion chamber containing a 3-D collagen matrix, allowing simultaneous application of WSS and observation of angiogenic events. They demonstrated that the extent of EC network formation from invading cells is enhanced in the presence of 3 dyn/cm^2 WSS [81], which is within the range of WSS for maximal invasion in our study (3 to 5 dyn/cm^2). The networks generated in their study did not extend more than 50 μm beneath the monolayer but rather extended parallel to the matrix surface. In our system, the ECs did not form shallow networks but rather migrated predominantly orthogonal to the monolayer surface to depths >100 μm. In this study, S1P was incorporated in the collagen matrix and resulted in the ECs migrating orthogonal to the monolayer in a manner that more closely represents the morphology of sprouting ECs in vivo.

It is intriguing that invasion distance and density show different dependencies on WSS magnitude (cf. Figs. 4, *D* and *E*). It is well established that low and high WSS have distinct effects on cell signaling, migration, morphology, proliferation, and apoptosis in ECs cultured in 2-D culture [89, 99, 100]. This is the first study to investigate the effects of different WSS magnitudes on EC invasion into 3-D matrices. WSS levels of 5.3 and 12 dyn/cm^2 induced similar levels of Ki-67 staining and caspase-3 cleavage. Thus, other mechanisms unrelated to cell proliferation and apoptosis are involved in regulating the sensitivity of invasion to the magnitude of WSS. Recently, Venkataraman et al. [101] reported data supporting a role for ECs in maintaining plasma levels of S1P. Furthermore, these authors demonstrated that 15 dyn/cm^2 WSS increased the secretion

of S1P from cultured ECs with concomitant upregulation of sphingosine kinase expression and downregulation of the expressions of sphingosine lyase and sphingosine phosphatase. With the consideration of the results of this new report and the present study, it appears that WSS regulates both the generation of S1P as well as the ability of S1P to induce EC invasion. The role of WSS-induced S1P generation in our system may not be critical in our system due to the high concentration present in the matrix; however, such localized S1P generation may be important in regulating EC invasion *in vivo*. Although flow has long been recognized as a regulator of angiogenesis [102], few studies have directly evaluated the role of flow-induced WSS on angiogenesis *in vivo*. Nasu et al. [75] studied the growth and flow rate distribution of microvessels in tumors and concluded their observations indicated that vessel growth in tumors depends more on local hemodynamics than on vascular growth factors. Typical WSS magnitudes in the microvasculature are reported to be in the range of 5 to 150 dyn/cm^2 [103, 104]; however, WSS levels in postcapillary venules in mouse cremaster muscle have been estimated to be in the range of 1 to 5 dyn/cm^2 [105]. Ichioka et al. [74] measured changes in blood flow and vascular growth in response to long-term administration of the vasodilator prazosin in a rabbit ear chamber. They estimated that WSS in postcapillary venules increased from 3.7 to 5.3 dyn/cm^2, and this coincided with an increase in the rate of tissue vascularization within the chamber [74]. Our results support the finding that increasing WSS within the range of 3 to 5.3 dyn/cm^2 enhances the angiogenic response. This optimal WSS was also observed when testing additional EC microvascular cell lines HDMVECs and HRMVECs (cf. Fig. 8). It is important to note

that sprouting angiogenesis is primarily localized to postcapillary venules, which under quiescent conditions are exposed to relatively lower WSS than blood vessels in other areas of the vasculature.

In our experimental model, EC invasion was dependent on the magnitude of WSS in the only perfusion media with the same viscosity. However, WSS is the product of fluid viscosity and shear rate. Our results indicate that shear rate rather than wall shear stress appeared to regulate S1P-induced EC invasion. WSS is the shearing force exerted by flow over the EC surface and can modulate many signal transduction pathways mediated by mechano-sensor molecules [106, 107]. On the other hand, shear rate can modulate the diffusional accumulation of vasoactive agonists like ATP to the cell surface, which are known to induce a Ca^{2+} response in cells. In mathematical models, the ATP concentration at the EC surface increases with the magnitude of applied shear stress [108-111].

In experimental model, Choi el al. [112] reported that the ATP concentration at the EC surface increases at higher shear stress (40 dyn/cm^2) rather than low shear stress (5 dyn/cm^2) progressely in the longitudinal direction using a backward facing step chamber. Flow-induced Ca^{2+} transient in cultured ECs is dominantly influenced by ATP concentration in the perfusing medium [113, 114]. Nollert el al. [109] demonstrated that the ATP concentration is determined by a balance between the convective transport of fresh ATP from upstream and the degradation of ATP at the ECs surface in a parallel plate flow system. Ando et al. also reported that cytoplasmic Ca^{2+} responses in ECs were increased by increasing flow rate and the regulated by WSS but not by shear rate. Importantly, cytoplasmic Ca^{2+} responses were increased and saturated after 5 dyn/cm^2 WSS. These data suggest that high shear rate over 5 dyn/cm^2 WSS may induce similar high cytoplasmic Ca^{2+} responses in our system. However, it is intriguing why EC invasion density is high at 5.3 dyn/cm^2 WSS and low at 12 dyn/cm^2 WSS. We hypothesized that downstream signaling pathways due to WSS may play a crucial role in S1P- induced EC invasion, which we address in the next chapters.

CHAPTER III

FLUID SHEAR STRESS AND SPHINGOSINE 1–PHOSPHATE ACTIVATE CALPAIN AND AKT TO PROMOTE MT1-MMP MEMBRANE TRANSLOCATION AND ENDOTHELIAL CELL INVASION *

Overview

Our results from Chapter II indicate that S1P and WSS cooperatively initiate EC invasion into 3-D collagen matrices [84]. In this chapter, we defined the signaling pathways activated during EC invasion in response to S1P and WSS. We investigate whether calpain controlled Akt and MT1-MMP, because these molecules have been demonstrated by others to regulate angiogenesis, yet a hierarchical signaling pathway where calpain regulated downstream activation of Akt, and MT1-MMP has not been demonstrated. S1P synergized with 5.3 dyn/cm^2 WSS and stimulated maximal calpain, Akt, and MT1-MMP activation, resulting in high levels of EC invasion. Our data indicate the combination of S1P and 5.3 dyn/cm^2 WSS activated calpains, which phosphorylated Akt and directed MT1-MMP membrane localization to initiate angiogenic sprouting responses in ECs.

*This manuscript has been submitted to the *Journal of Biological Chemistry.*

Introduction

Biochemical and Mechanical Stimuli Promote Angiogenesis and Vascular Remodeling

Pro-angiogenic factors such as S1P, VEGF, and bFGF, are potent stimulators of new blood vessel growth [5, 115-117]. Blood flow, like biochemical factors, is a strong regulator of vascular development and remodeling. Dickinson and colleagues demonstrated that fluid shear stress is crucial for normal vascular remodeling during development [23]. In Chapter II, we reported that 5.3 dyn/cm^2 WSS acted synergistically with S1P to stimulate robust endothelial sprouting responses [84]. While biochemical signals that stimulate angiogenesis are well-studied, signals downstream that integrate biochemical and hemodynamic signals to control new blood vessel growth are not completely defined. In this chapter, we take advantage of the 3-D EC invasion system to more completely understand the combined influence of WSS and S1P on the initiation of sprouting angiogenesis, where ECs transition from a quiescent to an invading phenotype.

Calpain Is a Plausible Candidate for Regulating the Transition From the Quiescent to Invasive Phenotype

Various exogenous stimuli activate calpains, including WSS [76, 118] and VEGF [119]. Calpains are intracellular calcium-activated cysteine proteases that function to regulate migration by cleaving talin, vinculin, paxillin, focal adhesion kinase and cortactin [120-122]. Calpain inhibitors block endothelial alignment in response to shear stress [123]. Calpain antagonists also block bFGF-induced corneal angiogenesis [124] and matrigel-induced angiogenesis *in vivo* that was attributed to VEGF induction of calpain 2 in lung endothelial cells [119]. Calpains are required for cell membrane release during cell spreading [121, 125, 126] and mediate membrane protrusion and cell movement in 2-D systems [127-130]. Thus, calpain activity is modulated in ECs by growth factors and mechanical stimuli, which support a role for calpain in initiating angiogenic sprouting events. These data have prompted us to investigate a functional requirement for calpain in initiating endothelial sprouting events induced by WSS and S1P in 3-D collagen matrices. Importantly, the molecular events downstream of calpain activation that initiate angiogenesis are poorly understood.

S1P- or WSS- Stimulated Akt Phosphorylation Plays a Key Role During EC Invasion

The serine/threonine kinase Akt is a central regulator of cell survival, migration, metabolism, and tube formation [32, 131]. A role for Akt has also been demonstrated during EC sprouting *in vitro* and angiogenesis *in vivo* [34]. The average length of sprouts was significantly reduced in Akt1 knockout mice compared to wild-type mice in an *ex vivo* aortic ring invasion assay [33]. Since Akt plays a crucial role in ECs, we investigate whether Akt is required for S1P- and WSS-induced EC invasion in 3D collagen matrices. In addition, it is well known that Akt is phosphorylated by S1P, VEGF, and WSS. The effects of VEGF and S1P on EC migration and tubulogenesis *in vitro* have been shown in separate studies to be dependent on Akt activity [132-134]. Activation of $S1P_1$ receptors in ECs has been reported to stimulate the activation of Akt via pertussis toxin-sensitive G proteins [135, 136]. Dimmler et al. [137] demonstrated that Akt phosphorylation increases monotonically with increasing WSS in the range of 0 to 45 dyn/cm^2 in 2-D cultures. In addition, both S1P and WSS induce dose-dependent Akt phosphorylation [138, 139]. Akt has several downstream targets implicated in angiogenesis, including endothelial nitric oxide synthase (eNOS) [138], hypoxia-inducible factor [140], and the transcription factor FOXO [141]. This study is the first to define the role of Akt in S1P- and WSS-induced EC invasion in 3D collagen matrices and demonstrate a new molecular pathway as a downstream of calpain or upstream of MT1-MMP.

MT1-MMP activation Is a Key Event in Angiogenic Sprouting and Invasion Events

Membrane-type matrix metalloproteinases (MT-MMPs) function alongside integrins and growth factors to direct angiogenic sprouting and lumen formation [48, 142-147]. Mice lacking MT1-MMP have developmental delays, a reduced lifespan and defective angiogenic sprouting responses [48, 148, 149]. The MT1-MMP cytoplasmic tail is phosphorylated by Src to regulate proteolytic activity and membrane localization [150], and S1P stimulates translocation of MT1-MMP to the membrane [151]. MT1-MMP is clearly required for vessel outgrowth and lumen formation [48, 142, 144, 145], but the intracellular molecular events that control MT1-MMP activation and membrane translocation following pro-angiogenic stimulation of EC are incompletely defined. Here, we investigated whether calpain activation acts upstream of pro-angiogenic factor-induced MT1-MMP membrane translocation and activation. We demonstrate for the first time an ability of calpain to regulate MT1-MMP in endothelial cells following activation by S1P and WSS.

Materials and methods

Gene Silencing Using ShRNA

Short hairpin RNA constructs were purchased from Sigma-Aldrich and prepared from glycerol stocks for calpain 1 (SHCLNG-NM_005186), calpain 2 (SHCLNG-NM_007148) and beta 2 microglobulin (SHCLNG-NM_004048). Lentiviruses were generated as described [152] using 1.5 μg of backbone Lentiplasmid, 4.5 μg of VIRAPOWER packaging mix (Invitrogen) and 12 μl lipofectamine 2000 into 100% confluent 293FT cells in T25 flask. Viral supernatants were harvested at 48h from 293FT cells at 48 h, passed through 0.45 μm filter (Millipore) using 10 ml syringe, incubated with 1 x 10^6 HUVECs at passage 3 and then added polybrene (12 μg/ml). HUVECs were changed fresh growth medium after 4h and 72h. ECs expressing shRNA were selected with puromycin (0.2 μg/ml) for two weeks prior to placing in invasion assays. Successful expression of mutant genes and protein silencing was confirmed by Western blot analysis.

Generation of a TIMP-1 Lentivirus

TIMP-1 was amplified from HUVECs cDNA generated in the laboratory and inserted into the pIEX-5 vector (Novagen) to generate a C-terminal S- and His-Tag. Inserts were cloned into pENTR4 vector (Invitrogen). Positive clones were recombined with the pLenti6/V5-Dest vector (Invitrogen) using the GATEWAY system according to manufacturer's instructions. For lentiviral production, the 293FT packaging cell

monolayers were seeded into two 25cm^2 flasks at 40-50% confluency. A TIMP-1 lentivirus was generated by combining 4µg of the pLenti6/V5 backbone vector with 12ug of VIRAPOWER packaging plasmid and 20µl lipofectamine 2000 into 293FT cells of two flasks. Media were changed 12-16h later. One 293FT supernatant was harvested at 48 h after transfection, centrifuged at 300xg for 5 min and incubated with 0.4x10^6 HUVECs in the presence of 12µg/ml Polybrene (Sigma). This procedure was repeated with the other 293 FT supernatant after 24h. Media were changed with growth media 72 h later after viral transduction. Cells were used for collagen matrix invasion assay 24h later. Successful gene transduction was monitored by Western blot analysis using antisera directed to the S-Tag epitope.

Inhibition Experiments

Wortmannin and GM6001 (EMD Biosciences) were dissolved in DMSO at 10 nM and 500 nM concentrations, respectively. ECs were preincubated with wortmannin (10 nM) or GM-6001 (500 nM) for 60 min during attachment to collagen matrices before shear stress exposure, and this was maintained throughout the application of WSS for 24h. Global (10 µM) was dissolved in ethanol; calpain inhibitor III (50 µM) and IV (31.6 µM) were dissolved in DMSO. Calpastatin human Recombinant Domain I and E64 were dissolved in M199 at 100 nM and 1µM concentrations, respectively. All inhibitors were obtained from Calbiochem. EGTA (200 mM) was dissolved in distilled water and then diluted 1:100 in M199. ECs were exposed to calpain inhibitors with shear stress exposure and maintained throughout the application of WSS for 18h. To subject ECs to

WSS magnitudes of 5.3 dyn/cm^2 in the presence of control or each inhibitor, two flow systems were run simultaneously. Each flow system contained two or three identical parallel-plate flow chambers (i.e. identical channel dimensions). ECs were exposed to inhibitors with shear stress exposure and maintained throughout the application of WSS for 18h. To subject ECs to WSS magnitudes of 5.3 dyn/cm^2 in the presence of control or each inhibitor, two flow systems were run simultaneously. Each flow system contained two or three identical parallel-plate flow chambers constructed to have identical channel dimensions and arranged in random and order.

Gelatin Zymography

To subject ECs to WSS magnitudes of 0.12, 5.3, and 12 dyn/cm^2, three flow systems were run simultaneously. Each flow system contained two identical parallel-plate flow chambers (i.e., identical channel dimensions) arranged in series. Conditioned media (4ml) were sampled from the reservoir at the time points indicated, centrifuged at 500g for 5 min, and frozen at -80°C. Aliquots of conditioned medium were concentrated ~10-fold using a Centricon centrifugal filter unit containing an Ultracel YM-10 membrane (Millipore) at 5000 rpm in a Beckman J2-21M centrifuge at 4°C. The concentrated media (30 μl) were prepared under non-reducing conditions and loaded in 8.5% acrylamide gels containing a final concentration of 1 mg/ml porcine gelatin. Following electrophoresis, the gels were rinsed 3 times in 100 ml of 2% Triton X-100 in water for 1 h and rinsed twice in distilled water before being placed in 25 mM Tris–HCl (pH 7.5) containing 5 mM $CaCl_2$ overnight at room temperature. The gels were stained

with 0.1% Amido Black in 30% methanol and 10% acetic acid for 15 min at room temperature and destained in 30% methanol and 10% acetic acid before image collection and analysis.

MT1-MMP Activation Assay

We used TIMP-1 cells to measure only MT1-MMP activity because TIMP-1 cells do not express any soluble MMPs. TIMP-1 cells were cultured in growth media with blast (1/1000) every 3 days and fed without blast 24h prior to beginning experiments. Other flasks containing confluent TIMP-1 cells were washed with only M199 twice and then fed with M199 and RSII (1/250) for 24h. After 24h, the culture media from flasks were collected and centrifuged at 350 Xg for 4 min. Supernatant were harvested and used for shear stress experiments. The cells were fed with growth media and blast (1/10000) again until they are confluent. MT1-MMP activity was measured using SensoLyte^{TM} 520 MMP-14 assay kit (Anaspec). The collagen matrices containing ECs were homogenized in assay buffer (Component D) containing 0.1% (v/v) Triton-X 100 at 4ºC for 10 min, vortexed every 5 min and then centrifuged for 10 min at 12,000 Xg, 4ºC for 10 min. The supernatant were collected and stored at -80°C until use. Assay buffer and MMP-14 substrate (Component A) were warmed to room temperature until thawed before setting up enzymatic reaction. MMP-14 substrate was diluted 1:100 in assay buffer and then added to the supernatant. The reagents were mixed gently, added to 96-well plate and measured fluorescence intensity at Ex/Em=490nm±20/520±20 nm

and continuously record data every 5 min for 60 min. Experiments are performed three times in triplicate wells. Average values are recorded, plotted with standard deviation.

Calpain Activity Assay

Calpain activity was measured using Calpain-Glo^{TM} protease assay kit (Promega). The collagen matrices containing ECs were collected and incubated in extraction buffer containing 0.9% Trinton X-100, 0.1M phenylmethylsulfonyl fluoride (PMSF) 1/100, 20 μg/ml Aprotinin in 1X PBS at 4ºC for 10 min,. The samples were vortexed every 5 min and then centrifuged for 10 min at 12,000 Xg, 4ºC for 10 min. The supernatant were collected and stored at -80°C until use. Assay buffer (Luciferin Detection Reagent and Calpain-Glo^{TM} Buffer) and an aliquot of Suc-LLVY-GloTM substrate were warmed to room temperature until thawed before setting up enzymatic reaction. This substrate was diluted 1:100 in assay buffer and then added to the supernatant. The reagents were mixed gently, added to 96-well plate and measured luminescence on a luminometer (Wallac 1420 Multilabel Counter from PerkinElmer Life Sciences). Experiments are performed three times in triplicate wells. Average values are recorded, plotted with standard deviation.

Western Blots

To subject ECs to WSS magnitudes of 0.12, 5.3, and 12 dyn/cm^2, three flow systems were run simultaneously with each flow system containing two identical parallel-plate flow chambers arranged in series; individual chambers were removed at

various times. The collagen matrices containing invading ECs were washed briefly with PBS before being placed directing into preheated (100ºC) 1.5X Laemmli sample buffer (15% glycerol, 3.45% SDS, 371 mM Tris (pH 6.8), 0.0013% Bromphenol Blue). The lysed cells were boiled for 10 min, incubated on ice for 5 min and frozen at -20°C. Proteins were loaded onto 10% SDS-polyacrylamide gels and transferred to polyvinylidene fluoride membranes (Fisher Scientific). After blocking in 5% non-fat dry milk at room temperature for 1 h, the membranes were incubated with monoclonal GAPDH (1:10000, Research Diagnostics, Inc., Flanders, NJ), vimentin (1:5000, Santa cruz biotechnology), polyclonal calpain-1 and -2 (1:2000, abcam) at room temperature for 3 h. In addition, membranes were incubated with monoclonal rabbit anti-phospho-Akt (Ser473) primary antibody (1:1000, Cell Signaling) at 4°C overnight in Tris-Tween-20 saline containing 5% BSA to detect phosphorylated Akt. The membranes were warmed to room temperature for 30 min and washed three times in Tris-Tween-20 saline before incubation with goat anti-rabbit secondary antibody and rabbit anti-mouse secondary antibody (1:5000, DAKO USA) in Tris-Tween-20 saline containing 5% milk for 1 h. The same Western blotting procedure was used with anti-Akt primary antibody (1:5000, Cell Signaling) to verify equal loading between samples or polyclonal antisera to cleaved caspase-3 fragments (Asp 175) primary antibody (1:1000, Cell Signaling Technologies) to quantify apoptosis. Immunoreactive proteins were visualized and developed using the enhanced chemiluminescence system (Millipore) and then the membranes were exposed to films (Denville Scientific Inc., Metuchen, NJ).

Image Analysis and Quantification

Images of the western blots were scanned using an HP photosmart C4280 desktop scanner and polyacrylamide gels from gelatin zymograms were scanned with a FluorChem 8900 digital imaging system (Alpha Innotech San Leandro, CA). The band intensities were measured using Image J analysis software (NIH). Akt phosphorylation was expressed as the ratio of phosphorylated Akt to total Akt protein. Akt phosphorylation was normalized relative to the level of the static control at 0 h. The band intensities for active MMP-2 and MMP-2 pro-peptide (pro-MMP-2) were expressed relative to their maximal values.

Immunofluorescence

Coverslips and collagen matrices will be fixed in freshly prepared 4% paraformaldehyde in PBS for 10 min. Each will be blocked in Tris/Glycine buffer (0.3% Tris, 1.5% Glycine) for 1 h, followed by permeabilization with 0.5% Triton X-100 in PBS for 30 min with gentle agitation. Samples will be blocked in buffer containing 0.5% TX-100, 1% BSA, and 1% serum that is appropriate for Alexa-conjugated secondary antibodies (Molecular Probes) overnight at 4°C. Primary antibodies will be added in blocking buffer (1:50) for 3h at room temperature. We used several primary antibodies, such as monoclonal Vimentin antibodies (1:500, Santa Cruz Biotechnology), Vinculin antibodies (1:100, Sigma), polyclonal calpain-1 and -2 (1:300, abcam) or VE-cadherin antibodies (1:100, Alexis biochemicals). After washing (15 min for coverslips, 1h for collagen gels) in 0.1% TX-100 in PBS, secondary antibodies will be added in BSA-containing buffer for 1h (coverslips) or 2h (collagen gels). After washing, samples

will be mounted and imaged from the side using a Nikon ECLIPSE fluorescent microscope equipped with appropriate filters or performed at the Texas A&M Image Analysis Laboratory [3].

Transfection

Before transfection, glass microscope slides (75 x 50 x 1mm) were coated with collagen type I (20 μg/ml) for 30 min. For allowing DNA-liposome complexes formation, Plasmid DNA (6μg) expressing MT1-MMP, calpain 1 or calpain 2 fused to green fluorescent protein (GFP) and 12μl Lipofectamine 2000 (Invitrogen) were diluted separately in 500μl of OPTI-MEM (Invitrogen) for 5 min and then were mixed gently and incubated at room temperature for 20 min. During incubation, the cells were rinsed twice with 14ml PBS and removed with 2ml of 0.25% trypsin-EDTA (Invitrogen) at 37°C for 1 min. The trypsin was neutralized with 2ml FBS. Cells were resuspended in 3ml DMEM with 20% FBS and then 1ml of them was added into the mixed plasmid DNA and Lipofectamine reagent. The Cells were seeded onto the glass microscope slide for 2 h, placed to culture medium without antibiotic for 24 h. The next day, cells were treated with various combinations of WSS and S1P as indicated. Cells were fixed and imaged. To quantify MT1-MMP-GFP localization to the cell periphery, outlined section of cells were manually traced in Adobe Photoshop and the pixel intensity inside a 10-pixel-wide outline of the cell was quantified in Image J. To avoid measuring fluorescent intensity from perinuclear staining, any perinuclear staining that entered the outline was excluded from the analysis. The cell fluorescent intensity histogram was normalized by

setting the darkest cytoplasmic region in the cell to a pixel intensity of zero. The extent of MT1-MMP-GFP localization to the cell periphery was defined as the average pixel intensity within the analysis region. The quantification of MT1-MMP-GFP localization to the cell periphery was measured from three individual experiments (n=25 cells).

Membrane Fractionation

Cells were seeded on glass slides overnight and treated with or without 1 μM S1P for 1 h prior to the application of the indicated levels of shear stress for an additional 2 h. Membrane fractions were prepared by incubating the cells in lysis buffer [20mM HEPES, pH 7.4, 20mM NaCl, 1.5mM $MgCl_2$, 250mM sucrose, 1mM EDTA, 2mM phenylmethylsulfonyl fluoride, and Complete Protease Inhibitor Cocktail (Roche Diagnostics)]. Lysates were passed through a 27G needle 10 times using a 1mL syringe and kept on ice for 20 min. After homogenization, lysates were centrifuged at 1,000xg for 5 min at 4°C to remove unbroken cells. The supernatant was removed and centrifuged at 150,000xg for 30 min at 4°C in a TL-100 Ultracentrifuge (Beckman Instruments). The resulting supernatants corresponded to cytoplasmic fractions. Pellets were resuspended in lysis buffer containing 0.5% NP-40 and corresponded to membrane fractions.

Results

Calpains Are Required for S1P- and WSS-Induced EC Invasion in 3-D Collagen Matrices

Calpain 1 (μ-calpain) and calpain 2 (m-calpain) are the two major isoforms of calpain. Pharmacological inhibitors of calpains were used to demonstrate a functional requirement for calpains in EC invasion. ECs were stimulated with S1P and 5.3 dyn/cm^2 WSS in the presence of global calpain inhibitor, calpain inhibitor IV, and calpain inhibitor III for comparison to untreated controls (Fig. 9A). Each of these calpain inhibitors is cell-permeable and block both calpain I and II. Specially, global calpain inhibitor also blocks cathepsin B and cathepsin L. Calpain inhibitor IV inhibits cathepsin L and is an irreversible inhibitor of calpain II. Photographs of invading structures are shown in Figure 9B. Invasion responses were noticeably impaired in the presence of the global calpain inhibitor, calpain inhibitor IV and III. These findings support that calpains are required for EC invasion responses. To confirm the results obtained using these pharmacological inhibitors, gene silencing studies using recombinant lentiviruses delivering shRNA directed against calpain 1 (shCalp1), calpain 2 (shCalp2) were also performed. As controls, cells were left untreated (Control) or treated with shRNA directed against beta 2 microglobulin control (shβ2M). A side view of invasion responses is shown in Figure 10A and quantification of invading EC density are summarized in Figure 10B. Consistent with the results obtained using calpain inhibitors, both shCalp1 and shCalp2 treatment blocked invasion responses (Fig. 10B). In all

experiments, shβ2M control invaded to a comparable extent to control non-transfected cells. Selective knockdown of the appropriate calpain isoform with each shRNA was confirmed by Western blot analyses (Fig. 10C) and quantified by the densitometric analysis in Figure 10D. Multiple shRNA sequences that targeted calpain 1 and calpain 2 were delivered to the ECs to rule out off-target effects of RNA silencing treatments (Figure 11). These support the hypothesis that both calpain isoforms are required for S1P and WSS-induced EC invasion in 3-D collagen matrices.

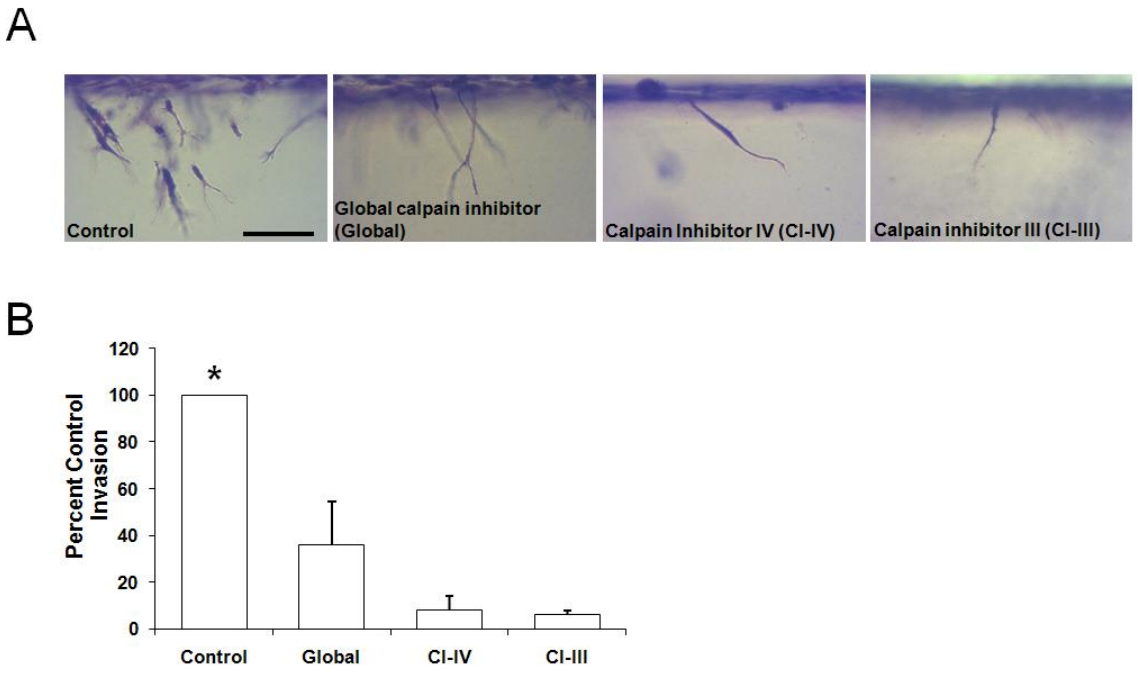

Figure. 9. Calpain inhibitors inhibited S1P and WSS-induced EC invasion. ***A:*** ECs were seeded on collagen matrices containing 1μM S1P and treated with 5.3 dyn/cm^2 WSS with vehicle, 10μM Global, 31.6 μM calpain inhibitor IV, or 50 μM calpain inhibitor III for 18 h. Cultures were fixed and stained to quantify the number of cells invading per field. Inhibitors were tested in three individual experiments (mean ± SD, n = 18 fields) and data were normalized to control values. Representative cross-sectional micrographs are shown for ECs left untreated control, 10μM Global, 31.6 μM calpain inhibitor IV, or 50 μM calpain inhibitor III for 18 h. The invasion densities quantified for each condition from three individual experiments are summarized (B: mean±S.D. * ANOVA and multiple comparison testing indicates a significant difference from control and shβ2M ($P<0.05$). Scale bar, 100μm.

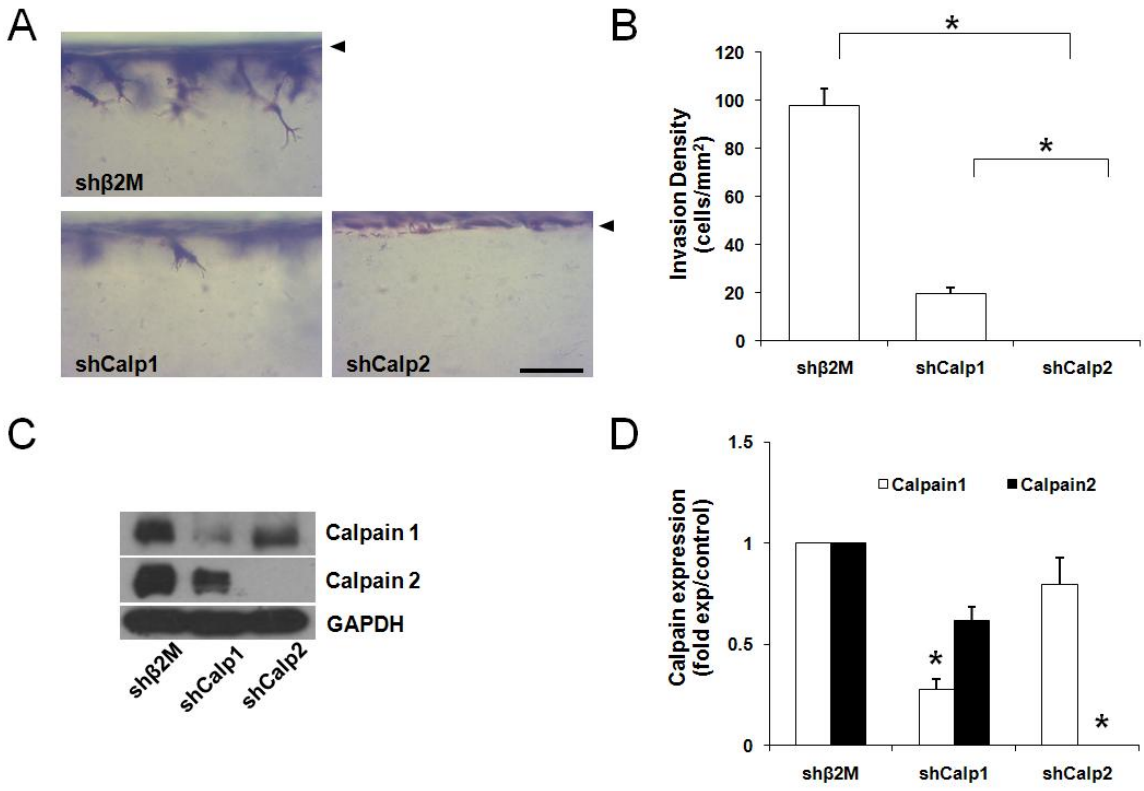

Figure. 10. Calpains are required for EC invasion induced by combined WSS and S1P stimuli. ***A and B*****:** ECs transduced with lentiviruses delivering shRNA directed to beta 2 microglobulin (shβ2M), calpain 1 (shCalp1) or calpain 2 (shCalp2) were stimulated with 1μM S1P and 5.3 dyn/cm^2 WSS for 24h. Cultures were fixed and stained (**A**) and the invasion densities quantified for each condition from five individual experiments are summarized (**B**; mean ± SD, n = 21 fields). ***C*****:** Culture extracts were immunoblotted with antibodies against calpain 1, 2 and GAPDH. Each blot is representative of 3 independent experiments. D**:** The invasion densities quantified for each condition from three individual experiments and the blots quantified by densitometric analysis from 3 independent experiments are summarized (B and D: mean±S.D). * ANOVA and multiple comparison testing indicates a significant difference from control and shβ2M ($P<0.05$). Scale bar, 100μm.

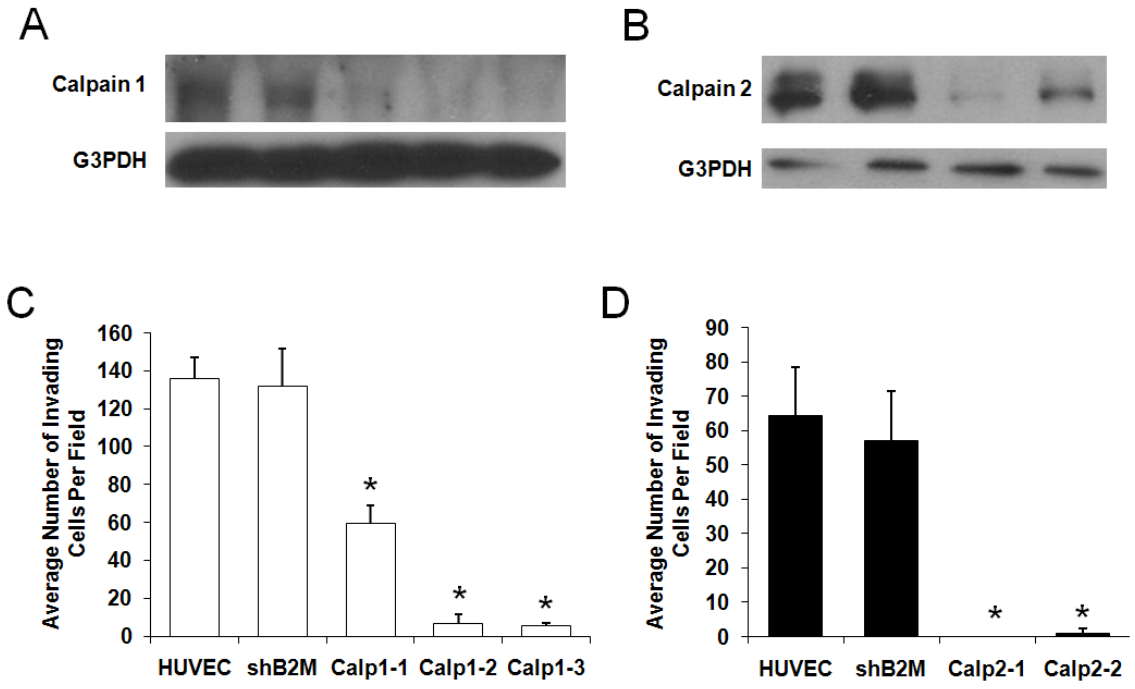

Figure. 11. Calpain 1 and 2 knockdown significantly reduced S1P and 5.3 dyn/cm^2 WSS induced EC invasion. ECs were non-transfected (HUVEC) or transduced with lentiviruses delivering shRNA directed to beta 2 microglobulin (shβ2M; negative control), multiple calpain 1 and 2 shRNA sequences to successful reduced or blocked invading structures. ***A and B*:** Western blot analyses confirm successful knockdown of multiple calpain 1 and 2. ***C and D*:** Untreated ECs (HUVEC) and ECs transduced with lentiviruses delivering shRNA directed to shβ2M, multiple shCalp1 or shCalp2 were stimulated with 1μM S1P and 5.3 dyn/cm^2 WSS for 24h. Cultures were fixed and stained and the invasion densities quantified for each condition from three individual experiments are summarized (mean ± SD). * ANOVA and multiple comparison testing indicates a significant difference from HUVEC and shβ2M ($P<0.05$).

Calpains Are Activated During S1P-and WSS-Induced Invasion

To determine whether S1P and/or WSS activates calpain, ECs cultured on 3-D collagen matrices containing or lacking S1P (1 μM) were treated with or without WSS (5.3 dyn/cm^2) for 6 h (Fig. 12). WSS applied alone significantly increased calpain activation compared to untreated ECs and ECs treated with S1P alone (Fig. 12A). In addition, combined S1P and WSS treatment induced even greater calpain activation. The extent of cell invasion was also highest following combined treatment with S1P and 5.3 dyn/cm^2 WSS (Fig. 12C), which is consistent with our previous report [84]. Thus, S1P synergized with 5.3 dyn/cm^2 WSS to activate calpain activation. We next determined the effect of the magnitude of WSS on calpain activation in 3-D collagen matrices containing S1P (Fig. 12B). 5.3 dyn/cm^2 WSS induced significantly higher calpain activation compared to 0.12 and 12 dyn/cm^2 WSS. In addition, S1P combined with 5.3 dyn/cm^2 WSS and more effectively induced invasion than 0.12 and 12 dyn/cm^2 WSS (Fig. 12D). We next determined whether S1P- or WSS- induced calpain activation corresponded with the protein amounts of calpains and calpastatin. ECs seeded onto 3-D collagen matrices were pretreated with or without 1μM S1P for 1h and then exposed to static conditions or 5.3 dyn/cm^2 WSS for 6h (Fig. 13). The protein amounts of calpains and calpastatin decreased with a time, but were not significantly changed by WSS and/or S1P application. These results demonstrate calpain is a critical component of successful invasion in response to WSS and S1P, but that overall calpain activation levels do not completely explain the changes in invasion responses (data not shown).

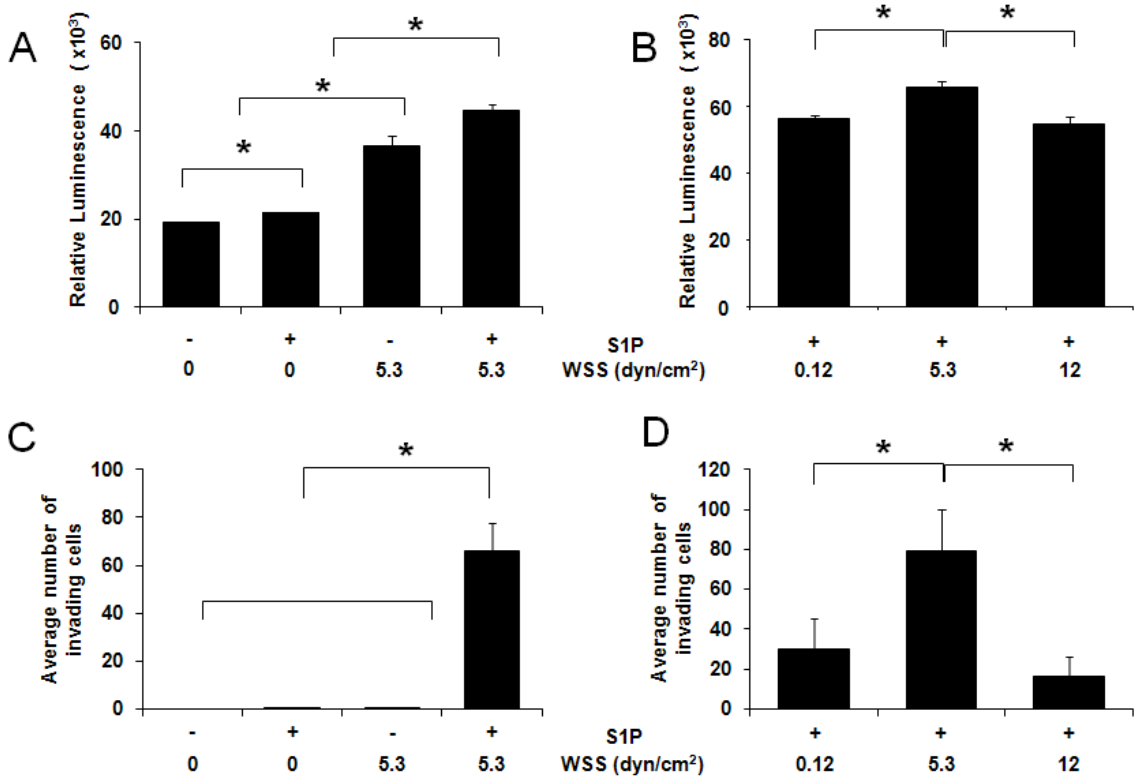

Figure. 12. S1P and WSS synergistically activate calpains. ECs on collagen matrices were subjected to the indicated magnitudes of WSS in the absence or presence of S1P for 6h. The cultures were then either lysed to measure calpain activity (***A*** and ***B***) or stained and imaged to quantify the average number of invading cells (***C*** and ***D***). As described in MATERIALS AND METHODS, calpain activation was measured as luminescent intensity (mean±SD; n=3) using the Calpain-Glo™ protease assay kit. Western blot analyses were performed with antibodies directed to GAPDH to verify equal loading between samples (not shown). Each data point was derived by averaging three individual wells from three individual experiments. Invasion responses were measured after 18h of treatment. * ANOVA and multiple comparison testing indicates a significant difference between groups ($P<0.05$).

S1P and 5.3 dyn/cm^2 Preferentially Regulate Calpain Membrane Localization

Calpain activation is often associated with translocation to the membrane and is facilitated by hydrophobic interactions with the lipid bilayer [153, 154]. Since alterations in calpain activation levels did not exclusively explain invasion responses (cf. Fig. 12), we next determined whether calpain 1 or 2 are translocated to the membrane by S1P and 5.3 dyn/cm^2. ECs were treated with nothing (control), 5.3 dyn/cm^2 WSS alone, S1P alone, or S1P together with 5.3 dyn/cm^2 WSS. Following each treatment, membrane fractions were isolated and analyzed for calpain 1 or 2 levels (Fig. 13). Combined treatment with S1P and 5.3 dyn/cm^2 WSS resulted in the highest levels of both endogenous calpain 1 and 2 detected in membrane isolates Thus, the combination of S1P and 5.3 dyn/cm^2 WSS enhanced calpain 1 and 2 membrane translocation compared to other treatments.

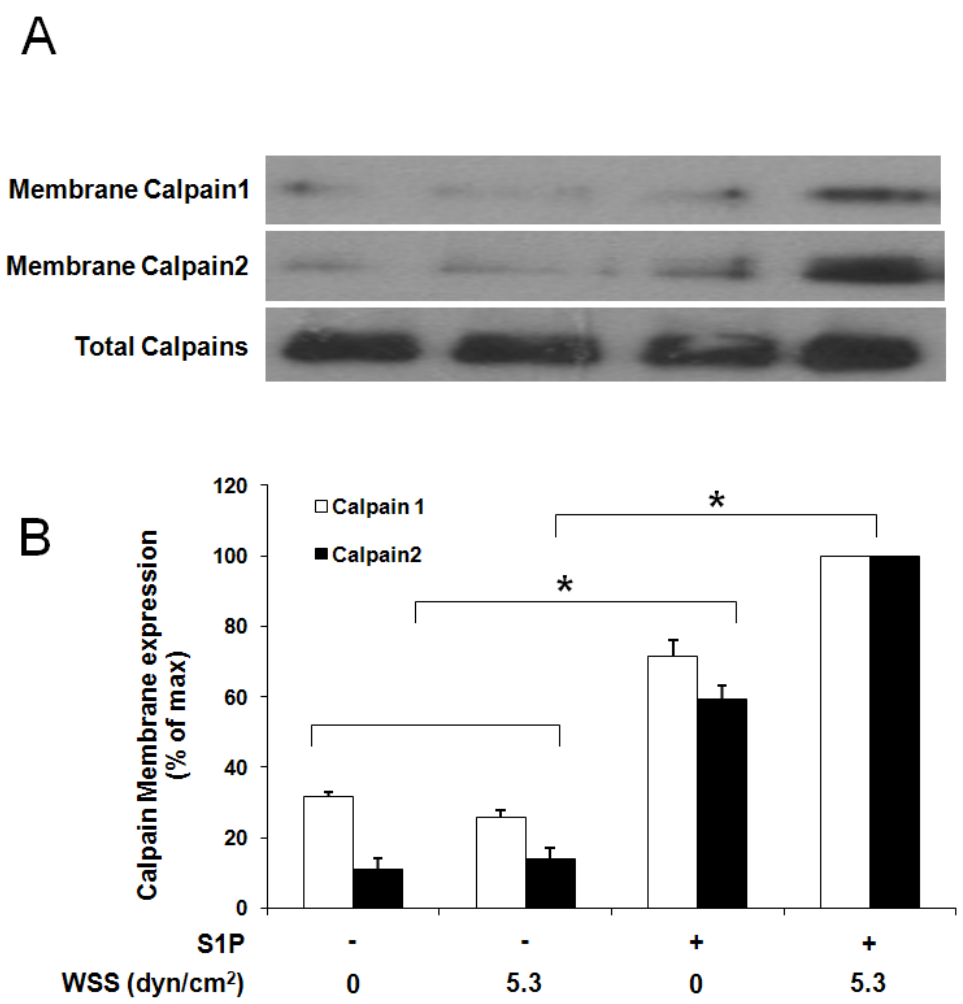

Figure. 13. S1P-induced calpain expression is enhanced by 5.3 dyn/cm^2 WSS. ***A***: ECs were treated in the absence or presence of S1P (1μM) for 1 h prior to WSS treatment and maintained in the flow media for the duration of 2 h WSS treatment (5.3 dyn/cm^2). Cell membranes were isolated as described in MATERIALS AND METHODS. Representative Western blots (***A***) indicate Calpain 1 and 2 levels in the membrane *(top and middle blot)* and total cell fractions *(bottom blot).* The blots were quantified by densitometric analysis from 2 independent experiments (**B**: mean±S.D.). * Significant difference from other groups.

WSS and S1P-Induced Invasion Responses Required for Akt Phosphorylation

A role for Akt has previously been demonstrated during EC sprouting *in vitro* and angiogenesis *in vivo* [33]. Both S1P and WSS have been reported to induce dose-dependent Akt phosphorylation [138, 139]. To determine whether S1P or WSS stimulated Akt phosphorylation in ECs seeded onto 3-D collagen matrices, cultures were exposed to static conditions or 5.3 dyn/cm^2 WSS on collagen matrices in the absence or presence of S1P (Fig. 14*A*). In the absence of S1P (Fig. 14*A*, *left*), WSS did not induce a noticeable increase in Akt phosphorylation compared with static controls (0 dyn/cm^2). There was a significant increase in Akt phosphorylation, however, when ECs were seeded on collagen matrices containing S1P for 1h that subsided after 8 h (Fig. 14*A*, *right*). The level of Akt phosphorylation at the 1h time point was noticeably enhanced by the addition of 5.3 dyn/cm^2 WSS. We next determined whether the WSS-induced Akt phosphorylation varied depending on the magnitude of WSS applied to ECs on S1P-containing collagen matrices using Western blot and densiometric analyses (Fig. 14, *B* and *C*, respectively). Consistent with the results in Fig. 14*A*, 5.3 dyn/cm^2 WSS increased Akt phosphorylation relative to the static control. This robust increase was not observed with 0.12 and 12 dyn/cm^2 WSS. All together, these results suggested that WSS-induced

invasion may involve Akt phosphorylation and that the increase in Akt phosphorylation was maximal at an intermediate WSS magnitude of ~5 dyn/cm^2, which also induced the maximal density of invasion (cf. Fig. 4). PI3K is the major kinase that activates Akt. To demonstrate a functional requirement for phosphorylated Akt in invasion responses, ECs were treated with the specific PI3K inhibitor wortmannin (Fig. 15*B*). Although Akt was transiently phosphorylated in ECs sheared in the presence of the vehicle (control), the increase in Akt phosphorylation after the application of WSS was completely blocked in the presence of 10 nM wortmannin (Fig. 15*A*). Furthermore, wortmannin treatment significantly attenuated EC invasion, as demonstrated by the photographs shown in Fig. 15A (top vs. bottom). Quantification of these responses demonstrated that invasion distance (Fig. 15*C*) and density (Fig. 15*D*) were significantly reduced by wortmannin treatment in response to 5.3 dyn/cm^2 WSS. These results confirm that Akt phosphorylation is involved in mediating S1P and WSS-induced invasion responses.

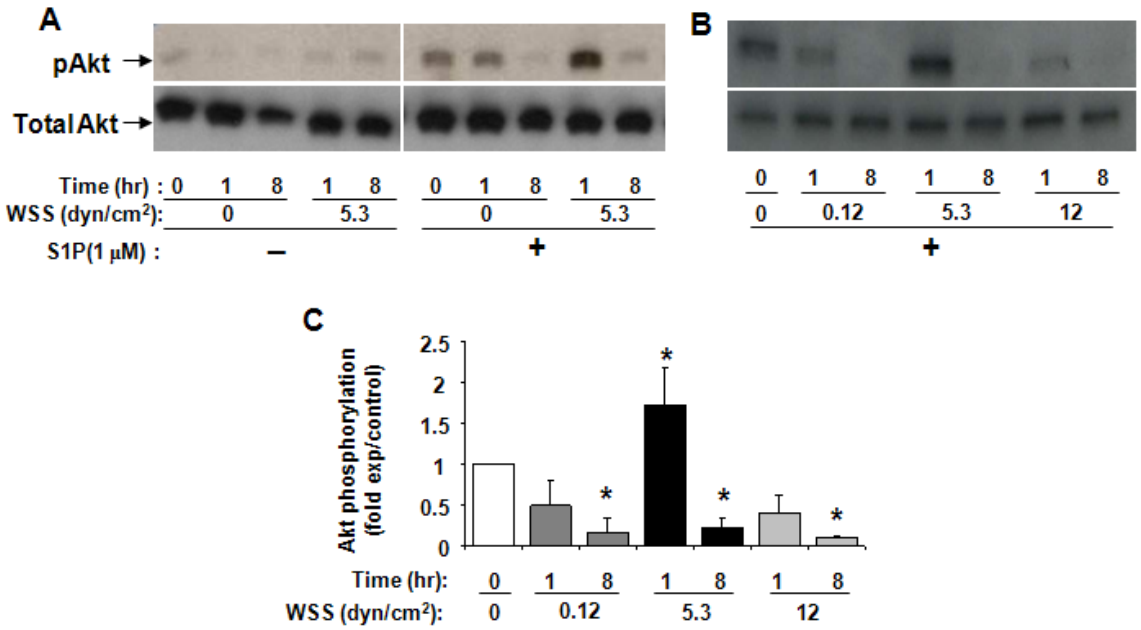

Figure 14. **S1P-induced Akt activation is enhanced by 5.3 dyn/cm^2 WSS. A:** ECs were subjected to WSS magnitudes of 0 (static control) and 5.3 dyn/cm^2 for 0,1, and 8 h, in the absence or presence of S1P. The cells were then lysed, and proteins were then collected as described in MATERIALS AND METHODS. Western blot analysis was performed with an antibody directed against the phosphorylated form of Akt (top blot) and an antibody directed against all forms of Akt (bottom blot). Each blot is representative of 3 independent experiments. **B and C:** ECs were subjected to steady WSS magnitudes of 0 (static control), 0.12, 5.3, or 12 dyn/cm^2 for the indicated durations in the presence of S1P. Western blots for the phosphorylated form of Akt (top blot) and total Akt (bottom blot) are representatively shown (B) and quantified by densitometric analysis from 3 independent experiments (C; means±SD). *Significant difference from static control ($P< 0.05$).

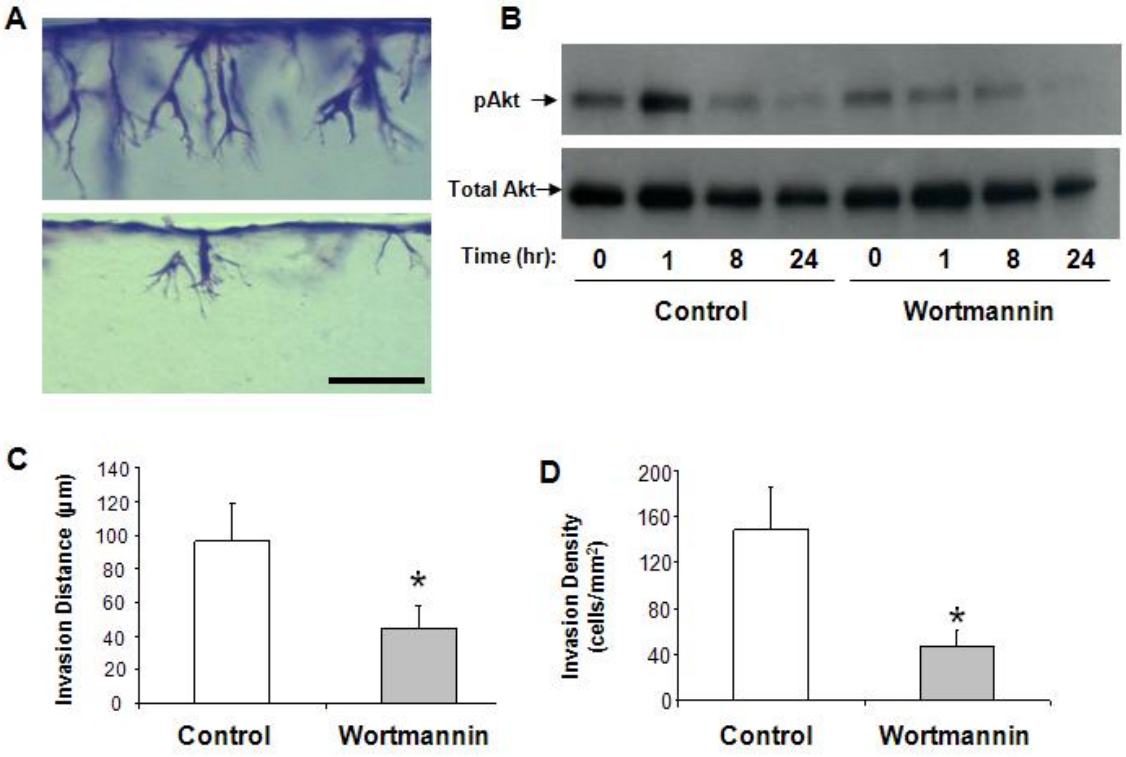

Figure 15. Wortmannin inhibits the effects of WSS on Akt phosphorylation and attenuates EC invasion. ECs were subjected to 5.3 dyn/cm^2 WSS for 0, 1, 8, and 24 h in the presence of S1P and either DMSO vehicle or 10 nM wortmannin. Western blot analyses were performed with an antibody directed against the phosphorylated form of Akt (***B***; *top blot*) and an antibody directed against all forms of Akt (***B***; *bottom blot*). The invasion distance (***C***; n =150 sprouts) and density (**D**; n =12 fields) of invading ECs were plotted as a function of WSS magnitude (means ±SD). *Significant difference between groups (*t*-test; P <0.05). Scale bar, 100 μm.

WSS and S1P-Induced Invasion Responses Required MMP-2 Activation

Because MMP-2 activation has been previously correlated with S1P and growth factor-induced EC invasion [4], we determined the effects of WSS magnitude on MMP-2 expression and activation. ECs were subjected to 0.12, 5.3, and 12 dyn/cm^2 WSS in the presence of S1P before performing gelatin zymography using conditioned media collected from the flow system at time points indicated (Fig. 16A). MMP-2 levels increased with time in cultures subjected to 0.12 and 5.3 dyn/cm^2 WSS, whereas high WSS (12 dyn/cm^2) resulted in suppression of pro- and activated forms of MMP-2. Quantification and two-way ANOVA of the zymograms (Fig. 16, B and C) indicated that the pro-MMP-2 band intensities were statistically lowest in the perfusate from the cells subjected to 12 dyn/cm^2 WSS, whereas the activated MMP-2 band intensities were statistically highest in perfusate from cells subjected to 5.3 dyn/cm^2 WSS. These results suggested that MMP activity is important for EC invasion in response to WSS+ S1P and that MMP-2 expression and activation are maximal at 5.3 dyn/cm^2 WSS, whereas MMP-2 expression and activation is largely suppressed by 12 dyn/cm^2 WSS. To confirm that metalloproteinase activity is functionally important in EC invasion induced by WSS and S1P, we tested the effect of the hydroxamate-based metalloproteinase inhibitor GM6001 along with vehicle (control) on the invasion response of ECs subjected to 5.3 dyn/cm^2 WSS. Photographs illustrate that GM6001 treatment (500 nM) completely blocked EC invasion (Fig. 17, A vs. B), which is quantified in Fig. 17C. Gelatin zymography confirmed complete blockade of MMP-2 activation by GM6001 (data not shown). These

results confirm a requirement for MMP activity in mediating S1P and WSS-induced invasion responses.

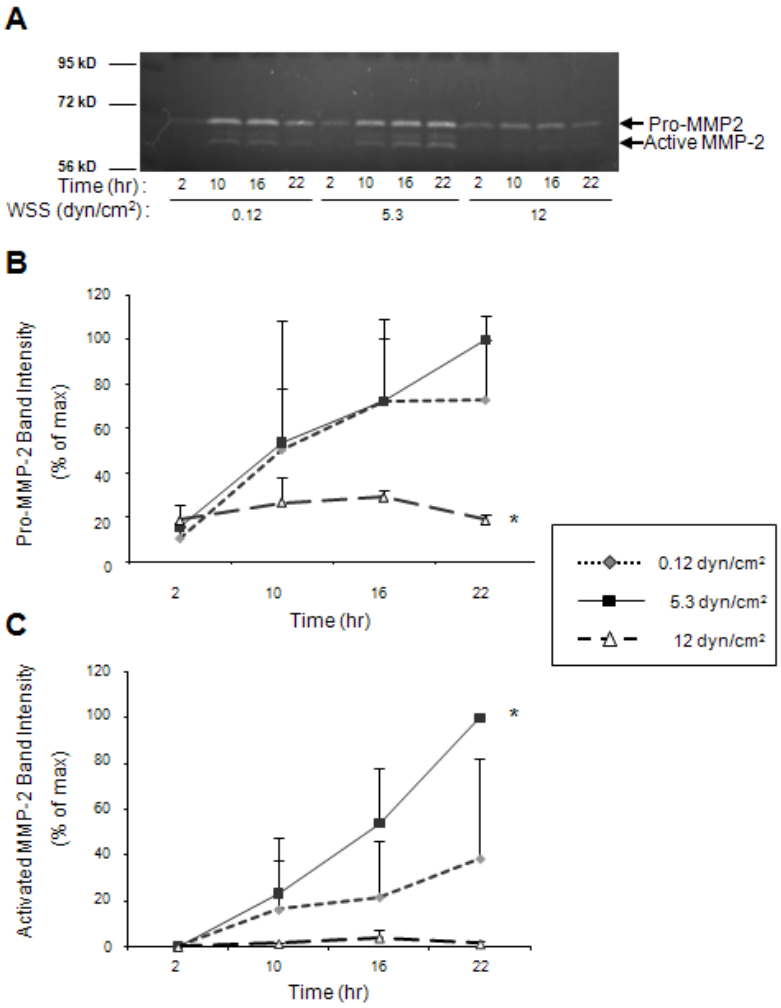

Figure 16. Matrix metalloproteinase (MMP)-2 activation is maximal in response to S1P and 5.3 dyn/cm^2 WSS. ECs were subjected to steady WSS ranging from 0.12 to 12 dyn/cm^2 in the presence of S1P, and samples of the conditioned media were collected at the indicated time points. The concentrations of MMP-2 propeptide (pro-MMP-2) and active MMP-2 are representatively shown by gel zymography ***(A)*** and quantified by densitometric analysis from 2 independent experiments (***B* and *C***, respectively; means ±SD). The band intensities were normalized relative to the highest intensity for each form of MMP-2. *Two-way ANOVA indicates a significant difference from the other WSS magnitudes (P<0.05).

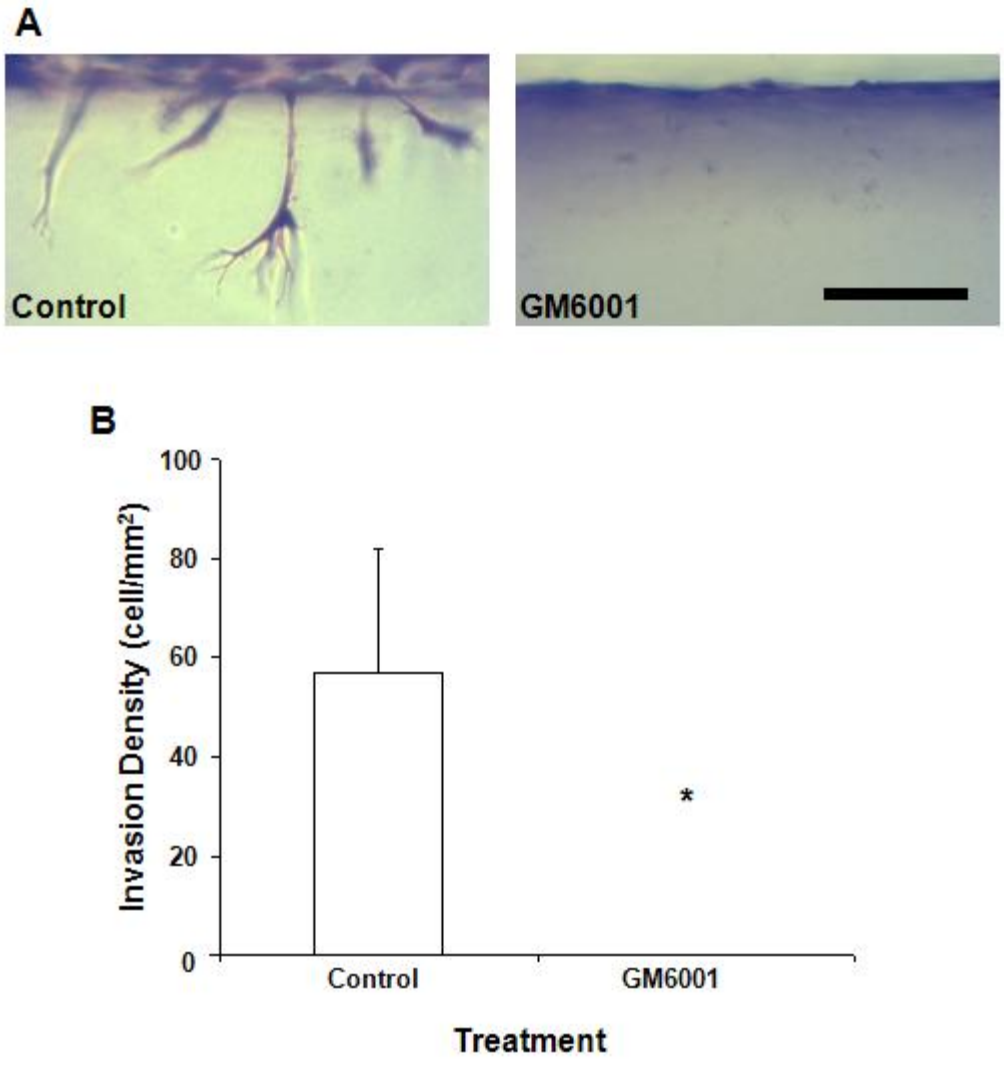

Figure 17. Invasion in response to the combined applications of S1P and WSS is blocked by MMP inhibition. Representative cross-sectional micrographs are shown for ECs that were subjected to 5.3 dyn/cm^{2}WSS for 24 h in the presence of S1P and either DMSO vehicle **(A)** or 500 nM GM6001 **(B).** The invasion density (**C**; n =24 fields) of invading ECs was quantified for each condition (means's). *Significant difference from vehicle control (t-test; $P<0.05$). Scale bar, 100 μm.

Calpain Activation Regulates MT1-MMP

MT-MMP plays a key role in matrix proteolysis and has been demonstrated to regulate angiogenic sprouting events [48, 144, 147, 155]. Compared to control cultures, calpain inhibition resulted in extremely thin invading structures (Fig. 18A and 9), suggesting a possible defect in matrix proteolysis. To test for a connection between calpain and MT1-MMP activity, MMP-2 activation levels, as an indicator of MT1-MMP activity in HUVEC [156] were determined using gelatin zymography(Fig. 18E). MMP-2 levels in the presence of vehicle increased with time, while calpain inhibitor III reduced both pro- and activated forms of MMP-2. Quantification of pro-MMP-2 and MMP-2 activation band intensities from zymograms (Fig. 18F-G) indicated that the MMP-2 intensities were statistically lower in the perfusate from cells treated with calpain inhibitor III. The significant morphological changes caused by calpain inhibition (cf. Fig. 18A) were then quantified, including attenuated sprout diameter (Fig. 18B), nucleus penetration distance (Fig. 18C), and invasion distance (Fig. 18D). Sprouts were still observed, arguing against a gross defect in the ability of the ECs to migrate. Rather, these results indicate that the cells lacking calpain activity can send thin processes into the matrix, but their nuclei cannot penetrate into the dense collagen 3-D matrix. Altogether, impaired morphological responses and decreased levels of pro- and activated

MMP-2 resulting from calpain inhibition support that calpain may regulate MT1-MMP function during S1P- and WSS-induced sprouting. We next quantified MT1-MMP activation in 3-D cultures treated with S1P, WSS in the presence and absence of calpain inhibitor III. ECs were allowed to invade for 3 h before measuring MT1-MMP activity using a fluorogenic substrate. While S1P and WSS each alone induced significant increases in MT1-MMP activity, a much larger increase in MT1-MMP activity was measured with S1P and WSS applied simultaneously (Fig. 19A). Further, S1P combined with 5.3 dyn/cm^2 WSS elicited the highest MT1-MMP activation that was significantly elevated compared to 0.12 and 12 dyn/cm^2 WSS (Fig. 19B). This activation was at least partially calpain-dependent since treatment with the calpain inhibitor III significantly reduced overall levels of MT1-MMP activation (Fig. 19C). The inhibitor completely inhibited calpain activation (Fig. 19D), as expected.

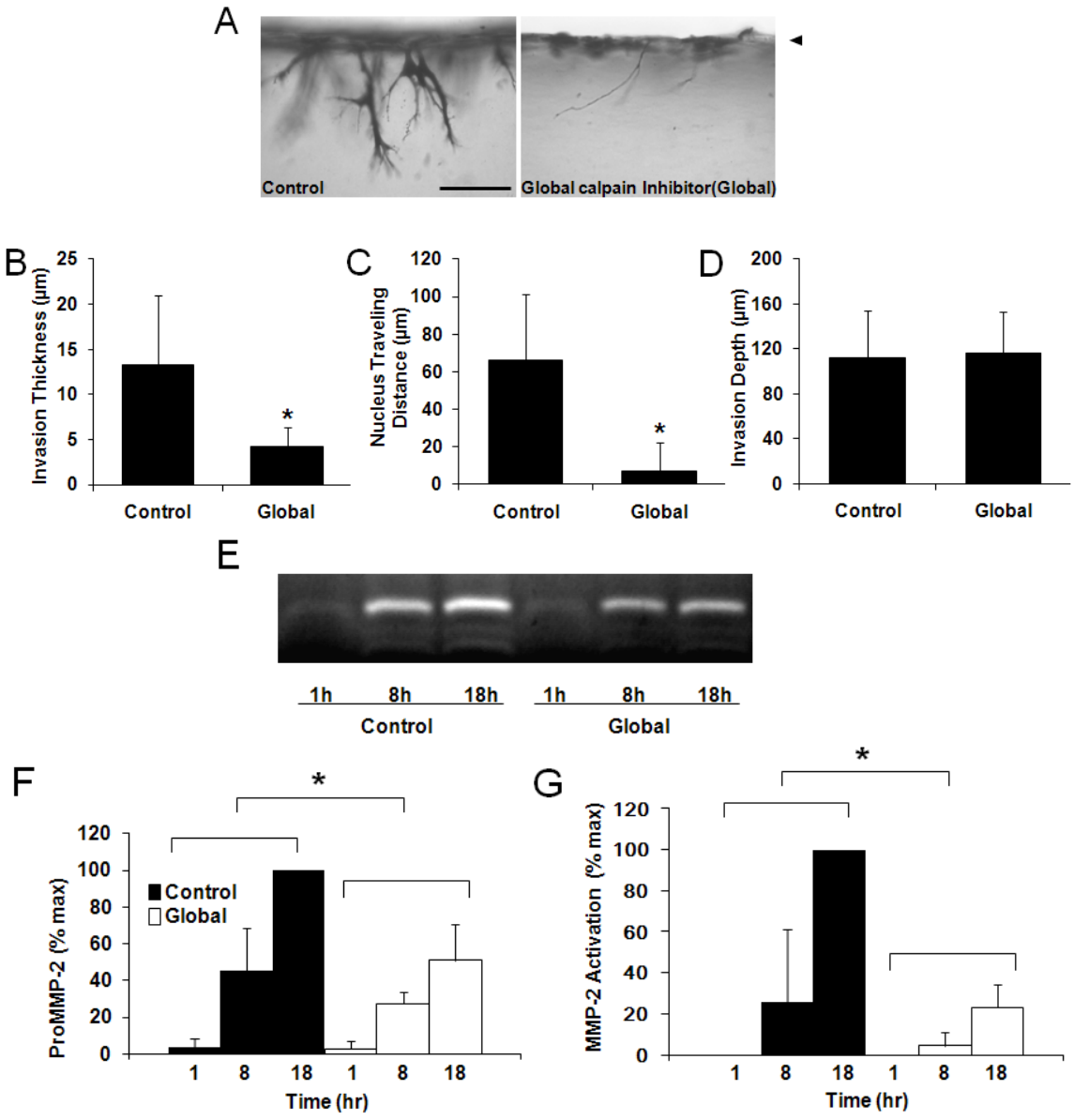

Figure. 18. Calpain blockade significantly reduced EC invasion and altered sprout morphology. ***A***: Photographs of cell invasion responses after 18 h of exposure to 1 μm S1P and 5.3 dyn/cm^2 WSS in the absence (left) and presence (right) of 50 μM calpain inhibitor III. The diameter of invading sprouts (***B***), the nucleus penetration distance (***C***), and overall invasion distance (***D***) were quantified (mean ± SD) * Significant difference from vehicle control (t-Test; P<0.05). Three individual experiments were performed (n=50 cells). Results shown are from a representative experiment. Scale bar, 100 μm.

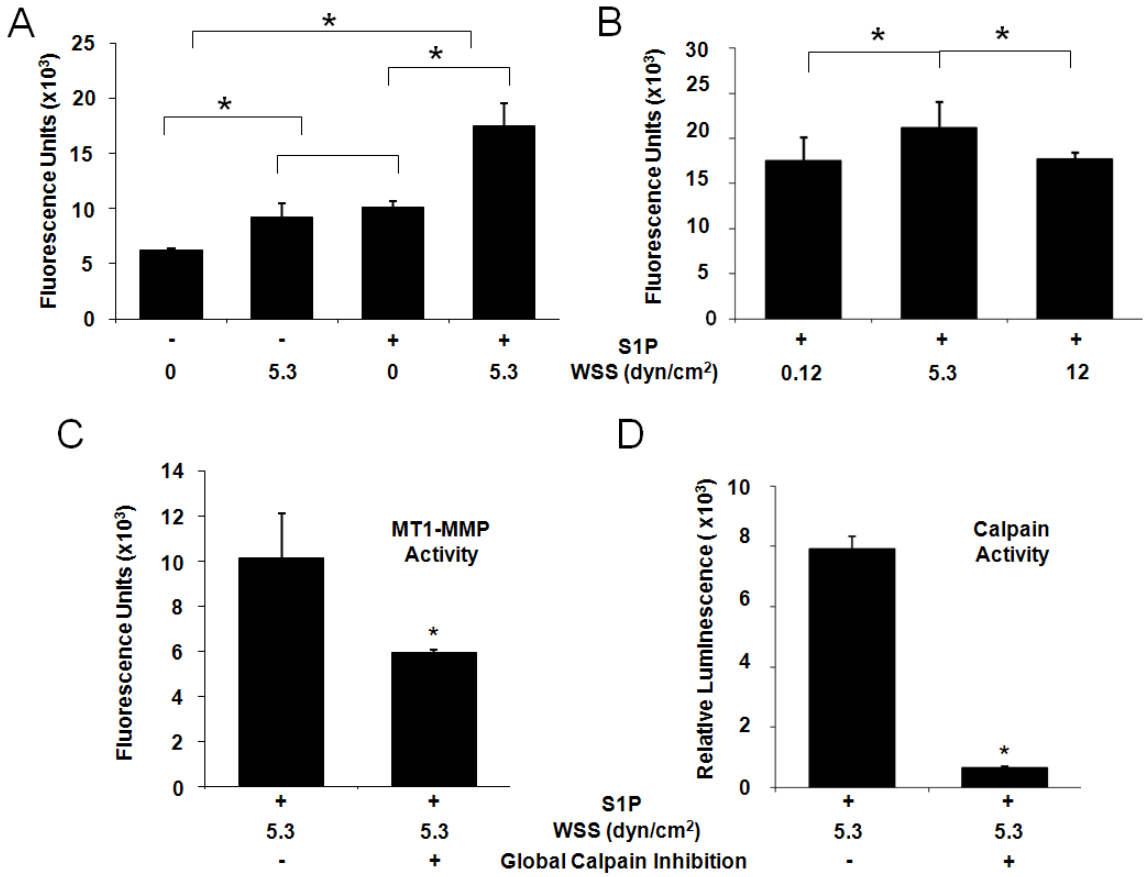

Figure. 19. S1P and WSS activate MT1-MMP. ECs were subjected to the indicated magnitude of WSS in the absence or presence of S1P for 3 h. ***A-C***: MT1-MMP activity was measured using the SensoLyte™ 520 MMP-14 protease assay kit as described in MATERIALS AND METHODS. MT1-MMP (***C***) and calpain (***D***) activation were measured in ECs subjected to 5.3 dyn/cm^2 WSS + S1P in the presence and absence of the calpain inhibitor III(50μM). Each data point was an average of triplicate wells from three individual experiments * ANOVA and multiple comparison test ($P<0.05$). * t-Test ($P<0.05$).

Like calpain activity, changes in the global levels of MT1-MMP activation did not completely explain the observed invasion responses elicited by S1P and 5.3 dyn/cm^2 WSS. Thus, we next investigated levels of MT1-MMP expression. To determine whether MT1-MMP expression was alterd by S1P and 5.3 dyn/cm^2 WSS, ECs seeded onto 3-D collagen matrices were pretreated with or without 1μM S1P for 1h and then exposed to static conditions or 5.3 dyn/cm^2 WSS (Fig. 20). Pro-MT1-MMP was high and active MT1-MMP was low regardless of the addition of S1P before exposure to 5.3 dyn/cm^2 WSS at 0 h (Fig. 20, lanes 1 and 2). After the application of 5.3 dyn/cm^2 WSS, Pro-MT1-MMP was decreased and active MT1-MMP was increased significantly compared with static controls (0 dyn/cm^2) at 2 and 6 h (Fig. 20, lanes 5-6 and 9-10 vs lanes 3-4 and 7-8). We next determined whether the effects of WSS magnitude influence MT1-MMP expression. We applied 0, 0.12, 5.3, and 12 dyn/cm^2 WSS to collagen matrices containing S1P. Pro-MT1-MMP was generally lower in cells treated with 0.12 dyn/cm^2 compared to 12 dyn/cm^2 and 5.3 dyn/cm^2 WSS (Fig. 20, lane 11). 12 dyn/cm^2 WSS induced minimal active MT1-MMP at 6 h significantly compared to 5.3 dyn/cm^2 WSS. All together, these results suggest that WSS-induced invasion may involve an increase in active MT1-MMP expression.

It is not clear why HUVECs show decreased active MT1-MMP expression and cell invasion at 12 dyn/cm^2 WSS. Thus, we next determined whether the effects of WSS magnitude influence membrane translocation of MT1-MMP. S1P can stimulate MT1-MMP translocation to the membrane [52], but the effects of shear stress on MT1-MMP localization have not been reported. Experiments were conducted to apply WSS in the presence or absence of S1P. We transfected ECs with GFP-labeled MT1-MMP to detect changes in the localization of MT1-MMP in response to S1P and/or WSS. Cells on collagen-coated slides were pretreated with 0 or 1μM S1P for 1h, subjected to 0.12, 5.3 or 12 dyn/cm^2 WSS for 2h, fixed, and imaged (Fig. 21). In the absence of S1P, almost no localization of MT1-MMP-GFP to the cell periphery was observed at any level of WSS except 5.3 dyn/cm^2 WSS (Fig. 21A). In the presence of S1P, 5.3 dyn/cm^2 WSS elicited maximal localization of MT1-MMP-GFP to the cell periphery (indicated by white arrowheads), which was not observed for 0.12 or 12 dyn/cm^2 WSS (Fig. 21A). Importantly, MT1-MMP-GFP membrane translocation was almost completely inhibited by blocking calpain (Fig. 21A).

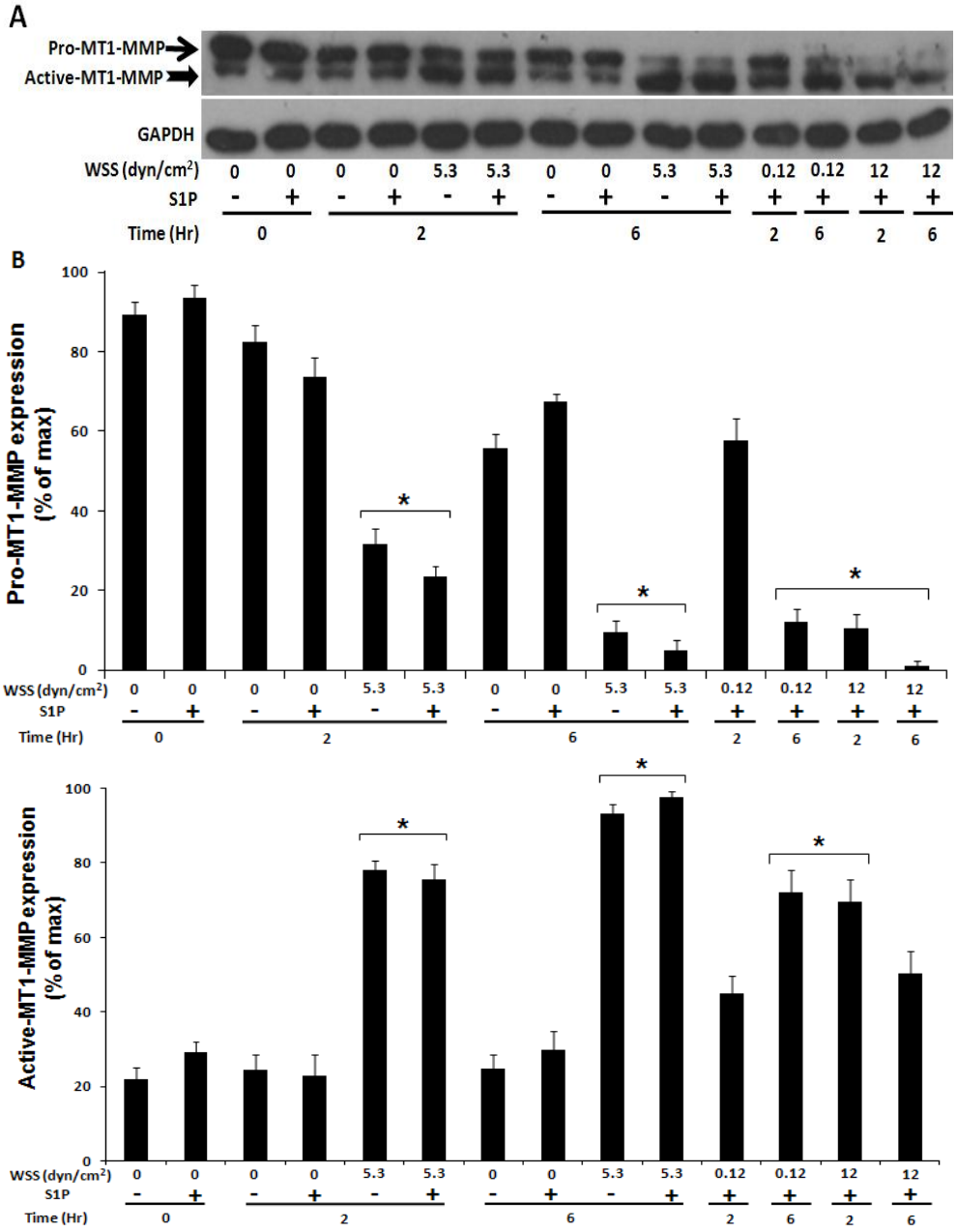

Figure. 20. Active MT1-MMP expression level is enhanced by 5.3 dyn/cm^2 WSS. ***A***: ECs were subjected to steady WSS magnitudes of 0 (static control), 0.12, 5.3, or 12 dyn/cm^2 WSS in the absence or presence of S1P for 0, 2, and 6h. The cells were then lysed, and proteins were then collected as described in MATERIALS AND METHODS. Western blot analysis was performed with an antibody directed against all forms of MT1-MMP (top blot) and GAPDH (bottom blot) and quantified by densitometric analysis from 3 independent experiments. Each blot is representative of 3 independent experiments. **B**: * The bracketed groups were significant difference from the control group (land 1 and 2) (ANOVA and multi-comparison testing; mean ± SD, $P<0.05$).

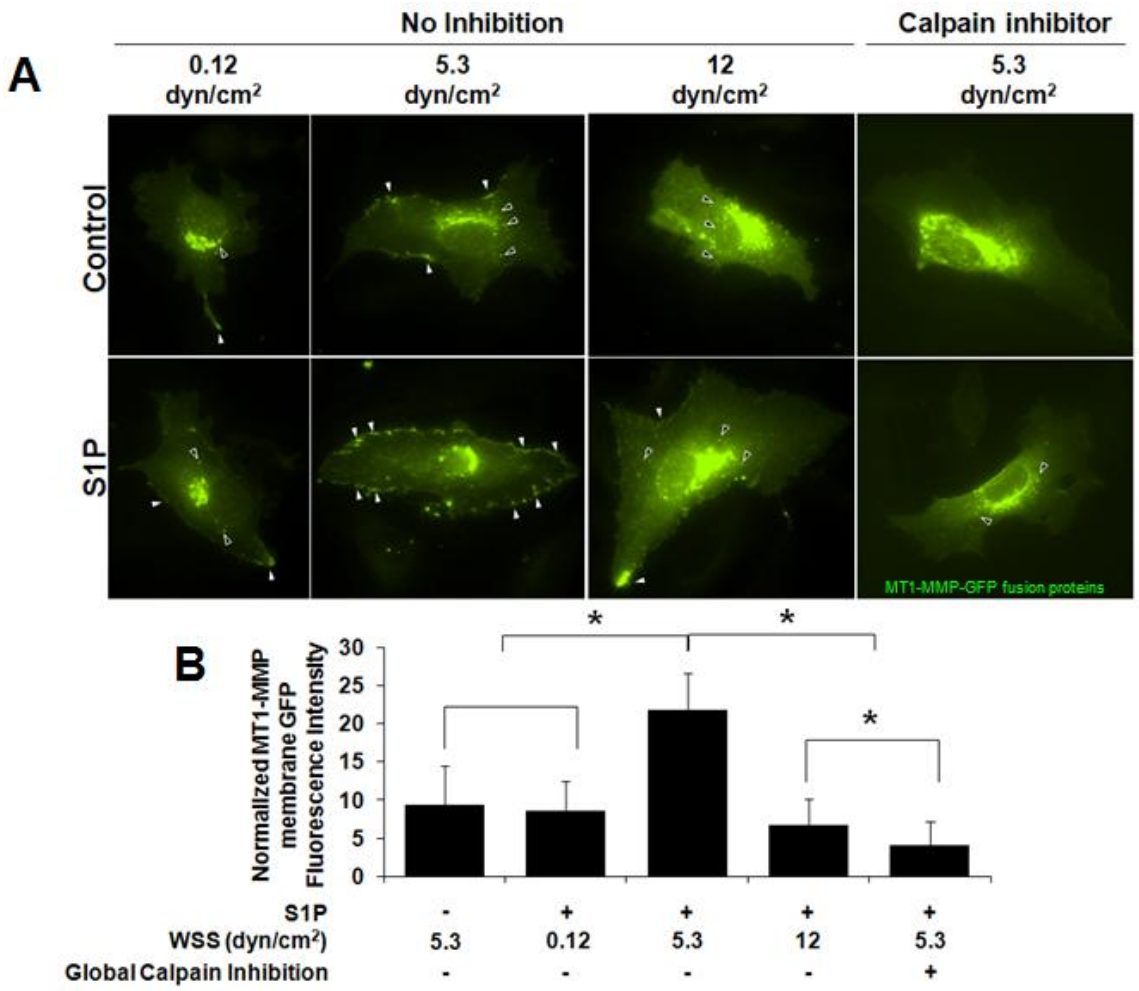

Figure. 21. Combined S1P and WSS treatment induced calpain-dependent membrane translocation of MT1-MMP. ECs transiently transfected with vectors expressing MT1-MMP-GFP chimeras were treated with the indicated magnitudes of WSS in the absence or presence of S1P. Transfection efficiency was roughly 20%. In calpain inhibition experiments, cells were pretreated with either the calpain inhibitor, Global (10μM) or the calpain inhibitor III (50μM) for 1 h prior to S1P and WSS treatments and the inhibitor was maintained in the perfusion media. ***A***: White arrowheads indicate MT1-MMP-GFP localization to the cell periphery; black arrowheads indicate perinuclear localization. Scale bar, 20 μm. ***B***: MT1-MMP peripheral GFP fluorescence intensities were quantified as described in MATERIALS and METHODS. Note the maximal induction was observed with exposure to 5.3 dyn/cm^2 in the presence of S1P. * significant difference from other groups.

Interestingly, treatments that did not induce MT1-MMP-GFP membrane translocation resulted in strong perinuclear MT1-MMP-GFP localization (indicated by black arrowheads). Signal intensity was quantified by tracing intensity along the cell periphery (Fig. 21B) as described in the Materials and Methods. The reliability of MT1-MMP-GFP fusion proteins was confirmed in separate experiments using two independent antibodies directed to MT1-MMP (data not shown). These data indicate that calpain inhibition attenuates MT1-MMP translocation to the cell membrane, which is necessary for robust invasion (cf. Fig. 9). To confirm MT1-MMP membrane localization, ECs were treated with nothing (control), WSS alone, S1P alone, or S1P together with WSS. Following each treatment, membrane fractions were isolated and analyzed for MT1-MMP levels (Fig. 22). Consistent with the fluorescent imaging results from Figure 21, combined treatment with S1P and WSS resulted in the highest levels of endogenous MT1-MMP detected in membrane isolates (Fig. 22A). In addition, higher levels of MT1-MMP were detected following 5.3 dyn/cm^2 compared to 0.12 or 12 dyn/cm^2 WSS (Fig. 22B). Quantification of MT1-MMP membrane localization is shown in Figures 22C and D, where MT1-MMP intensity in the starting material was expressed as a percentage of the total levels of MT1-MMP.

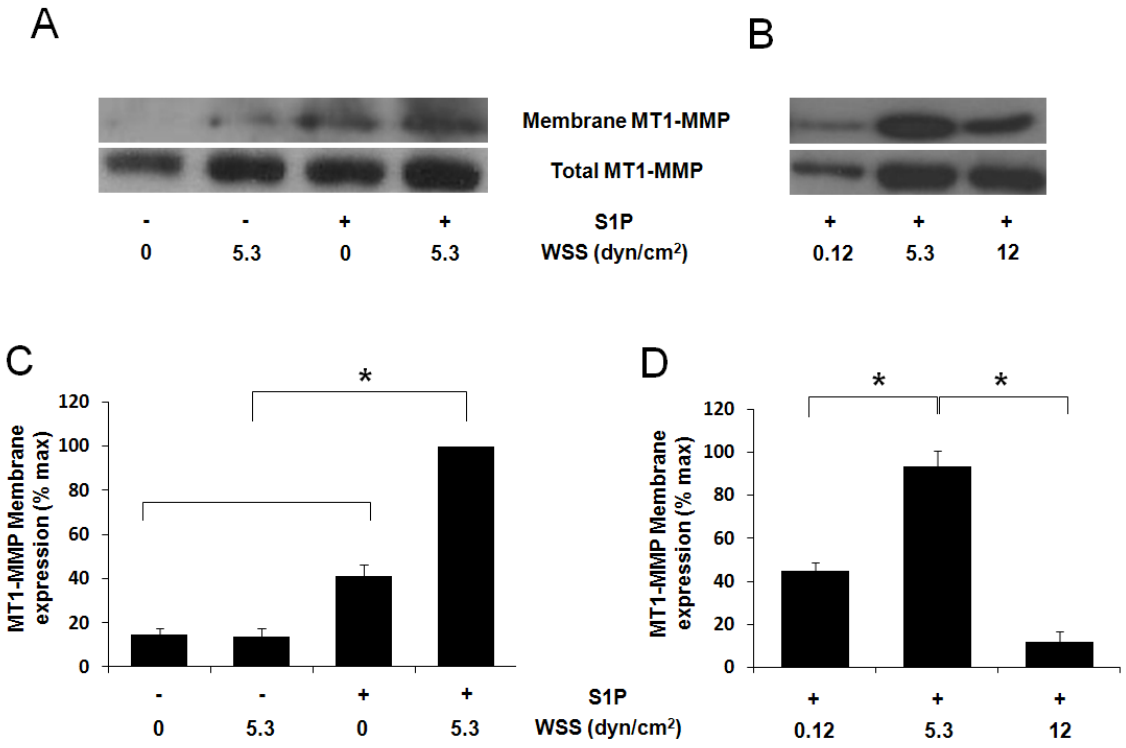

Figure. 22. S1P and 5.3 dyn/cm^2 WSS stimulate MT1-MMP membrane translocation. ***A and C***: ECs were treated in the absence or presence of S1P (1μM) for 1 h prior to WSS treatment and maintained in the flow media for the duration of 2 h WSS treatment (5.3 dyn/cm^2). ***B and D***: ECs were treated with S1P (1μM) for 1 h and then subjected to 2 h of WSS at the indicated magnitudes. Cell membranes were isolated as described in MATERIALS AND METHODS. Representative Western blots (***A*** and ***B***) indicate MT1-MMP levels in the membrane *(top blot)* and total cell fractions *(bottom blot).* The blots were quantified by densitometric analysis from 3 independent experiments (C and D: mean±S.D.). * Significant difference from other groups.

S1P/WSS-induced Akt Phosphorylation Was Calpain-dependent and Partially Acted Upstream of MT1-MMP Activity

Akt phosphorylation is involved in mediating S1P and WSS-induced invasion responses (cf., Fig. 8) and is required for cell motility in angiogenesis [34, 84, 131, 157]. However, Miyazaki et al. [76] recently reported that calpeptin, a calpain inhibitor, did not reduce Akt phosphorylation induced by shear stress of 30 dyn/cm^2, while Youn et al. [157] showed that VEGF-induced Akt phosphorylation was attenuated by both calpeptin and global calpain inhibitors. To determine whether S1P and WSS-induced calpain activation regulates Akt phosphorylation to enhance EC invasion in 3-D collagen matrices, ECs exposed to 5.3 dyn/cm^2 WSS were cultured in the absence and presence of global calpain inhibitor. Calpain inibition significantly attenuated Akt phosphorylation (Figs. 23A and B) and MT1-MMP activity (data not shown)**.** Akt inhibition with wortmannin blocked WSS+S1P-induced MT1-MMP activation (Fig. 23C). These results suggest that calpain-induced Akt phosphorylation mediated MT1-MMP activity.

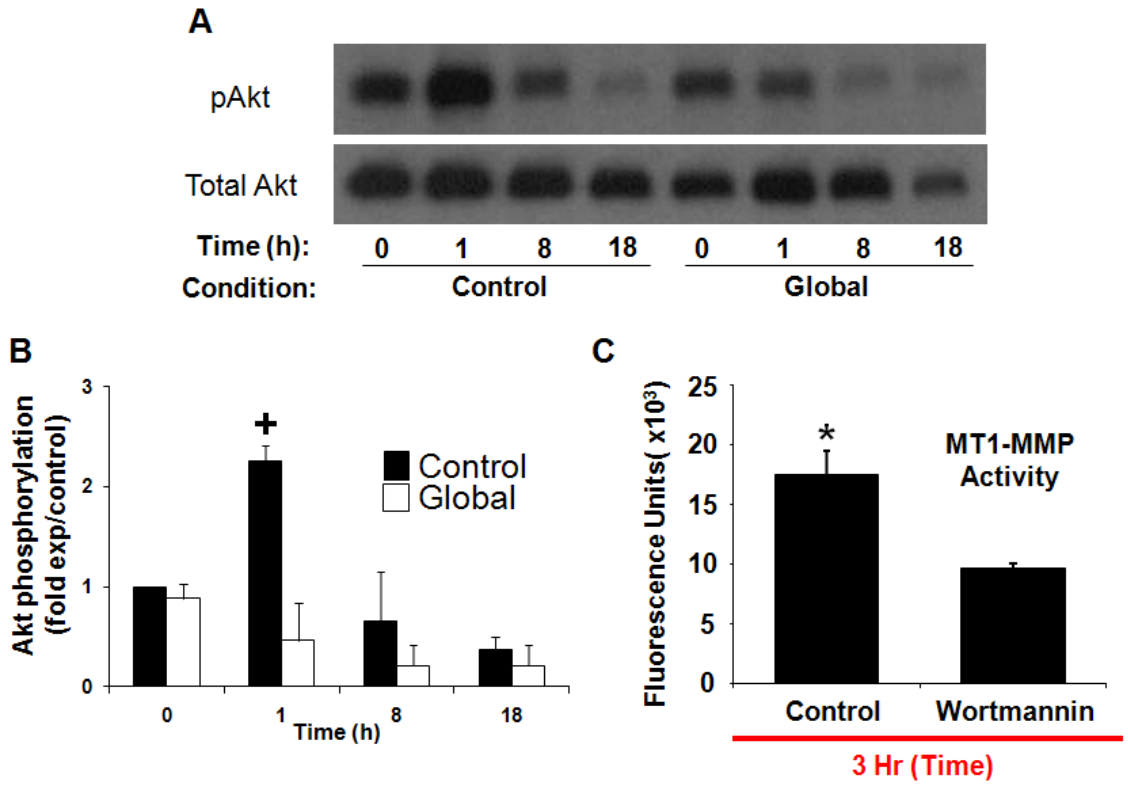

Figure. 23. Calpain inhibition attenuated Akt phosphorylation and Akt inhibition reduces MT1-MMP activation. ECs were subjected to 5.3 dyn/cm^2 WSS for 0, 1, 8, 17 h In the presence of S1P and either control or global calpain inhibitor (Global, 10μM). Western blot analysis was performed with an antibody directed against the phosphorylated form of Akt (*A; top blot*) and an antibody directed against all forms of Akt (***A****; bottom blot*). **B;** Western blots for the phosphorylated form of Akt and total Akt quantified by densitometric analysis from 3 independent experiments (means ±SD). **C;** Wortmannin significantly attenuates MT1-MMP activity. ECs were subjected to 5.3 dyn/cm^2 WSS for 3 and 20 h In the presence of S1P and either control or 10nM wortmannin. * significant difference between groups (T-test , $P<0.01$). + Two-way ANOVA indicates a significant difference from Global ($P<0.01$).

Discussion

In Chapter II, we reported that EC invasion in 3-D collagen matrices requires S1P co-administered with either growth factors (VEGF and bFGF) or WSS, with WSS providing a stronger invasion response [84]. We also showed a biphasic dependence on WSS magnitude with the highest invasion observed at 5.3 dyn/cm^2 WSS, but the lowest invasion observed at 12 dyn/cm^2 WSS [84]. This same biphasic dependence on WSS magnitude was observed for the activations of calpain, Akt, and MT1-MMP. VEGF-induced angiogenesis into matrigel plugs *in vivo* is blocked by calpain inhibition [119], which implicates calpain in regulating EC invasion through an unknown mechanism. Our data indicate that calpain regulates MT1-MMP to allow ECs to digest the collagen matrix in response to S1P and WSS. While WSS has previously been shown to activate calpain [76], this is the first study to demonstrate both S1P and WSS activates calpain. We provide several lines of evidence that invasion induced by S1P and WSS is related to the activation and membrane translocation of calpains. First, pharmacological inhibition and shRNA against calpains strongly inhibited EC invasion (cf. Fig. 10). Second, activation and membrane translocation of calpains, and cell invasion were each maximal at 5.3 dyn/cm^2 WSS.

The 3-D model used in our experiments provides a more realistic environment for studying the effects of angiogenic factors on cell invasion than 2-D models. Still, it is important to consider our results in light of previous studies of the effects of WSS on calpain signaling in 2-D HUVEC cultures. Ariyoshi and colleagues [118] observed

increased calpain 2 localization to the membrane in HUVECs in response to 10 dyn/cm^2 WSS, though the effects of other WSS magnitudes were not tested. Miyazaki and colleagues [76] reported that WSS-induced proteolytic activity in HUVECs increased monotonically as WSS magnitude was raised from 0 to 30 dyn/cm^2. In contrast, we observe a biphasic dependence on WSS magnitude. It is not clear why HUVECs show decreased calpain activation and cell invasion at 12 dyn/cm^2 WSS, though this is an area we are actively investigating.

S1P and WSS Stimulate Akt Phosphorylation During EC Invasion

Our data indicate that Akt activity is required for S1P- and WSS-induced EC invasion in 3D collagen matrices, as demonstrated by a 40% reduction in the average length of sprouts from Akt1 knockout mice as compared to wild-type mice in an *ex vivo* aortic ring invasion assay [33]. The effects of VEGF and S1P on EC migration and tubulogenesis *in vitro* have also been shown in separate studies to be dependent on Akt activity [132-134]. Activation of $S1P_1$ receptors in ECs has been reported to stimulate the activation of Akt via pertussis toxin-sensitive G proteins [135, 136]. Pertussis toxin blocked S1P-induced migration [136], 3-D invasion [4], and tubulogenesis following preshearing [78]. Our data also provide evidence that Akt activation was stimulated by S1P and demonstrate for the first time that S1P synergizes with 5.3 dyn/cm^2 WSS to induce maximal Akt activation in 3-D collagen matrices. Interestingly, S1P-induced Akt activation was suppressed by 12 dyn/cm^2 WSS (cf. Fig. 14). Akt activation was also significantly decreased by inhibition of Akt and calpain in the presence of S1P and 5.3

dyn/cm^2 WSS. Recently, Youn et al. [157] also demonstrated that calpain 2 colocalized with ezrin to regulate Akt, endothelial nitric oxide synthase (eNOS) activation and nitric oxide (NO) production. Our data support that calpain may regulate Akt activation in 3D collagen matrices. Akt has several downstream targets implicated in angiogenesis, including eNOS [138], hypoxia-inducible factor [140], the transcription factor FOXO [141], and p21-activated kinase (PAK) [158-160]. Of note, both eNOS activity, FOXO expression, PAK are regulated by WSS in ECs [138, 141] [161]. It is not clear how calpain-mediated Akt activity is involved in S1P- and WSS-induced EC invasion, but this is an area we are actively investigating.

Calpains Regulate MT1-MMP Following Stimulation by S1P and WSS

MT1-MMP has an indispensible role in angiogenic sprouting into collagen matrices *in vitro* and *in vivo* [48, 49, 80]. Although S1P has previously been shown to stimulate MT1-MMP membrane translocation through Src-mediated phosphorylation of the cytoplasmic tail of MT1-MMP [52], the effects of WSS on MT1-MMP membrane translocation have not been reported.

We have previously shown that EC invasion correlates with MMP-2 activation as an indicator of MT1-MMP activity in ECs [162] (cf. Fig. 16). The expression of pro-MMP-2 and active-MMP-2 were maximal at an intermediate WSS magnitude of 5.3 dyn/cm^2 and minimal at a high WSS magnitude of 12 dyn/cm^2 in 3-D collagen matrices. These data are consistent with a previous report by Milkiewicz and colleagues [163] demonstrating that 16 dyn/cm^2 WSS downregulated both MMP-2 protein and

mRNA levels (vs. static control) in cultured microvascular ECs, while 5 dyn/cm^2 WSS did not. The ability of ECs to invade into collagen matrices despite a decrease in MMP-2 levels is also noteworthy and demonstrates MMP-2 is not required for EC invasion into 3-D collagen matrices. These data are consistent with previous reports that tissue inhibitor of metalloproteinase-1 (TIMP-1) [4, 144], an endogenous inhibitor of soluble MMPs, including MMP-2 and MMP-9, does not alter invasion responses [164]. Thus, we need to determine how shear stress regulates MT1-MMP and related angiogenic intracellular signaling cascades.

Here we demonstrated for the first time that calpains can regulate MT1-MMP membrane translocation and, to a lesser extent, MT1-MMP activation. Calpain inhibition resulted in narrow sprouts and the inability of the nucleus to penetrate collagen matrices (cf. Fig. 18). However, sprout defects were likely not due simply to inhibition of migration since sprout length appeared unaffected. Rather, these results suggest matrix proteolysis was impaired. We previously reported that 12 dyn/cm^2 WSS combined with S1P to stimulate invading ECs to extend more rapidly into collagen matrices with narrower lumens than sprouts from ECs subjected to lower magnitudes of WSS [84]. This sprout morphology observed with 12 dyn/cm^2 WSS is strikingly similar to invading structures treated with calpain inhibitors. Further, 12 dyn/cm^2 WSS-treated samples exhibited significantly lower calpain activation levels and MT1-MMP membrane localization than ECs treated with 5.3 dyn/cm^2 WSS. In our model, S1P combines with 5.3 dyn/cm^2 WSS to induce the highest EC invasion responses. Consistent with this data, 5.3 dyn/cm^2 WSS combined with S1P promoted the highest activation and membrane

localization of calpain, as well as the activation, expression, and membrane localization of MT1-MMP. These data demonstrate a correlation between calpain activation, MT1-MMP membrane translocation and EC invasion responses. Further, calpain inhibition partially reduced MT1-MMP activation and almost completely blocked membrane translocation stimulated by 5.3 dyn/cm^2 WSS combined with S1P. These data reveal for the first time that calpain regulates MT1-MMP.

Physiological Implications of These Findings

Wound healing is a complex process in which the skin or organ repairs itself after injury. Platelets accumulate at sites along damaged blood vessels and release a number of biochemical factors including VEGF, bFGF, and S1P [94-97]. Additional inflammatory mediators released locally result in vasodilatory responses that ultimately increase WSS via increased blood flow. This scenario fits with the possibility that WSS and S1P initiate EC sprouting into the wound from nearby preexisting vessels. We have previously reported that WSS synergizes with S1P to induce significant EC invasion in collagen matrices [84]. A wide range of WSS levels are used to study mechanotransduction events *in vitro*, with many studies utilizing shear stresses of 12 dyn/cm^2 or greater. WSS levels in post-capillary venules have been estimated at 1-5 dyn/cm^2 [74, 105, 165], which is consistent with a previous report of 0-5 dyn/cm^2 laminar shear stress in the mouse embryo [166]. Here, we find S1P combined with 5.3 dyn/cm^2 WSS induced maximal activation of calpain and MT1-MMP and membrane translocation of calpain and MT1-MMP, thus providing new insight into the intracellular

signaling events that stimulate S1P- and WSS-induced EC sprouting at physiological levels of WSS observed in post-capillary venules. More specifically, our results suggest that S1P and WSS activation calpains, which controls MT1-MMP membrane translocation, and to a lesser extent, activation, which are key steps for successful initiation of EC sprouting in 3-D collagen matrices.

These results provide a novel molecular mechanism of angiogenic sprout initiation induced by biochemical and mechanical stimuli, namely S1P and WSS. Altogether, these data demonstrate a requirement for calpain in directing MT1-MMP to the membrane in response to stimulation with S1P and 5.3 dyn/cm^2 WSS. This observation is significant in that these conditions optimally stimulate endothelial sprouting responses in 3-D collagen matrices and uncover a previously unknown mechanism for regulating intracellular MT1-MMP localization that appears to be controlled by calpain activation. The regulation of this pathway may underlie vascular remodeling and angiogenic events in a variety of scenarios, including embryonic development, wound healing, and tumor angiogenesis, where biochemical and mechanical cues are optimal for initiation of new blood vessel growth.

CHAPTER IV

FLUID SHEAR STRESS AND SPHINGOSINE 1-PHOSPHATE PHOSPHORYLATE PAK AND CLEAVE VIMENTIN TO ACTIVATE MT1-MMP AND INDUCE EC INVASION

Overview

Our results from Chapters II and III demonstrate that S1P and 5.3 dyn/cm^2 WSS synergistically enhances angiogenic sprouting through the activation of calpain, Akt, and MT1-MMP in 3-D collagen matrices. In this chapter, we define the roles of vimentin and PAK in initiating angiogenic sprout formation in response to S1P and WSS. Knockdown of the appropriate vimentin isoform with shRNA reduced MT1-MMP activation and inhibited S1P- and WSS-induced EC invasion in 3-D collagen matrices. A vimentin is a known substrate of calpain. A pharmacological inhibition of calpain significantly reduced vimentin cleavage resulting in decreased invasion responses. Akt inhibitor X also significantly decreased PAK and vimentin phosphorylation. All together, these data suggest that S1P- and WSS-activated calpain and Akt regulate vimentin cleavage and phosphorylation. The resulting vimentin fragments may bind and then transfer MT1-MMP to the membrane to facilitate cell invasion into the collagen matrix.

Introduction

Our results from Chapter III define that S1P- and WSS-activated calpains regulate Akt and MT1-MMP for initiating EC invasion in 3-D collagen matrices, but it is unclear how calpain activation or Akt phosphorylation specifically activated and translocated MT1-MMP to the membrane during EC invasion. In this chapter, we investigate the roles of a vimentin as a potential calpain substrate and as a controller of angiogenic sprouting formation. Since vimentin, the only intermediate filament protein found in ECs has recently emerged as a regulator of signal transduction involved in cell adhesion and migration [167-170], we hypothesized that S1P- and WSS-activated calpains may regulate vimentin networks, which may be directly linked to MT1-MMP translocation to the membrane during EC invasion in 3-D collagen matrices.

Vimentin is required for angiogenic sprouting events. Gilles et al. [54] reported that vimentin contributes to human mammary epithelial cell migration *in vitro* wound-healing models. Eckes el al. [55] observed that vimentin-deficient fibroblasts exhibit decreased motility, chemotactic migration, and delayed wound healing. Vimentin can also be cleaved by calpain [171]. Under mechanical stress, vimentin provides cells with mechanical resilience independent from the microtubule or actin filament networks. Cucina et al. [172] showed that vimentin is retracted and formed a dense network extending mainly around the nucleus after applying 6 dyn/cm^2 WSS for 24 h in ECs. Jackson et al. [173] reported that the amount of vimentin is increased in human fetal osteoblasts subjected to WSS. Helmke et al. [174, 175] demonstrated that GFP-vimentin

networks are rapidly displaced at the apical surface of ECs within 3 min after applying 12 dyn/cm^2 WSS.

Interestingly, the formation of capillary-like morphologies is diminished by reduction of MT1-MMP expression and vimentin cleavage in HUVECs [176]. MT1-MMP expression is directly correlated with vimentin expression in human breast carcinoma cell lines [177]. Based on these results, we hypothesized that S1P- and WSS-activated calpain would cleave cytoplasmic networks of vimentin and the vimentin fragments would colocalize with MT1-MMP. Vimentin filaments are composed of bundles of vimentin monomers consisting of a central rod domain that is flanked by an N-terminal head and C-terminal tail domain. When a phosphate group is added to the head region, the monomer is freed from the polymerized network [56, 57, 59, 178]. Thus, vimentin filament stability is dependent on its phosphorylation state.

Interestingly, the serine/threonine kinase PAK2 found in ECs phosphorylates vimentin [58, 59] and plays a crucial role in angiogenesis [36]. Thus, we hypothesized that PAK, a downstream effector of Akt, would regulate vimentin depolymerization and be required for S1P- and WSS- induced EC invasion.

Results

Vimentin Cleavage Is Required for S1P- and WSS-induced EC Invasion in 3-D Collagen Matrices

Vimentin plays a significant role in cell attachment and migration [54, 56, 58] and can directly associate with MT1-MMP [176, 177, 179]. Based on these results, we determined whether vimentin is necessary for S1P- and WSS-induced EC invasion and MT1-MMP activity. Two individual shRNA constructs directed to vimentin (shVim1 and shVim2) were compared to β2M negative control shRNA. Knockdown of vimentin with either construct significantly reduced EC invasion responses (Fig. 24B). Equal loading in lysates was confirmed using GAPDH-specific antisera (data not shown). Photographs of invading ECs that were not treated with shRNA (HUVEC) or treated with shRNA against sh β2M or shVim are shown in Fig. 24A. Selective knockdown of the appropriate vimentin isoform with each shRNA was confirmed by Western blot analyses (Fig. 24C). To measure MT1-MMP activity using a fluorogenic substrate, 5.3 dyn/cm^2 WSS applied to shβ2M, HUVEC, and shVim for 3 h in 3-D cultures containing S1P. Only shVim attenuated MT1-MMP activation compared to others (Fig. 24D). These results confirm that vimentin is required for S1P and WSS-induced EC invasion into 3-D collagen matrices.

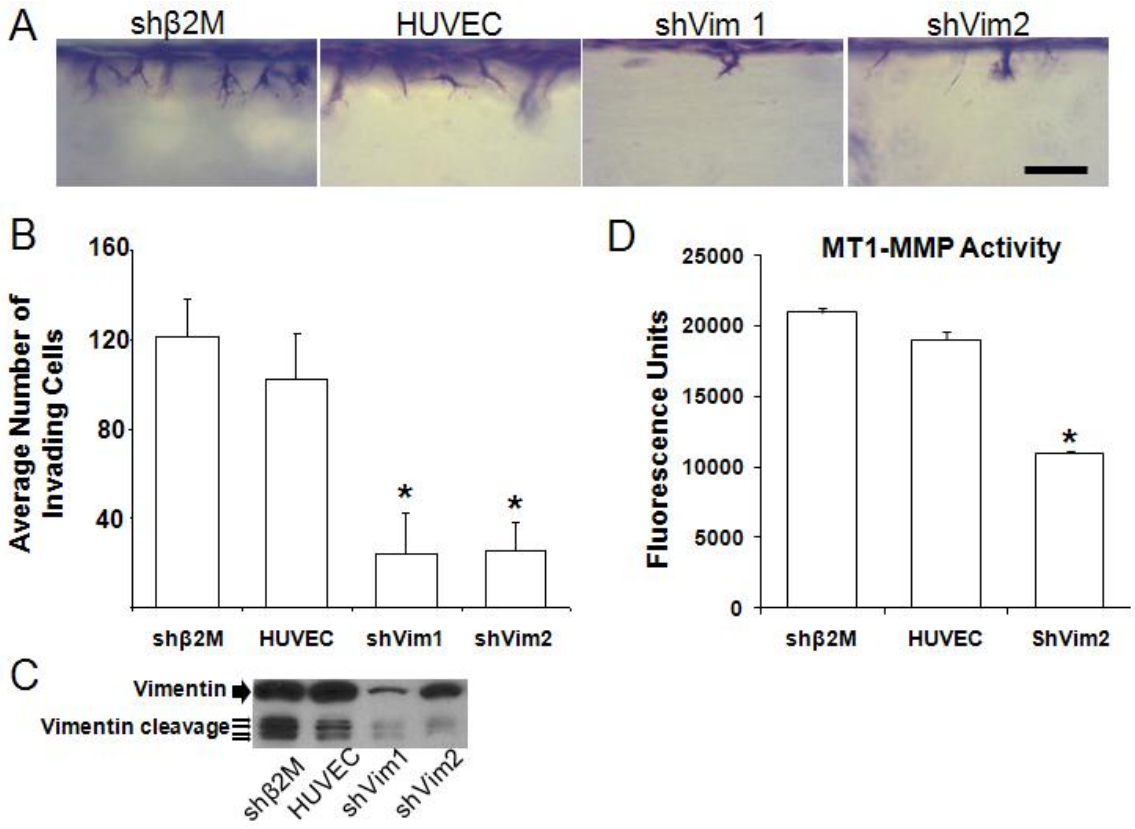

Figure 24. Vimentin cleavage is required for S1P and WSS-induced EC invasion in 3-D collagen matrices. Untreated control ECs and ECs transduced with lentiviruses delivering shRNA directed to beta 2 microglobulin (shβ2M), vimentin (shVim1 and shVim2) were stimulated with 1μM S1P and 5.3 dyn/cm^2 WSS for 24h. Cultures were fixed and stained for morphometric analysis **(A)** and the invasion density is quantified for each condition from three individual experiments (**B**; mean ± SD, n = 9 fields). Culture extracts were prepared and antibodies against vimentin and GAPDH, as an experimental control, were used for western blot analyses **(C)**. MT1-MMP activity was measured using the SensoLyte^{TM} 520 MMP-14 protease assay kit as described in MATERIALS AND METHODS. MT1-MMP activation ***(D)*** was measured in untreated control ECs and ECs transduced with lentiviruses delivering shRNA directed to shβ2M and shVim2 subjected to 5.3 dyn/cm^2 WSS + S1P. Each data point was an average of triplicate wells from three individual experiments. * indicates significant difference from control (P<0.05). Scale bar, 100 μm.

Vimentin Cleavage Is Enhanced by the Combination of S1P and 5.3 dyn/cm^2 WSS and Is Calpain-dependent

Vimentin, the only intermediate filament protein found in ECs, is cleaved in response to shear stress [175]. Based on this evidence, we determined whether S1P or WSS induced on vimentin cleavage during EC invasion. ECs cultured on 3-D collagen matrices containing or lacking S1P (1 μM) were treated with or without WSS (5.3 dyn/cm^2) and total cell extracts were collected after 3 h (Fig. 25A). The samples were probed in Western blots using vimentin-specific antisera. S1P alone or the combination S1P and 5.3 dyn/cm^2 WSS stimulated increased vimentin cleavage (3 thin arrowheads) compared to no treatment and 5.3 dyn/cm^2 WSS alone in Figure 25A. We next determined whether the effects of WSS magnitude influence on vimentin cleavage. We applied 0.12, 5.3, and 12 dyn/cm^2 WSS to ECs cultured on 3-D collagen matrices containing S1P. 5.3 dyn/cm^2 WSS induced greater vimentin cleavage than that occurring in response to 0.12 and 12 dyn/cm^2 WSS. Interestingly, immunofluorescence experiments revealed 12 dyn/cm^2 WSS induced prominent vimentin bundles that extended to the cell periphery (Fig. 26), suggesting polymerization of vimentin networks and minimal vimentin cleavage (Fig. 25B).

Since there is evidence that vimentin is cleaved by calpain [171], we next determined if networks of vimentin are cleaved by S1P/WSS-activated calpain. ECs exposed to 5.3 dyn/cm^2 WSS were cultured in the presence or absence of global calpain inhibitor, a pharmacological calpain inhibitor. Lysates were prepared from invading cultures treated with global calpain inhibitor and analyzed by Western blotting. Global

calpain inhibitor reduced vimentin cleavage during EC invasion in 3-D collagen matrices (Figs. 25C and 25D). These data support the hypothesis that calpains are responsible for vimentin cleavage during EC invasion responses.

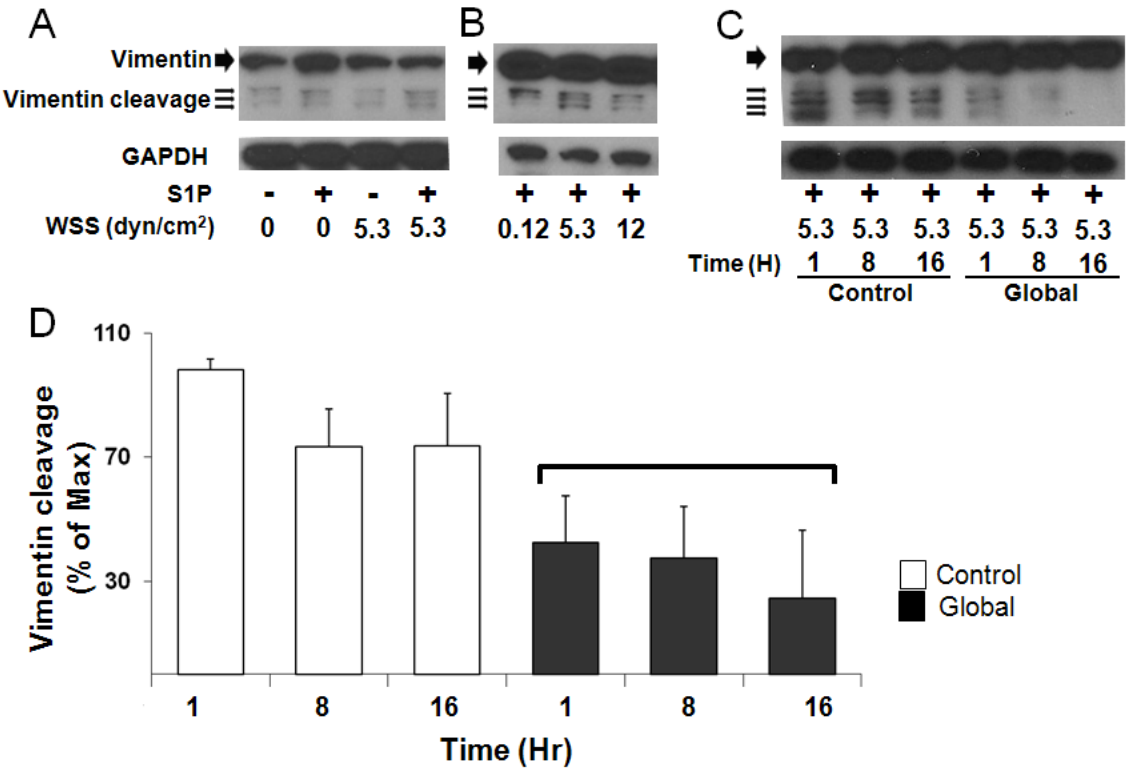

Figure. 25. S1P and 5.3 dyn/cm^2 WSS enhances vimentin cleavage and calpain inhibitor significantly attenuated vimentin cleavage. ***A***: ECs were treated in the absence or presence of S1P (1μM) for 1 hr prior to WSS treatment and maintained in the flow media for the duration of 3 h WSS treatment (5.3 dyn/cm^2). ***B***: ECs were treated with S1P (1μM) for 1 hr and then subjected to 3 h of WSS at the indicated magnitudes. ***C-D***: ECs were subjected to both S1P and 5.3 dyn/cm^2 WSS for 1, 8 and 16 h in the presence of either Ethanol control or global calpain inhibitor (Global; 10μM). Western blot analysis was performed with an antibody directed against the vimentin (**A, B and C**; upper blot) and GAPDH (**A, B and C**; lower blot). The blot is representative of 3 separate experiments. **C**; Western blots for the vimentin cleavage and GAPDH by densiometric analysis from 3 independent experiments (**C**; means ±SD). The bracketed groups were significant difference from the control group (ANOVA and multi-comparison testing; $P<0.05$).

WSS and Akt Phosphorylation Regulated Vimentin Bundles of ECs in 3-D Collagen Matrices

Tsuruta et al. [169] reported that 12 dyn/cm^2 WSS enhanced thick vimentin bundles. To determine whether S1P and WSS affect vimentin and MT1-MMP localization, experiments were conducted to apply WSS in the presence S1P. ECs were transfected with GFP-labeled MT1-MMP to detect changes of MT1-MMP localization in response to S1P and WSS. Cells were seeded on collagen-coated glass slides and pretreated with 1μM S1P for 1 h before being subjected to 0, 0.12, 5.3 and 12 dyn/cm^2 WSS for 2 h, fixed, and imaged (Fig.26). Localization of vimentin protein is shown by immunofluorescence staining with an anti-vimentin monoclonal primary antibody and FITC-conjugated secondary antibodies (vimentins are stained by red). Under static control conditions, the vimentin network is only arranged in a dense pattern around the nucleus (nuclei are stained by blue) rather than spreading out to the cell periphery. However, WSS induced dramatic spreading of the vimentin networks along direction of flow. 12 dyn/cm^2 WSS elicited thick and dense vimentin bundles compared to 5.3 dyn/cm^2 WSS. However, 5.3 dyn/cm^2 WSS elicited the greatest membrane localization of GFP-MT1-MMPcompared to that observed in response to 0.12 or 12 dyn/cm^2 WSS (Fig.26). In addition, both calpain inhibitor and Akt inhibitor X completely blocked MT1-MMP membrane localization in the presence of S1P and 5.3 dyn/cm^2 WSS (cf. Figs.22 and 26).

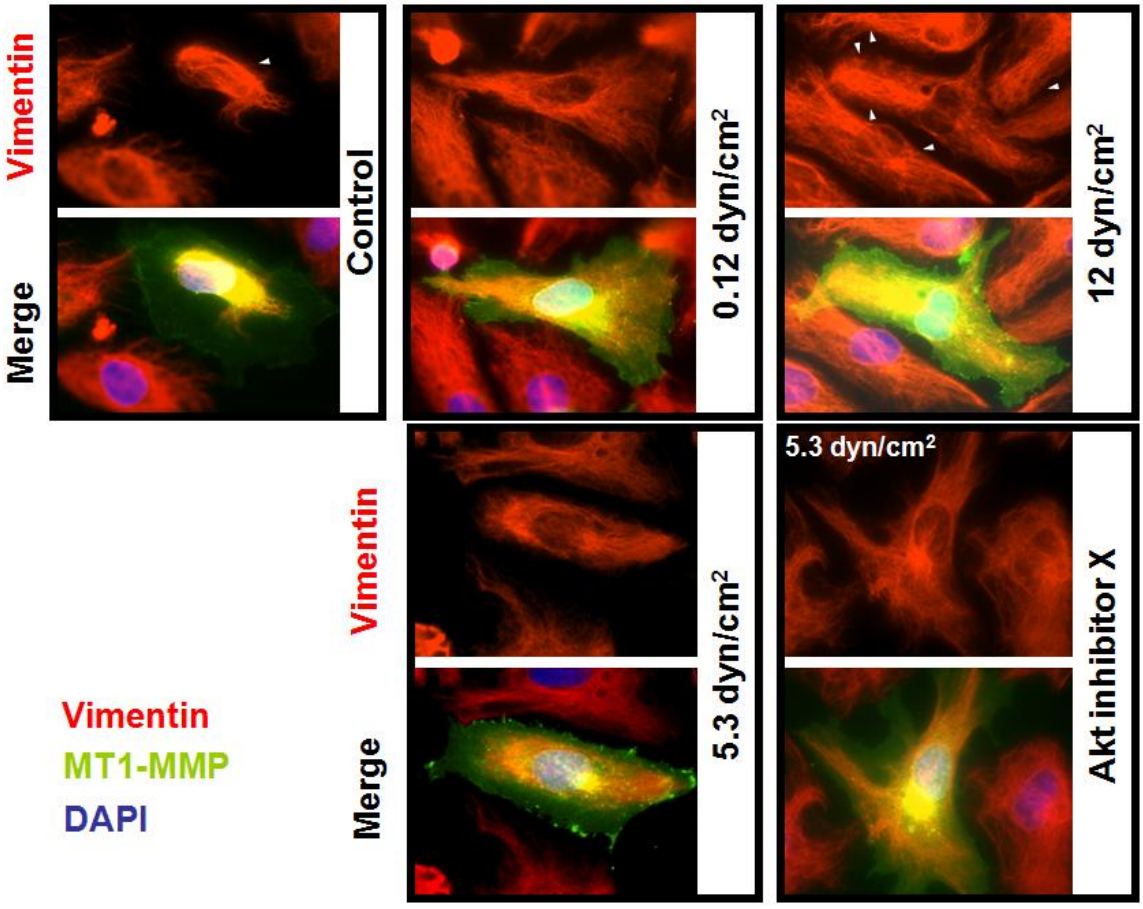

Figure 26. Akt blockade and 12 dyn/cm^2 WSS exhibited dense vimentin network with thick vimentin bundles in the presence of S1P. ECs subjected to WSS magnitudes of 0 (Control), 0.12, 5.3, or 12 or 5.3 dyn/cm^2 WSS + S1P were transiently transfected with vectors expressing MT1-MMP-green fluorescent protein (GFP) chimera. Localization of vimentin protein is shown by immunofluorescence stained with an anti-FLAG monoclonal primary antibody and FITC-conjugated secondary antibodies. Cells were treated identically to Figure 22 without (S1P+WSS) or with (S1P+WSS+Akt inhibitor X) pretreating with Akt inhibitor (10μM) for 1 h prior to beginning experiments. The compound was maintained in the flow media for the duration of 2 h WSS treatment. At the conclusion of the experiments, samples were fixed in fresh 4% paraformaldehyde and immunofluorescence was performed with antisera directed to vimentin. White arrowheads indicate vimentin bundles.

Vimentin and PAK Phosphorylation Are Enhanced by S1P and 5.3 dyn/cm^2 WSS in a Akt-dependent Manner

As shown above, S1P synergized with 5.3 dyn/cm^2 WSS increases vimentin cleavage which is required for EC invasion by knockdown of vimentin and calpain inhibitor (cf. Figs. 24 and 25). Altogether, these data suggested that S1P- and WSS-regulated vimentin cleavage had a very important role in facilitating EC invasion in 3-D collagen matrices. It was still unclear how S1P and WSS-activated calpain could induce vimentin filament disassembly. We hypothesized that calpain may directly cleave vimentin and calpain-dependent Akt can phosphorylate vimentin to induce vimentin depolymerization. S1P- and WSS-activated calpains are likely to responsible for vimentin cleavage since the calpain inhibitor significantly blocked vimentin cleavage, resulting in decreasing EC invasion (cf. Fig. 25). Interestingly, PAK regulated by Akt [180-182] phosphorylates vimentin at Ser-56 [183] and Ser-25, -38, -50, -65, and -72 [59]. Based on these results, we next determined whether Akt phosphorylate PAK and vimentin. ECs exposed to S1P and 5.3 dyn/cm^2 WSS were cultured in the presence or absence of Akt inhibitor X. Akt inhibitor X dose-dependently blocked EC invasion (Figs. 27A and 28) as well as attenuating MT1-MMP activity. Furthermore, it reduced PAK phosphorylation, vimentin cleavage, vimentin phosphorylation at Ser-6, -38, -56, and -72 (Fig. 29).

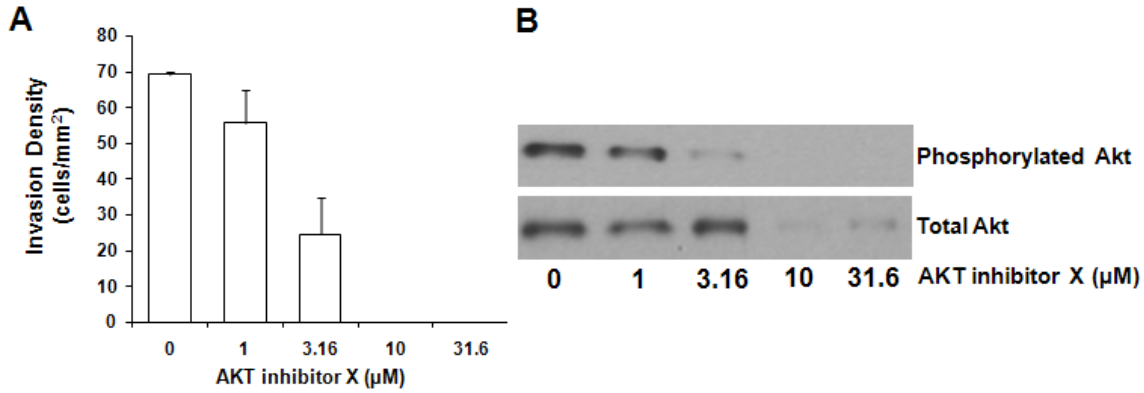

Figure 27. Akt inhibitor X reduces EC invasion in a dose-dependent manner. A; ECs were subjected to both S1P and GF for 18 h in the presence of either Ethanol control or Akt inhibitor X in a dose-dependent manner. **B;** Western blot analysis was performed with an antibody directed against the Akt phosphorylation (upper blot) and total Akt (lower blot). The blot is representative of 3 separate experiments (**A;** means ±SD).

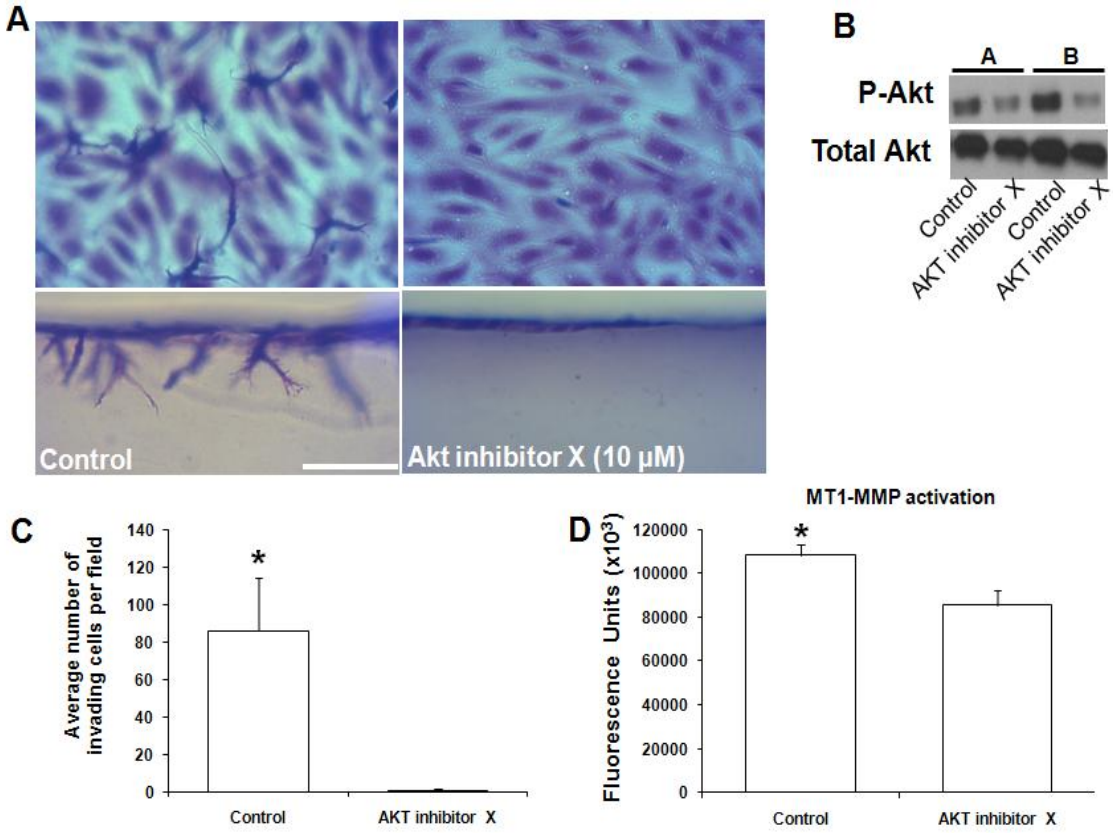

Figure 28. Akt inhibitor X significantly reduced EC invasion and MT1-MMP activation. A: Photographs of cell invasion responses after 24 h of exposure to 1 μm S1P and 5.3 dyn/cm^2 WSS in the presence (left) and absence (right) of 3 μM Akt inhibitor X. **B**: Western blot analysis was performed with an antibody directed against Akt phosphorylation (**B**; upper blot) and total Akt (**B**; lower blot). The blot is representative of 3 separate experiments. **C**: Cultures were fixed and stained to quantify the number of cells invading per field. **D**: MT1-MMP activation was measured in ECs subjected to S1P and 5.3 dyn/cm^2 WSS in the presence and absence of the Akt inhibitor X. Each data point was an average of triplicate wells from three individual experiments * t-test ($P<0.05$).

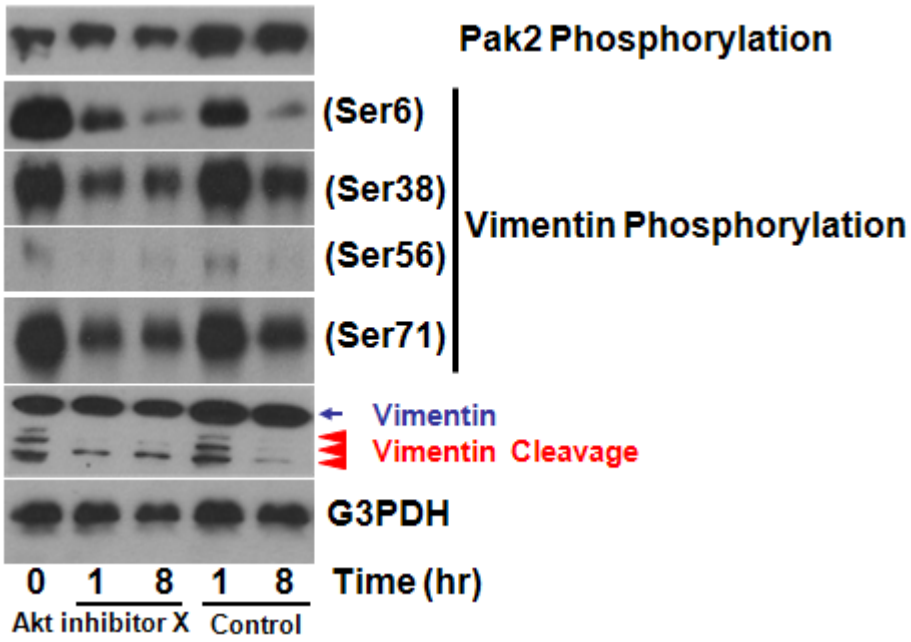

Figure 29. Akt inhibitor X downregulated Vimentin and PAK phosphorylation during S1P/WSS-induced EC invasion in 3-D collagen matrices. Akt inhibitor X significantly reduced vimentin cleavage, vimentin phosphorylation at ser -6, -38, -56, and -71 and Pak 2 phosphorylation. ECs were subjected to 5.3 dyn/cm^2 WSS for 1 and 8 h in the presence of S1P and either M199 control or Akt inhibitor X (10μM). Western blot analysis was performed with an antibody directed against the phospho-specific PAK, phospho-specific vimentin, total vimentin, and G3PDH. The blot is representative of 3 separate experiments.

PAK Phosphorylation Is Required for EC Invasion in 3-D Collagen Matrices

Kiosses et al. [36] demonstrated that dominant-negative PAK can block bFGF-induced angiogenesis in vivo. To demonstrate a functional requirement for phosphorylated PAK during S1P- and WSS- induced EC invasion, ECs were treated with either PAK inhibitory peptide or PAK control peptide (Fig. 30). The peptide was fused to the polybasic sequence from the HIV Tat protein to facilitate entry into ECs. The inhibitory peptide selectively binds to an SH3 domain from the adapter protein NCK to disrupt binding with PAK, which then inhibits PAK activity. The PAK inhibitory peptide treatment significantly attenuated EC invasion (Figs. 30A and B). PAK inhibitory peptide also reduced both PAK and Akt phosphorylation by Western blot analyses (Fig. 30C). These results confirm that PAK activity is required for S1P- and WSS-induced EC invasion and indicate that PAK acts upstream of Akt.

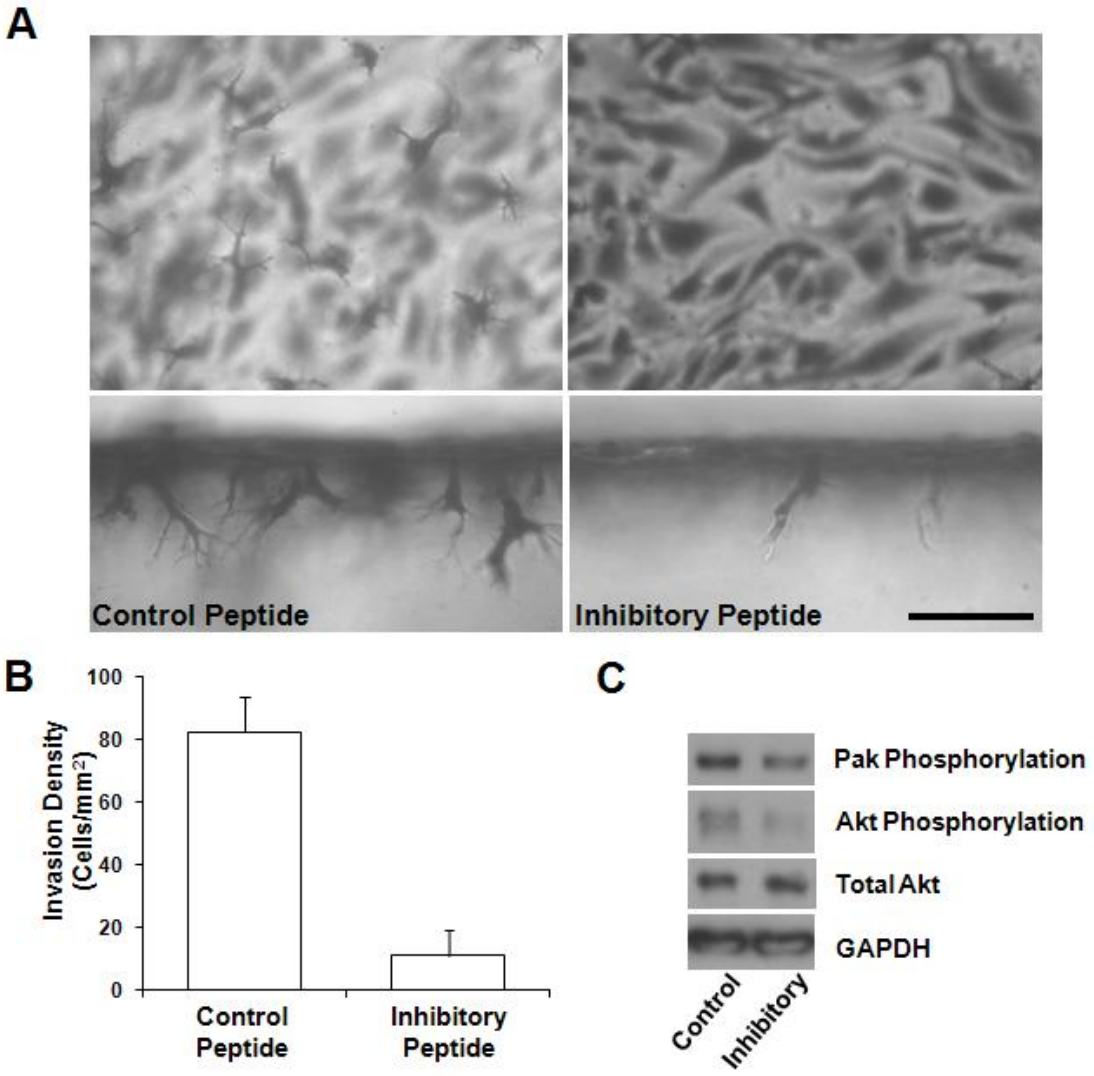

Figure 30. PAK phosphorylation is required for S1P and WSS-induced EC invasion in 3-D collagen matrices. ECs were subjected to 5.3 dyn/cm^2 WSS for 1 and 24 h in the presence of S1P and either PAK control peptide or PAK inhibitory peptide (20ug/ml). Western blot analysis was performed with an antibody directed against the phospho-specific PAK, phospho-specific Akt, total Akt, and G3PDH. The blot is representative of 3 separate experiments.

Discussion

In this chapter, we defined a novel mechanism by which S1P and WSS synergistically induce EC invasion through vimentin remodeling. Vimentin knockdown with shRNA greatly attenuated invasion caused by WSS and S1P, which indicates vimentin is necessary in this process. Further, WSS+S1P induced vimentin disassembly in a WSS magnitude-dependent manner as evidenced by the appearance of vimentin cleavage products in western blots (cf. Fig. 25A) and by retraction of the vimentin network observed in immunostainings (cf. Fig. 26). A WSS of 5.3 dyn/cm^2 was found to be optimal for inducing vimentin cleavage. This is consistent with the optimal WSS for activating Akt, calpain, MMP-2, MT1-MMP and cell invasion as shown in the previous chapters. We provide strong evidence indicating that the activation of MT1-MMP in response to WSS and S1P occurs as a consequence of vimentin network disassembly through calpain and Akt activation.

Vimentin appears to regulate invasion in a manner dependent on calpain and Akt. This is supported by the attenuation of vimentin cleavage when cells were treated with global calpain inhibitor or with Akt Inhibitor X. Akt inhibition also blocked the retraction of the vimentin network from the cell periphery in response to 5.3 dyn/cm^2 WSS and S1P. Calpain can induce vimentin filament disassembly directly through cleavage [169]. Akt likely regulates vimentin filament disassembly via phosphorylation of vimentin head domains, which then reduces filament stability. Tsuruta and Jones [169] demonstrated that 12 dyn/cm^2 WSS-induced thick vimentin bundles assembled and associated with large focal contacts that restricted EC movement. Interestingly, our immunofluorescence experiments also revealed that WSS dramatically changes vimentin organization, where 12 dyn/cm^2 WSS synergized with S1P to produce long and thick vimentin filaments. These results are consistent with the reduction in vimentin cleavage observed with 12 dyn/cm^2 WSS.

We suggest that vimentin disassembly is dependent on the magnitude of WSS and the activities of calpain, Akt and PAK2. Izawa and Inagaki [57] reported that PAK, a downstream effector of Akt, phosphorylates vimentin at Ser-25,-38,-50,-65, and-72 in the mouse vimentin head domain. Tang et al. [58] demonstrated that PAK-regulated vimentin phosphorylation at Ser -56 is required for smooth muscle cell motility. While it is well known that depolymerized vimentin is necessary for disrupted vimentin networks, a study of vimentin phosphorylation has not been reported in EC sprouting events. Our results showed that Akt-dependent PAK phosphorylation is required for S1P- and WSS-induced EC invasion. Further, inhibition of PAK with an inhibitor peptide reduced EC invasion as well as Akt phosphorylation. We suggest that Akt and PAK each phosphorylate vimentin to result in vimentin network disassembly. Our results provide a clue as to how MT1-MMP can translocate to the membrane in response to disassembly of the vimentin network. The vimentin network has a radial organization, extending outwards from the cell centre and interacts with microtubules [184, 185]. All forms of vimentin filaments in living cells move along microtubules both towards and away from the cell center [184, 186]. The vimentin cleavage fragments cleaved by calpain interact with and transport phosphorylated ERK 1/2 on dynein [187]. Based on these results, we hypothesize that calpain-cleaved vimentin binding to MT1-MMP may be transported to the cell periphery by kinesin. Further investigation is needed to determine the molecular interaction amongst MT1-MMP, vimentin and kinesin.

CHAPTER V

CONCLUSIONS

We established for the first time a novel model to study the synergic effects of biochemical factors and mechanical stimuli during EC invasion in 3-D collagen matrices. The results in Chapter II provide new sights into the roles of the S1P and WSS during EC invasion with the very interesting result that WSS is a strong positive modulator of S1P-induced EC invasion. The results in Chapters III and IV went on to define the roles of MT1-MMP, calpain, Akt, PAK and vimentin in S1P- and WSS-induced EC invasion in 3-D collagen matrices.

Many groups studied EC angiogenesis in 2D culture, but this approach is fundamentally limited in its ability to recapitulate the environment that ECs experience *in vivo* during angiogenesis. In support of this claim, Davis and colleagues [50, 193] recently demonstrated that the activation of MT1-MMP and Cdc42 plays a key role in regulating lumen and tube formation in 3D collagen matrices, but not in 2D collagen surface. The addition of physiological flow adds yet another dimension to the model that has provided unpredicted results. Specifically, fluid forces can enhance EC invasion to a comparable extent as the well-known proangiogenic growth factors VEGF and FGF.

Another unexpected finding was that the effect of WSS is greatest at a magnitude of 5.3 dyn/cm^2. A wide range of WSS levels are used to study mechanotransduction events *in vitro*, with many studies utilizing shear stresses of 12 dyn/cm^2 or greater.

However, typical WSS magnitudes in the microvasculature are reported to be in the range of 5 to 150 dyn/cm^2 [103, 104]. WSS levels in postcapillary venules in mouse cremaster muscle have been estimated to be in the range of 1 to 5 dyn/cm^2 [105]. Ichioka et al. [74] reported that increasing WSS in postcapillary venules from 3.7 to 5.3 dyn/cm^2.singificantly enhanced angiogenesis in a rabbit ear window model. WSS levels in post-capillary venules have been estimated at 1-5 dyn/cm^2 [165], which is consistent with a previous report of 0-5 dyn/cm^2 laminar shear stress in the mouse embryo [166]. It is important to note that sprouting angiogenesis is primarily localized to postcapillary venules, which under quiescent conditions are exposed to relatively lower WSS than blood vessels in other areas of the vasculature.

The synergistic effects of WSS and S1P are particularly relevant to understanding angiogenesis that occurs during wound healing. Wound healing is a complex process in which the skin or organ repairs itself after injury. Platelets from damaged blood vessels accumulate into the wound where they can create a provisional matrix, release a number of biochemical factors including VEGF, bFGF, and S1P [89-92]. The high concentration of these factors in the wound provides a directional cue for EC invasion toward the provisional matrix. Additional inflammatory mediators released locally result in vasodilatory responses that ultimately increase WSS via increased blood flow.

Although my experiments were only performed on ECs subjected to laminar fluid shear stress, my findings may also help to understand the endothelial response to other mechanical stimuli. Interstitial flow, for example, causes migration of ECs and

smooth muscle cells[188] [189] [190] and cyclic stretch triggers angiogenic events in coronary microvascular ECs [191] and epithelial cells [192]. The overall goal of this research is to provide a better understanding of the role of laminar fluid shear stress on angiogenic sprouting events in 3-D collagen matrices. My findings in this dissertation may help to explain why the synergistic effect of S1P and wall shear stress is important in angiogenesis.

These studies provide a novel molecular mechanism of angiogenic sprouting events induced by S1P and WSS and underlie embryonic development, wound healing, and tumor angiogenesis, where biochemical and mechanical cues are optimal for initiation of new blood vessel growth. While these studies herein have provided significant insight into the molecular mechanisms that mediate the effects of WSS and S1P on EC invasion, it is expected that the experimental model developed as a result of this dissertation will be useful to further explore the processes that regulate angiogenesis.

REFERENCES

1. **Folkman J, D'Amore PA.** Blood vessel formation: what is its molecular basis? *Cell* 87(7): 1153-5, 1996.

2. **Carmeliet P.** Manipulating angiogenesis in medicine. *J Intern Med* 255(5): 538-61, 2004.

3. **Bayless KJ, Davis GE.** The Cdc42 and Rac1 GTPases are required for capillary lumen formation in three-dimensional extracellular matrices. *J Cell Sci* 115(Pt 6): 1123-36, 2002.

4. **Bayless KJ, Davis GE.** Sphingosine-1-phosphate markedly induces matrix metalloproteinase and integrin-dependent human endothelial cell invasion and lumen formation in three-dimensional collagen and fibrin matrices. *Biochem Biophys Res Commun* 312(4): 903-13, 2003.

5. **Hla T.** Physiological and pathological actions of sphingosine 1-phosphate. *Semin Cell Dev Biol* 15(5): 513-20, 2004.

6. **Lee MJ, Van Brocklyn JR, Thangada S, Liu CH, Hand AR, et al.** Sphingosine-1-phosphate as a ligand for the G protein-coupled receptor EDG-1. *Science* 279(5356): 1552-5, 1998.

7. **Vogler R, Sauer B, Kim DS, Schafer-Korting M, Kleuser B.** Sphingosine-1-phosphate and its potentially paradoxical effects on critical parameters of cutaneous wound healing. *J Invest Dermatol* 120(4): 693-700, 2003.

8. **Hla T, Lee MJ, Ancellin N, Liu CH, Thangada S, et al.** Sphingosine-1-phosphate: extracellular mediator or intracellular second messenger? *Biochem Pharmacol* 58(2): 201-7, 1999.

9. **Oyama O, Sugimoto N, Qi X, Takuwa N, Mizugishi K, et al.** The lysophospholipid mediator sphingosine-1-phosphate promotes angiogenesis in vivo in ischaemic hindlimbs of mice. *Cardiovasc Res* 78(2): 301-7, 2008.

10. **Yan G, Chen S, You B, Sun J.** Activation of sphingosine kinase-1 mediates induction of endothelial cell proliferation and angiogenesis by epoxyeicosatrienoic acids. *Cardiovasc Res* 78(2): 308-14, 2008.

11. **Gingras D, Michaud M, Di Tomasso G, Beliveau E, Nyalendo C, et al.** Sphingosine-1-phosphate induces the association of membrane-type 1 matrix metalloproteinase with p130Cas in endothelial cells. *FEBS Lett* 582(3): 399-404, 2008.

12. **Li Z, Paik JH, Wang Z, Hla T, Wu D.** Role of guanine nucleotide exchange factor P-Rex-2b in sphingosine 1-phosphate-induced Rac1 activation and cell migration in endothelial cells. *Prostaglandins Other Lipid Mediat*x 76(1-4): 95-104, 2008.

13. **Su SC, Maxwell SA, Bayless KJ.** Annexin 2 regulates endothelial morphogenesis by controlling AKT activation and junctional integrity. *J Biol Chem* 285(52): 40624-34, 2010.

14. **Zhao YD, Ohkawara H, Rehman J, Wary KK, Vogel SM, et al.** Bone marrow progenitor cells induce endothelial adherens junction integrity by sphingosine-1-phosphate-mediated Rac1 and Cdc42 signaling. *Circ Res* 105(7): 696-704, 2009.

15. **Sun X, Shikata Y, Wang L, Ohmori K, Watanabe N, et al.** Enhanced interaction between focal adhesion and adherens junction proteins: involvement in sphingosine 1-phosphate-induced endothelial barrier enhancement. *Microvasc Res* 77(3): 304-13, 2009.

16. **Mehta D, Konstantoulaki M, Ahmmed GU, Malik AB.** Sphingosine 1-phosphate-induced mobilization of intracellular Ca2+ mediates rac activation and adherens junction assembly in endothelial cells. *J Biol Chem* 280(17): 17320-8, 2005.

17. **Takabe K, Paugh SW, Milstien S, Spiegel S.** "Inside-out" signaling of sphingosine-1-phosphate: therapeutic targets. *Pharmacol Rev* 60(2): 181-95, 2008.

18. **Spiegel S, Takabe K, Paugh SW, Milstien S, Spiegel S.** Sphingosine-1-phosphate: an enigmatic signalling lipid. *Nat Rev Mol Cell Biol* 4(5): 397-407, 2003.

19. **Kim RH, Takabe K, Milstien S, Spiegel S.** Export and functions of sphingosine-1-phosphate. *Biochim Biophys Acta* 1791(7): 692-6, 2009.

20. **Li YS, Haga JH, Chien S.** Molecular basis of the effects of shear stress on vascular endothelial cells. *J Biomech* 38(10): 1949-71, 2005.

21. **Nerem RM.** Hemodynamics and the vascular endothelium. *J Biomech Eng* 115(4B): 510-4, 1993.

22. **Takahashi M, Ishida T, Traub O, Corson MA, Berk BC.** Mechantransduction in endothelial cells: temporal signaling events in response to shear stress. *J Vasc Res* 34(3): 212-9, 1997.

23. **Lucitti JL, Jones EA, Huang C, Chen J, Fraser SE, et al.** Vascular remodeling of the mouse yolk sac requires hemodynamic force. *Development* 134(18): 3317-26, 2007.

24. **Nasu R, Kimura H, Akagi K, Murata T, Tanaka Y.** Blood flow influences vascular growth during tumor angiogenesis. *British Journal of Cancer* 79(5-6): 780-6, 1999.

25. **Carragher NO, Frame MC.** Calpain: a role in cell transformation and migration. *Int J Biochem Cell Biol* 34(12): 1539-43, 2002.

26. **Suzuki K, Sorimachi H.** A novel aspect of calpain activation. *FEBS Lett* 433(1-2): 1-4, 1998.

27. **Ono Y, Sorimachi H, Suzuki K.** Structure and physiology of calpain, an enigmatic protease. *Biochem Biophys Res Commun* 245(2): 289-94, 1998.

28. **Sorimachi H, Ishiura S, Suzuki K.** Structure and physiological function of calpains. *Biochem J* 328 (Pt 3): 721-32, 1997.

29. **Dourdin N, Bhatt AK, Dutt P, Greer PA, Arthur JS, et al.** Reduced cell migration and disruption of the actin cytoskeleton in calpain-deficient embryonic fibroblasts. *J Biol Chem* 276(51): 48382-8, 2001.

30. **Carragher NO, Fincham VJ, Riley D, Frame MC.** Cleavage of focal adhesion kinase by different proteases during SRC-regulated transformation and apoptosis. Distinct roles for calpain and caspases. *J Biol Chem* 276(6): 4270-5, 2001.

31. **Carragher NO, Levkau B, Ross R, Raines EW.** Degraded collagen fragments promote rapid disassembly of smooth muscle focal adhesions that correlates with cleavage of pp125(FAK), paxillin, and talin. *J Cell Biol* 147(3): 619-30, 1999.

32. **Manning BD, Cantley LC.** AKT/PKB signaling: navigating downstream. *Cell* 129(7): 1261-74, 2007.

33. **Wu H, Riha GM, Tang H, Li M, Yao Q, et al.** Differentiation and proliferation of endothelial progenitor cells from canine peripheral blood mononuclear cells. *J Surg Res* 126(2): 193-8, 2005.

34. **Chen J, Somanath PR, Razorenova O, Chen WS, Hay N, et al.** Akt1 regulates pathological angiogenesis, vascular maturation and permeability in vivo. *Nat Med* 11(11): 1188-96, 2005.

35. **Kiosses WB, et al.** A role for p21-activated kinase in endothelial cell migration. *J Cell Biol* 147(4): 831-44, 1999.

36. **Kiosses WB, Daniels RH, Otey C, Bokoch GM, Schwartz MA.** A dominant-negative p65 PAK peptide inhibits angiogenesis. *Circ Res* 90(6): 697-702, 2002.

37. **Orr AW, Stockton R, Simmers MB, Sanders JM, Sarembock IJ, et al.** Matrix-specific p21-activated kinase activation regulates vascular permeability in atherogenesis. *J Cell Biol* 176(5): 719-27, 2007.

38. **Tang Y, Chen Z, Ambrose D, Liu J, Gibbs JB, et al.** Kinase-deficient Pak1 mutants inhibit Ras transformation of Rat-1 fibroblasts. *Mol Cell Biol* 17(8): 4454-64, 1997.

39. **King AJ, Sun H, Diaz B, Barnard D, Miao W, et al.** The protein kinase Pak3 positively regulates Raf-1 activity through phosphorylation of serine 338. *Nature* 396(6707): 180-3, 1998.

40. **Zhang S, Han J, Sells MA, Chernoff J, Knaus UG, et al.** Rho family GTPases regulate p38 mitogen-activated protein kinase through the downstream mediator Pak1. *J Biol Chem* 270(41): 23934-6, 1995.

41. **Bagrodia S, Dérijard B, Davis RJ, Cerione RA.** Cdc42 and PAK-mediated signaling leads to Jun kinase and p38 mitogen-activated protein kinase activation. *J Biol Chem* 270(47): 27995-8, 1995.

42. **Manser E, Leung T, Salihuddin H, Zhao ZS, Lim L.** A brain serine/threonine protein kinase activated by Cdc42 and Rac1. *Nature* 367(6458): 40-6, 1994.

43. **Buday L, Wunderlich L, Tamas P.** The Nck family of adapter proteins: regulators of actin cytoskeleton. *Cell Signal* 14(9): 723-31, 2002.

44. **Bokoch GM, Wang Y, Bohl BP, Sells MA, Quilliam LA, et al.** Interaction of the Nck adapter protein with p21-activated kinase (PAK1). *J Biol Chem* 271(42): 25746-9, 1996.

45. **Galisteo ML, Chernoff J, Su YC, Skolnik EY, Schlessinger J.** The adaptor protein Nck links receptor tyrosine kinases with the serine-threonine kinase Pak1. *J Biol Chem* 271(35): 20997-1000, 1996.

46. **Zeng Q, Lagunoff D, Masaracchia R, Goeckeler Z, Côté G, et al.** Endothelial cell retraction is induced by PAK2 monophosphorylation of myosin II. *J Cell Sci* 113 (Pt 3): 471-82, 2000.

47. **Koh W, Mahan RD, Davis GE.** Cdc42- and Rac1-mediated endothelial lumen formation requires Pak2, Pak4 and Par3, and PKC-dependent signaling. *J Cell Sci* 121(Pt 7): 989-1001, 2008.

48. **Chun TH, Chun TH, Sabeh F, Ota I, Murphy H, McDonagh KT, et al.** MT1-MMP-dependent neovessel formation within the confines of the three-dimensional extracellular matrix. *J Cell Biol* 167(4): 757-67, 2004.

49. **Pepper MS.** Role of the matrix metalloproteinase and plasminogen activator-plasmin systems in angiogenesis. *Arterioscler Thromb Vasc Biol* 21(7): 1104-17, 2001.

50. **Fisher KE, Sacharidou A, Stratman AN, Mayo AM, Fisher SB, et al.** MT1-MMP- and Cdc42-dependent signaling co-regulate cell invasion and tunnel formation in 3D collagen matrices. *J Cell Sci* 122(Pt 24): 4558-69, 2009.

51. **Hotary KB, Yana I, Sabeh F, Li XY, Holmbeck K, et al.** Matrix metalloproteinases (MMPs) regulate fibrin-invasive activity via MT1-MMP-dependent and -independent processes. *J Exp Med* 195(3): 295-308, 2002.

52. **Langlois S, Gingras D, Beliveau R.** Membrane type 1-matrix metalloproteinase (MT1-MMP) cooperates with sphingosine 1-phosphate to induce endothelial cell migration and morphogenic differentiation. *Blood* 103(8): 3020-8, 2004.

53. **Eriksson JE, He T, Trejo-Skalli AV, Härmälä-Braskén AS, Hellman J, et al.** Specific in vivo phosphorylation sites determine the assembly dynamics of vimentin intermediate filaments. *J Cell Sci* 117(Pt 6): 919-32, 2004.

54. **Gilles C, Polette M, Zahm JM, Tournier JM, Volders L, et al.** Vimentin contributes to human mammary epithelial cell migration. *J Cell Sci* 112 (Pt 24): 4615-25, 1999.

55. **Eckes B, Dogic D, Colucci-Guyon E, Wang N, Maniotis A, et al.** Impaired mechanical stability, migration and contractile capacity in vimentin-deficient fibroblasts. *J Cell Sci* 111 (Pt 13): 1897-907, 1998.

56. **Ivaska J, Pallari HM, Nevo J, Eriksson JE.** Novel functions of vimentin in cell adhesion, migration, and signaling. *Exp Cell Res* 313(10): 2050-62, 2007.

57. **Izawa I, Inagaki M.** Regulatory mechanisms and functions of intermediate filaments: a study using site- and phosphorylation state-specific antibodies. *Cancer Sci* 97(3): 167-74, 2006.

58. **Tang DD, Bai Y, Gunst SJ.** Silencing of p21-activated kinase attenuates vimentin phosphorylation on Ser-56 and reorientation of the vimentin network during stimulation of smooth muscle cells by 5-hydroxytryptamine. *Biochem J* 388(Pt 3): 773-83, 2005.

59. **Goto H, Tanabe K, Manser E, Lim L, Yasui Y, Inagaki M.** Phosphorylation and reorganization of vimentin by p21-activated kinase (PAK). *Genes Cells* 7(2): 91-7, 2002.

60. **Zhu QS, Rosenblatt K, Huang KL, Lahat G, Brobey R, et al.** Vimentin is a novel AKT1 target mediating motility and invasion. *Oncogene*, doi:10.1038, 2010.

61. **Traub P, Scherbarth A, Willingale-Theune J, Paulin-Levasseur M, Shoeman R.** Differential sensitivity of vimentin and nuclear lamins from Ehrlich ascites tumor cells toward Ca^{2+}-activated neutral thiol proteinase. *Eur J Cell Biol* 46(3): 478-90, 1988.

62. **Nelson WJ, Traub P.** Proteolysis of vimentin and desmin by the Ca2+-activated proteinase specific for these intermediate filament proteins. *Mol Cell Biol* 3(6): 1146-56, 1983.

63. **Li QF, Spinelli AM, Wang R, Anfinogenova Y, Singer HA, et al.** Critical role of vimentin phosphorylation at Ser-56 by p21-activated kinase in vimentin cytoskeleton signaling. *J Biol Chem* 281(45): 34716-24, 2006.

64. **Perlson E, Hanz S, Ben-Yaakov K, Segal-Ruder Y, Seger R, et al.** Vimentin-dependent spatial translocation of an activated MAP kinase in injured nerve. *Neuron* 45(5): 715-26, 2005.

65. **Helfand BT, Chou YH, Shumaker DK, Goldman RD.** Intermediate filament proteins participate in signal transduction. *Trends Cell Biol* 15(11): 568-70, 2005.

66. **Helfand BT, Loomis P, Yoon M, Goldman RD.** Rapid transport of neural intermediate filament protein. *J Cell Sci* 116(Pt 11): 2345-59, 2003.

67. **Carmeliet P, Jain RK.** Angiogenesis in cancer and other diseases. *Nature* 407(6801): 249-57, 2000.

68. **Folkman J, Shing Y.** Angiogenesis. *J Biol Chem* 267(16): 10931-4, 1992.

69. **Gerwins P, Skoldenberg E, Claesson-Welsh L.** Function of fibroblast growth factors and vascular endothelial growth factors and their receptors in angiogenesis. *Crit Rev Oncol Hematol* 34(3): 185-94, 2000.

70. **Davis GE, Black SM, Bayless KJ.** Capillary morphogenesis during human endothelial cell invasion of three-dimensional collagen matrices. *In Vitro Cell Dev Biol Anim* 36(8): 513-9, 2000.

71. **Chalfant CE, Spiegel S.** Sphingosine 1-phosphate and ceramide 1-phosphate: expanding roles in cell signaling. *J Cell Sci* 118(Pt 20): 4605-12, 2005.

72. **Oyama O, Sugimoto N, Qi X, Takuwa N, Mizugishi K, et al.** The lysophospholipid mediator sphingosine-1-phosphate promotes angiogenesis in vivo in ischaemic hindlimbs of mice. *Cardiovasc Res 78(2):301-7*, 2008.

73. **Clark AJ, Gaddie R, Stewart CP.** The metabolism of the isolated heart of the frog. *J Physiol* 72(4): 443-66, 1931.

74. **Ichioka S, Shibata M, Kosaki K, Sato Y, Harii K, et al.** Effects of shear stress on wound-healing angiogenesis in the rabbit ear chamber. *J Surg Res* 72(1): 29-35, 1997.

75. **Nasu R, Kimura H, Akagi K, Murata T, Tanaka Y.** Blood flow influences vascular growth during tumour angiogenesis. *Br J Cancer* 79(5-6): 780-6, 1999.

76. **Miyazaki T, Honda K, Ohata H.** Requirement of Ca2+ influx- and phosphatidylinositol 3-kinase-mediated m-calpain activity for shear stress-induced endothelial cell polarity. *Am J Physiol Cell Physiol* 293(4): C1216-25, 2007.

77. **Gloe T, Sohn HY, Meininger GA, Pohl U.** Shear stress-induced release of basic fibroblast growth factor from endothelial cells is mediated by matrix interaction via integrin alpha(v)beta3. *J Biol Chem* 277(26): 23453-8, 2002.

78. **Cullen JP, Sayeed S, Sawai RS, Theodorakis NG, Cahill PA, et al.** Pulsatile flow-induced angiogenesis: role of G(i) subunits. *Arterioscler Thromb Vasc Biol* 22(10): 1610-6, 2002.

79. **Saunders WB, Bayless KJ, Davis GE.** MMP-1 activation by serine proteases and MMP-10 induces human capillary tubular network collapse and regression in 3D collagen matrices. *J Cell Sci* 118(Pt 10): 2325-40, 2005.

80. **Stratman AN, Saunders WB, Sacharidou A, Koh W, Fisher KE, et al.** Endothelial cell lumen and vascular guidance tunnel formation requires MT1-MMP-dependent proteolysis in 3-dimensional collagen matrices. *Blood* 114(2): 237-47, 2009.

81. **Ueda A, Koga M, Ikeda M, Kudo S, Tanishita K.** Effect of shear stress on microvessel network formation of endothelial cells with in vitro three-dimensional model. *Am J Physiol Heart Circ Physiol* 287(3): H994-1002, 2004.

82. **Maciag T, Cerundolo J, Ilsley S, Kelley PR, Forand R, et al.** An endothelial cell growth factor from bovine hypothalamus: identification and partial characterization. *Proc Natl Acad Sci USA 76*(11): 5674-8, 1979.

83. **Bornstein MB.** Reconstituted rattail collagen used as substrate for tissue cultures on coverslips in Maximow slides and roller tubes. *Lab Invest* 7(2): 134-7, 1958.

84. **Kang H, Bayless KJ, Kaunas R.** Fluid shear stress modulates endothelial cell invasion into three-dimensional collagen matrices. *Am J Physiol Heart Circ Physiol* 295(5): H2087-97, 2008.

85. **Hughes SK, Wacker BK, Kaneda MM, Elbert DL.** Fluid shear stress modulates cell migration induced by sphingosine 1-phosphate and vascular endothelial growth factor. *Ann Biomed Eng* 33(8): 1003-14, 2005.

86. **Igarashi J, Erwin PA, Dantas AP, Chen H, Michel T, et al.** VEGF induces S1P1 receptors in endothelial cells: Implications for cross-talk between sphingolipid and growth factor receptors. *Proc Natl Acad Sci USA* 100(19): 10664-9, 2003.

87. **Murata N, Sato K, Kon J, Tomura H, Okajima F.** Quantitative measurement of sphingosine 1-phosphate by radioreceptor-binding assay. *Anal Biochem* 282(1): 115-20, 2000.

88. **Thi MM, lacobas DA, lacobas S, Spray DC.** Fluid shear stress upregulates vascular endothelial growth factor gene expression in osteoblasts. *Ann N Y Acad Sci* 1117: 73-81, 2007.

89. **Dardik A, Chen L, Frattini J, Asada H, Aziz F, et al.** Differential effects of orbital and laminar shear stress on endothelial cells. *J Vasc Surg* 41(5): 869-80, 2005.

90. **Levesque MJ, Nerem RM, Sprague EA.** Vascular endothelial cell proliferation in culture and the influence of flow. *Biomaterials* 11(9): 702-7, 1990.

91. **Schluter C, Duchrow M, Wohlenberg C, Becker MH, Key G, et al.** The cell proliferation-associated antigen of antibody Ki-67: a very large, ubiquitous nuclear protein with numerous repeated elements, representing a new kind of cell cycle-maintaining proteins. *J Cell Biol* 123(3): 513-22, 1993.

92. **Lin K, Hsu PP, Chen BP, Yuan S, Usami S, et al.** Molecular mechanism of endothelial growth arrest by laminar shear stress. *Proc Natl Acad Sci USA* 97(17): 9385-9, 2000.

93. **Dewey CF, Bussolari SR, Gimbrone MA Jr, Davies PF, et al.** The dynamic response of vascular endothelial cells to fluid shear stress. *J Biomech Eng* 103(3): 177-85, 1981.

94. **Martin P, Leibovich SJ.** Inflammatory cells during wound repair: the good, the bad and the ugly. *Trends Cell Biol* 15(11): 599-607, 2005.

95. **Martyre MC,** Le Bousse-Kerdiles MC, Romquin N, Chevillard S, Praloran V, **et al.** Elevated levels of basic fibroblast growth factor in megakaryocytes and platelets from patients with idiopathic myelofibrosis. *Br J Haematol* 97(2): 441-8, 1997.

96. **Mohle R, Green D, Moore MA, Nachman RL, Rafii S.** Constitutive production and thrombin-induced release of vascular endothelial growth factor by human megakaryocytes and platelets. *Proc Natl Acad Sci USA* 94(2): 663-8, 1997.

97. **Yatomi Y, Igarashi Y, Yang L, Hisano N, Qi R, et al.** Sphingosine 1-phosphate, a bioactive sphingolipid abundantly stored in platelets, is a normal constituent of human plasma and serum. *J Biochem* 121(5): 969-73, 1997

98. **Shen YH, Shoichet MS, Radisic M.** Vascular endothelial growth factor immobilized in collagen scaffold promotes penetration and proliferation of endothelial cells. *Acta Biomater* 4(3): 477-89, 2008.

99. **Mohan S, Mohan N, Sprague EA.** Differential activation of NF-kappa B in human aortic endothelial cells conditioned to specific flow environments. *Am J Physiol* 273(2 Pt 1): C572-8, 1997.

100. **Hsu PP, Li S, Li YS, Usami S, Ratcliffe A, et al.** Effects of flow patterns on endothelial cell migration into a zone of mechanical denudation. *Biochem Biophys Res Commun* 285(3): 751-9, 2001.

101. **Venkataraman K, Lee YM, Michaud J, Thangada S, Ai Y, et al.** Vascular endothelium as a contributor of plasma sphingosine 1-phosphate. *Circ Res* 102(6): 669-76, 2008.

102. **Clark ER.** Studies on the growth of blood vessels in the tail of the frog larva by observation and experiment on the living animal. *Amer J Anat* 23: 73-88, 1918.

103. **House SD, Lipowsky HH.** Microvascular hematocrit and red cell flux in rat cremaster muscle. *Am J Physiol* 252(1 Pt 2): H211-22, 1987.

104. **Pries AR, Secomb TW, Gaehtgens P.** Design principles of vascular beds. *Circ Res* 77(5): 1017-23, 1995.

105. **Kim MB, Sarelius IH.** Distributions of wall shear stress in venular convergences of mouse cremaster muscle. *Microcirculation* 10(2): 167-78, 2003.

106. **Chien S.** Role of shear stress direction in endothelial mechanotransduction. *Mol Cell Biomech* 5(1): 1-8, 2008.

107. **Ishida T, Takahashi M, Corson MA, Berk BCl.** Fluid shear stress-mediated signal transduction: how do endothelial cells transduce mechanical force into biological responses? *Ann N Y Acad Sci* 811: 12-23; discussion 23-4, 1997.

108. **Nollert MU, Diamond SL, McIntire LV.** Hydrodynamic shear stress and mass transport modulation of endothelial cell metabolism. *Biotechnol Bioeng* 38(6): 88-602, 1991.

109. **Nollert MU, McIntire LV.** Convective mass transfer effects on the intracellular calcium response of endothelial cells. *J Biomech Eng* 114(3): p. 321-6, 1992.

110. **Shen J, Gimbrone MA Jr, Luscinskas FW, Dewey CF Jr.** Regulation of adenine nucleotide concentration at endothelium-fluid interface by viscous shear flow. *Biophys J* 64(4): 1323-30, 1993.

111. **John K, Barakat AI.** Modulation of ATP/ADP concentration at the endothelial surface by shear stress: effect of flow-induced ATP release. *Ann Biomed Eng* 29(9): 740-51, 2001.

112. **Choi HW, Barakat AI.** Modulation of ATP/ADP concentration at the endothelial surface by shear stress: effect of flow disturbance. *Conf Proc IEEE Eng Med Biol Soc* 7: 5065-8, 2004.

113. **Mo M, Eskin SG, Schilling WP.** Flow-induced changes in Ca2+ signaling of vascular endothelial cells: effect of shear stress and ATP. *Am J Physiol* 260(5 Pt 2): H1698-707, 1991.

114. **Dull RO, Davies PF.** Flow modulation of agonist (ATP)-response (Ca2+) coupling in vascular endothelial cells. *Am J Physiol* 261(1 Pt 2): H149-54, 1991.

115. **Carmeliet P.** Blood vessels and nerves: common signals, pathways and diseases. *Nat Rev Genet* 4(9): 710-20, 2003.

116. **Carmeliet P, Collen D.** Molecular basis of angiogenesis. Role of VEGF and VE-cadherin. *Ann N Y Acad Sci* 902: 249-62; discussion 262-4, 2000.

117. **English D, Garcia JG, Brindley DN.** Platelet-released phospholipids link haemostasis and angiogenesis. *Cardiovasc Res* 49(3): 588-99, 2001.

118. **Ariyoshi H, Yoshikawa N, Aono Y, Tsuji Y, Ueda A, et al.** Localized activation of m-calpain in migrating human umbilical vein endothelial cells stimulated by shear stress. *J Cell Biochem*. 81(1): 184-92, 2001

119. **Su Y, Cui Z, Li Z, Block ER.** Calpain-2 regulation of VEGF-mediated angiogenesis. *Faseb J* 20(9): 1443-51, 2006.

120. **Carragher NO, Fonseca BD, Frame MC.** Calpain activity is generally elevated during transformation but has oncogene-specific biological functions. *Neoplasia* 6(1): 53-73, 2004.

121. **Franco S, Perrin B, Huttenlocher A.** Isoform specific function of calpain 2 in regulating membrane protrusion. *Exp Cell Res* 299(1): 179-87, 2004.

122. **Wells A, Huttenlocher A, Lauffenburger DA.** Calpain proteases in cell adhesion and motility. *Int Rev Cytol* 245: 1-16, 2005.

123. **Butcher JT, Penrod AM, García AJ, Nerem RM.** Unique morphology and focal adhesion development of valvular endothelial cells in static and fluid flow environments. *Arterioscler Thromb Vasc Biol* 24(8): 1429-34, 2004.

124. **Tamada Y, Fukiage C, Boyle DL, Azuma M, Shearer TR.** Involvement of cysteine proteases in bFGF-induced angiogenesis in guinea pig and rat cornea. *J Ocul Pharmacol Ther* 16(3): 271-83, 2000.

125. **Flevaris P, Stojanovic A, Gong H, Chishti A, Welch E, et al.** A molecular switch that controls cell spreading and retraction. *J Cell Biol* 179(3): 553-65, 2007.

126. **Potter DA, Tirnauer JS, Janssen R, Croall DE, Hughes CN, et al.** Calpain regulates actin remodeling during cell spreading. *J Cell Biol* 141(3): 647-62, 1998.

127. **Cortesio CL, Chan KT, Perrin BJ, Burton NO, Zhang S, et al.** Calpain 2 and PTP1B function in a novel pathway with Src to regulate invadopodia dynamics and breast cancer cell invasion. *J Cell Biol* 180(5): 957-71, 2008.

128. **Calle Y, Carragher NO, Thrasher AJ, Jones GE.** Inhibition of calpain stabilises podosomes and impairs dendritic cell motility. *J Cell Sci* 119(Pt 11): 2375-85, 2006.

129. **Marzia M, Chiusaroli R, Neff L, Kim NY, Chishti AH, et al.** Calpain is required for normal osteoclast function and is down-regulated by calcitonin. *J Biol Chem* 281(14): 9745-54, 2006.

130. **Linder S, Aepfelbacher M.** Podosomes: adhesion hot-spots of invasive cells. *Trends Cell Biol* 13(7): 376-85, 2003.

131. **Shiojima I, Walsh K.** Role of Akt signaling in vascular homeostasis and angiogenesis. *Circ Res* 90(12): 1243-50, 2002.

132. **Dimmeler S, Zeiher AM.** Akt takes center stage in angiogenesis signaling. *Circ Res* 86(1): 4-5, 2000.

133. **Kureishi Y, Luo Z, Shiojima I, Bialik A, Fulton D, et al.** The HMG-CoA reductase inhibitor simvastatin activates the protein kinase Akt and promotes angiogenesis in normocholesterolemic animals. *Nat Med* 6(9): 1004-10, 2000.

134. **Morales-Ruiz M, Lee MJ, Zöllner S, Gratton JP, Scotland R, et al.** Sphingosine 1-phosphate activates Akt, nitric oxide production, and chemotaxis through a Gi protein/phosphoinositide 3-kinase pathway in endothelial cells. *J Biol Chem* 276(22): 19672-7, 2001.

135. **Gonzalez E, Kou R, Michel T.** Rac1 modulates sphingosine 1-phosphate-mediated activation of phosphoinositide 3-kinase/Akt signaling pathways in vascular endothelial cells. *J Biol Chem* 281(6): 3210-6, 2006.

136. **Lee MJ, Evans M, Hla T.** The inducible G protein-coupled receptor edg-1 signals via the G(i)/mitogen-activated protein kinase pathway. *J Biol Chem* 271(19): 11272-9, 1996.

137. **Dimmeler S, Assmus B, Hermann C, Haendeler J, Zeiher AM.** Fluid shear stress stimulates phosphorylation of Akt in human endothelial cells: involvement in suppression of apoptosis. *Circ Res* 83(3): 334-41, 1998.

138. **Dimmeler S, Fleming I, Fisslthaler B, Hermann C, Busse R, et al.** Activation of nitric oxide synthase in endothelial cells by Akt-dependent phosphorylation. *Nature* 399(6736): 601-5, 1999.

139. **Igarashi J, Bernier SG, Michel T.** Sphingosine 1-phosphate and activation of endothelial nitric-oxide synthase. differential regulation of Akt and MAP kinase pathways by EDG and bradykinin receptors in vascular endothelial cells. *J Biol Chem* 276(15): 12420-6, 2001.

140. **Gordan JD, Simon MC.** Hypoxia-inducible factors: central regulators of the tumor phenotype. *Curr Opin Genet Dev* 17(1): 71-7, 2007.

141. **Chlench S, Mecha Disassa N, Hohberg M, Hoffmann C, Pohlkamp T, et al.** Regulation of Foxo-1 and the angiopoietin-2/Tie2 system by shear stress. *FEBS Lett* 581(4): 673-80, 2007.

142. **Hotary K, Allen E, Punturieri A, Yana I, Weiss SJ.** Regulation of cell invasion and morphogenesis in a three-dimensional type I collagen matrix by membrane-type matrix metalloproteinases 1, 2, and 3. *J Cell Biol* 149(6): 1309-23, 2000.

143. **Hiraoka N, Allen E, Apel IJ, Gyetko MR, Weiss SJ.** Matrix metalloproteinases regulate neovascularization by acting as pericellular fibrinolysins. *Cell* 95(3): 365-377, 1998.

144. **Saunders WB, Bohnsack BL, Faske JB, Anthis NJ, Bayless KJ, et al.** Coregulation of vascular tube stabilization by endothelial cell TIMP-2 and pericyte TIMP-3. *J Cell Biol* 175(1): 179-91, 2006.

145. **Yana I, Sagara H, Takaki S, Takatsu K, Nakamura K, et al.** Crosstalk between neovessels and mural cells directs the site-specific expression of MT1-MMP to endothelial tip cells. *J Cell Sci 1*20(Pt 9): 1607-14, 2007.

146. **Nisato RE, Hosseini G, Sirrenberg C, Butler GS, Crabbe T, et al.** Dissecting the role of matrix metalloproteinases (MMP) and integrin alpha(v)beta3 in angiogenesis in vitro: absence of hemopexin C domain bioactivity, but membrane-Type 1-MMP and alpha(v)beta3 are critical. *Cancer Res* 65(20): 9377-87, 2005.

147. **Hiraoka N, Allen E, Apel IJ, Gyetko MR, Weiss SJ.** Matrix metalloproteinases regulate neovascularization by acting as pericellular fibrinolysins. *Cell* 95(3): 365-77, 1998.

148. **Holmbeck K, Bianco P, Caterina J, Yamada S, Kromer M, et al.** MT1-MMP-deficient mice develop dwarfism, osteopenia, arthritis, and connective tissue disease due to inadequate collagen turnover. *Cell* 99(1): 81-92, 1999.

149. **Zhou Z, Apte SS, Soininen R, Cao R, Baaklini GY, et al.** Impaired endochondral ossification and angiogenesis in mice deficient in membrane-type matrix metalloproteinase I. *Proc Natl Acad Sci U S A* 97(8): 4052-7, 2000.

150. **Langlois S, Nyalendo C, Di Tomasso G, Labrecque L, Roghi C, et al.** Membrane-type 1 matrix metalloproteinase stimulates cell migration through epidermal growth factor receptor transactivation. *Mol Cancer Res* 5(6): 569-83, 2007.

151. **Nyalendo C, Michaud M, Beaulieu E, Roghi C, Murphy G, et al.** Src-dependent phosphorylation of membrane type I matrix metalloproteinase on cytoplasmic tyrosine 573: role in endothelial and tumor cell migration. *J Biol Chem* 282(21): 15690-9, 2007.

152. **Su SC, Mendoza EA, Kwak HI, Bayless KJ.** Molecular profile of endothelial invasion of three-dimensional collagen matrices: insights into angiogenic sprout induction in wound healing. *Am J Physiol Cell Physiol* 295(5): C1215-29, 2008.

153. **Hood JL, Brooks WH, Roszman TL.** Subcellular mobility of the calpain/calpastatin network: an organelle transient. *Bioessays* 28(8): 850-9, 2006.

154. **Hood JL, Logan BB, Sinai AP, Brooks WH, Roszman TL.** Association of the calpain/calpastatin network with subcellular organelles. *Biochem Biophys Res Commun* 310(4): 1200-12, 2003.

155. **Hotary KB, Allen ED, Brooks PC, Datta NS, Long MW, et al.** Membrane type I matrix metalloproteinase usurps tumor growth control imposed by the three-dimensional extracellular matrix. *Cell* 114(1): 33-45, 2003.

156. **Lafleur MA, Handsley MM, Knäuper V, Murphy G, Edwards DR.** Endothelial tubulogenesis within fibrin gels specifically requires the activity of membrane-type-matrix metalloproteinases (MT-MMPs). *J Cell Sci* 115(Pt 17): 3427-38, 2002.

157. **Youn JY, Wang T, Cai H.** An ezrin/calpain/PI3K/AMPK/eNOSs1179 signaling cascade mediating VEGF-dependent endothelial nitric oxide production. *Circ Res* 104(1): 50-9, 2009.

158. **Higuchi M, Onishi K, Kikuchi C, Gotoh Y.** Scaffolding function of PAK in the PDK1-Akt pathway. *Nat Cell Biol* 10(11): 1356-64, 2008.

159. **Kierbel A, Gassama-Diagne A, Mostov K, Engel JN.** The phosphoinositol-3-kinase-protein kinase B/Akt pathway is critical for Pseudomonas aeruginosa strain PAK internalization. *Mol Biol Cell* 16(5): 2577-85, 2005.

160. **Somanath PR, Vijai J, Kichina JV, Byzova T, Kandel ES.** The role of PAK-1 in activation of MAP kinase cascade and oncogenic transformation by Akt. *Oncogene* 28(25): 2365-9, 2009.

161. **Orr AW, Sanders JM, Bevard M, Coleman E, Sarembock IJ, et al.** The subendothelial extracellular matrix modulates NF-kappaB activation by flow: a potential role in atherosclerosis. *J Cell Biol* 169(1): 191-202, 2005.

162. **Lafleur MA, Forsyth PA, Atkinson SJ, Murphy G, Edwards DR..** Perivascular cells regulate endothelial membrane type-1 matrix metalloproteinase activity. *Biochem Biophys Res Commun* 282(2): 463-73, 2001.

163. **Milkiewicz M, Kelland C, Colgan S, Haas TL..** Nitric oxide and p38 MAP kinase mediate shear stress-dependent inhibition of MMP-2 production in microvascular endothelial cells. *J Cell Physiol* 208(1): 229-37, 2006.

164. **Baker AH, Edwards DR, Murphy G.** Metalloproteinase inhibitors: biological actions and therapeutic opportunities. *J Cell Sci* 115(Pt 19): 3719-27, 2002.

165. **Boisseau MR.** Roles of mechanical blood forces in vascular diseases. A clinical overview. *Clin Hemorheol Microcirc* 33(3): 201-7, 2005.

166. **Jones EA, Baron MH, Fraser SE, Dickinson ME.** Measuring hemodynamic changes during mammalian development. *Am J Physiol Heart Circ Physiol* 287(4): H1561-9, 2004.

167. **McInroy L, Maatta A.** Down-regulation of vimentin expression inhibits carcinoma cell migration and adhesion. *Biochem Biophys Res Commun* 360(1): 109-14, 2007.

168. **Nieminen M, Henttinen T, Merinen M, Marttila-Ichihara F, Eriksson JE, et al.** Vimentin function in lymphocyte adhesion and transcellular migration. *Nat Cell Biol* 8(2): 156-62, 2006.

169. **Tsuruta D, Jones JC.** The vimentin cytoskeleton regulates focal contact size and adhesion of endothelial cells subjected to shear stress. *J Cell Sci* 116(Pt 24): 4977-84, 2003.

170. **Whipple RA, Balzer EM, Cho EH, Matrone MA, Yoon JR, et al.** Vimentin filaments support extension of tubulin-based microtentacles in detached breast tumor cells. *Cancer Res* 68(14): 5678-88, 2008.

171. **Yoshida H, Murachi T, Tsukahara I.** Degradation of actin and vimentin by calpain II, a Ca2+-dependent cysteine proteinase, in bovine lens. *FEBS Lett* 170(2): 259-62, 1984.

172. **Cucina A, Sterpetti AV, Pupelis G, Fragale A, Lepidi S, et al.** Shear stress induces changes in the morphology and cytoskeleton organisation of arterial endothelial cells. *Eur J Vasc Endovasc Surg* 9(1): 86-92, 1995.

173. **Jackson WM, Jaasma MJ, Tang RY, Keaveny TM.** Mechanical loading by fluid shear is sufficient to alter the cytoskeletal composition of osteoblastic cells. *Am J Physiol Cell Physiol* 295(4): C1007-15, 2008.

174. **Helmke BP, Goldman RD, Davies PF.** Rapid displacement of vimentin intermediate filaments in living endothelial cells exposed to flow. *Circ Res* 86(7): 745-52, 2000.

175. **Helmke BP, Rosen AB, Davies PF.** Mapping mechanical strain of an endogenous cytoskeletal network in living endothelial cells. *Biophys J* 84(4): 2691-9, 2003.

176. **Langlois S, Di Tomasso G, Boivin D, Roghi C, Murphy G, et al.** Membrane type 1-matrix metalloproteinase induces endothelial cell morphogenic differentiation by a caspase-dependent mechanism. *Exp Cell Res* 307(2): 452-64, 2005.

177. **Pulyaeva H, Bueno J, Polette M, Birembaut P, Sato H, et al.** MT1-MMP correlates with MMP-2 activation potential seen after epithelial to mesenchymal transition in human breast carcinoma cells. *Clin Exp Metastasis* 15(2): 111-20, 1997.

178. **Goto H, Kosako H, Tanabe K, Yanagida M, Sakurai M, et al.** Phosphorylation of vimentin by Rho-associated kinase at a unique amino-terminal site that is specifically phosphorylated during cytokinesis. *J Biol Chem* 273(19): 11728-36, 1998.

179. **Jiang L, Wang M, Zhang J, Monticone RE, Telljohann R, et al.** Increased aortic calpain-1 activity mediates age-associated angiotensin II signaling of vascular smooth muscle cells. *PLoS One* 3(5): e2231, 2008.

180. **Tang Y, Zhou H, Chen A, Pittman RN, Field J, et al.** The Akt proto-oncogene links Ras to Pak and cell survival signals. *J Biol Chem* 275(13): 9106-9, 2000.

181. **Zhou GL, Zhuo Y, King CC, Fryer BH, Bokoch GM, et al.** Akt phosphorylation of serine 21 on Pak1 modulates Nck binding and cell migration. *Mol Cell Biol* 23(22): 8058-69, 2003.

182. **Mao K, Kobayashi S, Jaffer ZM, Huang Y, Volden P, et al.** Regulation of Akt/PKB activity by P21-activated kinase in cardiomyocytes. *J Mol Cell Cardiol* 44(2): 429-34, 2008.

183. **Chan W, Kozma R, Yasui Y, Inagaki M, Leung T, et al.** Vimentin intermediate filament reorganization by Cdc42: involvement of PAK and p70 S6 kinase. *Eur J Cell Biol* 81(12): 692-701, 2002.

184. **Prahlad V, Yoon M, Moir RD, Vale RD, Goldman RD.** Rapid movements of vimentin on microtubule tracks: kinesin-dependent assembly of intermediate filament networks. *J Cell Biol* 143(1): 159-70, 1998.

185. **Yoon M, Moir RD, Prahlad V, Goldman RD.** Motile properties of vimentin intermediate filament networks in living cells. *J Cell Biol* 143(1): 147-57, 1998.

186. **Helfand BT, Mikami A, Vallee RB, Goldman RD.** A requirement for cytoplasmic dynein and dynactin in intermediate filament network assembly and organization. *J Cell Biol* 157(5): 795-806, 2002.

187. **Perlson E, Michaelevski I, Kowalsman N, Ben-Yaakov K, Shaked M.** Vimentin binding to phosphorylated Erk sterically hinders enzymatic dephosphorylation of the kinase. *J Mol Biol* 364(5): 938-44, 2006.

188. **Shi ZD, Ji XY, Berardi DE, Qazi H, Tarbell JM.** Interstitial flow induces MMP-1 expression and vascular SMC migration in collagen I gels via an ERK1/2-dependent and c-Jun-mediated mechanism. *Am J Physiol Heart Circ Physiol* 298(1): H127-35, 2010.

189. **Boardman KC, Swartz MA.** Interstitial flow as a guide for lymphangiogenesis. *Circ Res* 92(7): 801-8, 2003.

190. **Semino CE, Kamm RD, Lauffenburger DA.** Autocrine EGF receptor activation mediates endothelial cell migration and vascular morphogenesis induced by VEGF under interstitial flow. *Exp Cell Res* 312(3): 289-98, 2006.

191. **Zheng W, Christensen LP, Tomanek RJ.** Differential effects of cyclic and static stretch on coronary microvascular endothelial cell receptors and vasculogenic/angiogenic responses. *Am J Physiol Heart Circ Physiol* 295(2): H794-800, 2008.

192. **Desai LP, White SR, Waters CM.** Cyclic mechanical stretch decreases cell migration by inhibiting phosphatidylinositol 3-kinase- and focal adhesion kinase-mediated JNK1 activation. *J Biol Chem* 285(7): 4511-9, 2010.

193. **Sacharidou A, Koh W, Stratman AN, Mayo AM, Fisher KE.** Endothelial lumen signaling complexes control 3D matrix-specific tubulogenesis through interdependent Cdc42- and MT1-MMP-mediated events. *Blood* 115(25): 5259-69, 2010.

VITA

HO JIN KANG was born in JEJU Island, the Republic of KOREA, the middle of three to GILSUN KANG and KYOUNGJA KIM. He graduated from Sehwa High School in 1997. He received his Bachelor of Science in control and instrumentation engineering from the Korea University in 2000. In August 2000, he entered graduate school at the Korea University and received his Master of Science with a major in mechatronics in August 2002. He began his doctoral studies in biomedical engineering at Texas A&M University in January 2005 and graduated with his Ph. D. in May 2011. Dr. Kang can be reached at The Department of Biomedical Engineering 337 Zachry Engineering Center, 3120 TAMU, College Station, TX, 77843. His email is hobbang4@hotmail.com

PUBLICATIONS

Hojin Kang, Kayla J. Bayless and Roland R. Kaunas (2008) Fluid shear stress modulates endothelial cell invasion into three-dimensional collagen matrices. American Journal of Physiology *Heart and Circulatory Physiology*, 295: H2087-2097.

Hojin Kang, Roland R. Kaunas and Kayla J. Bayless (2011) Fluid shear stress and sphingosine 1-phosphate activate Calpain to promote MT1-MMP membrane translocation and endothelial invasion in collagen matrices. *The Journal of Biological Chemistry* (in review).